A tour de modeling and analysis of stellar atmospheres throughout the HRD

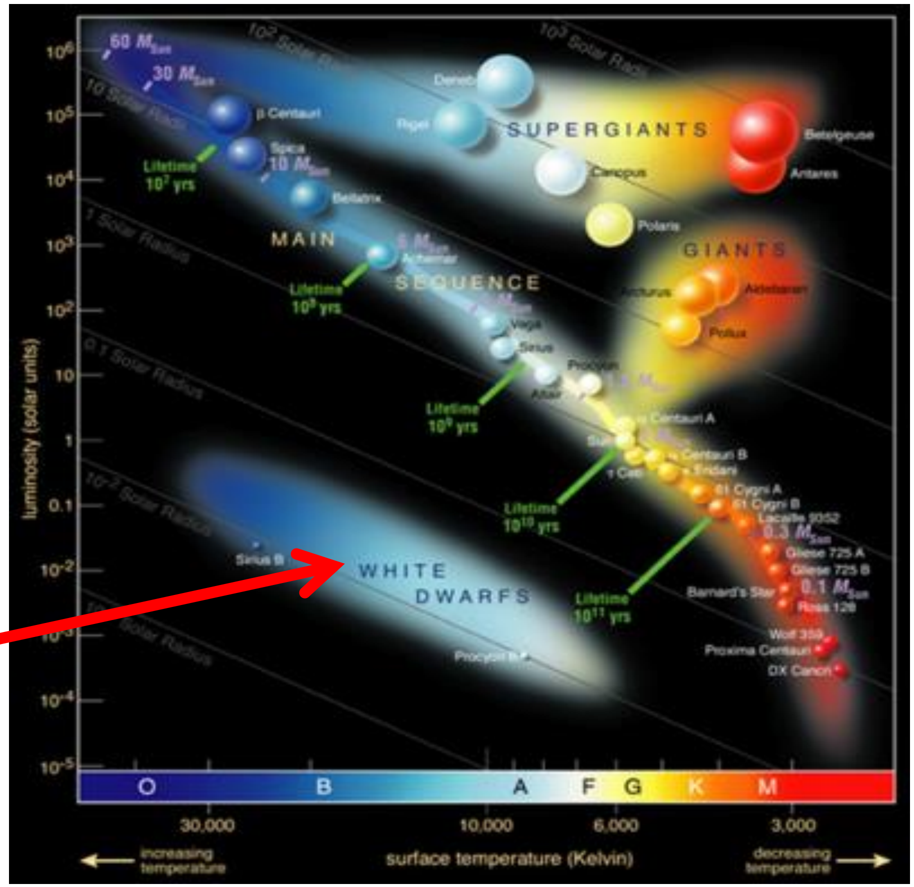

except for
white dwarfs

Some different types of stars…

Hot luminous stars:
Massive,
main-sequence (MS)
or evolved, ~10 Rsun.
Strong, fast stellar
winds

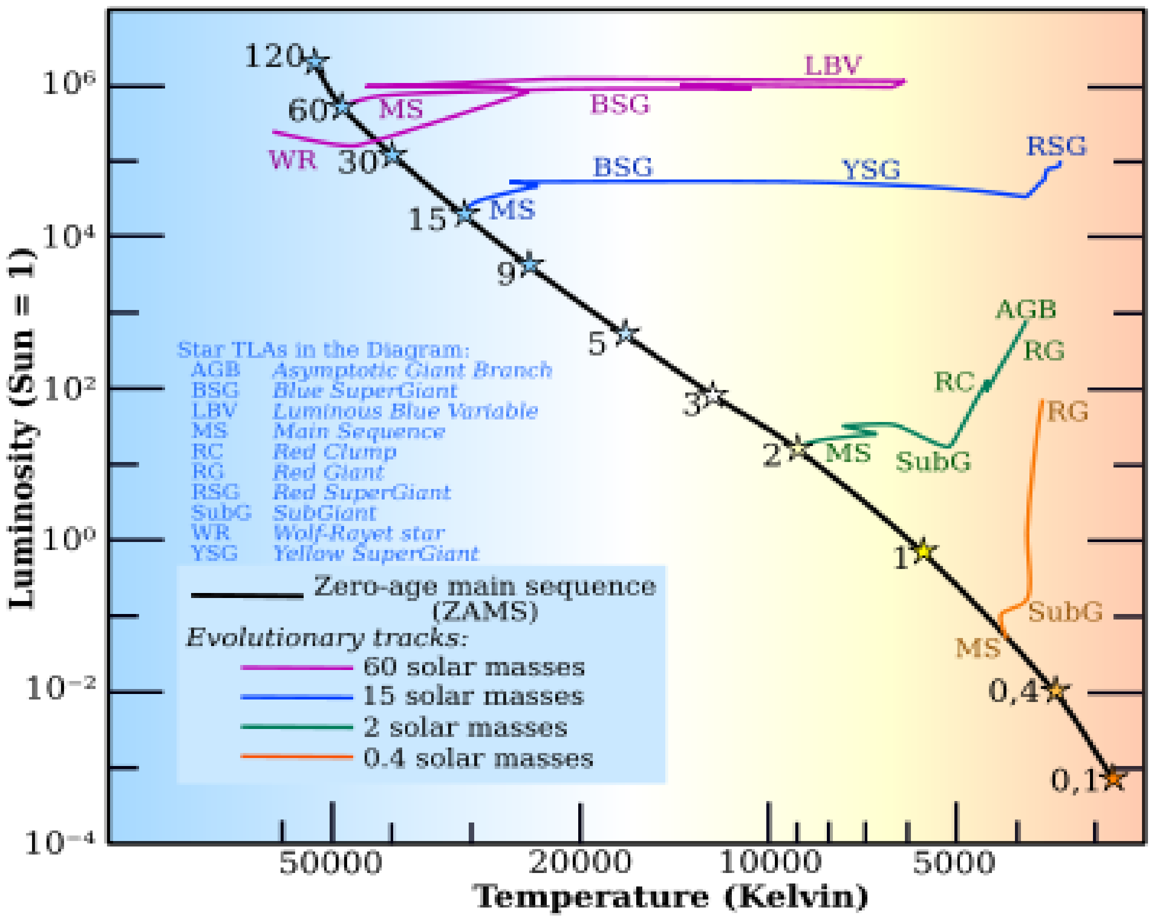

Cool, luminous stars
(RSG, AGB):
Massive or low/interme-
diate mass, evolved,
several 100 (!) Rsun.
Strong, slow stellar winds

Solar-type stars:
Low-mass, on or near MS,
hot surrounding coronae,
weak stellar wind
(e.g. solar wind)

A tour de modeling and analysis of stellar atmospheres throughout the HRD

Different regimes require different key input physics and assumptions

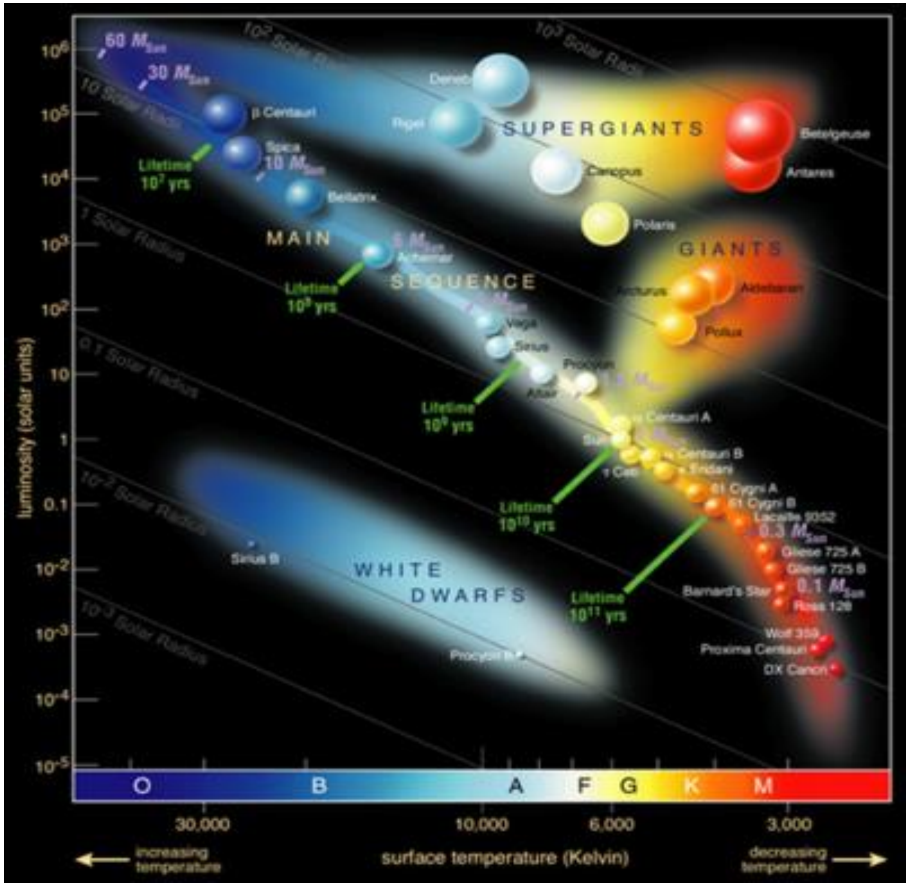

- LTE or NLTE
- Spectral line blocking/blanketing
- (sub-) Surface convection
- Geometry and dimensionality
- Velocity fields and outflows

Spectroscopy and Photometry

ALSO:
Analysis
of different
WAVELENGTH
BANDS
is different

(X-ray, UV, optical, infra-red…)

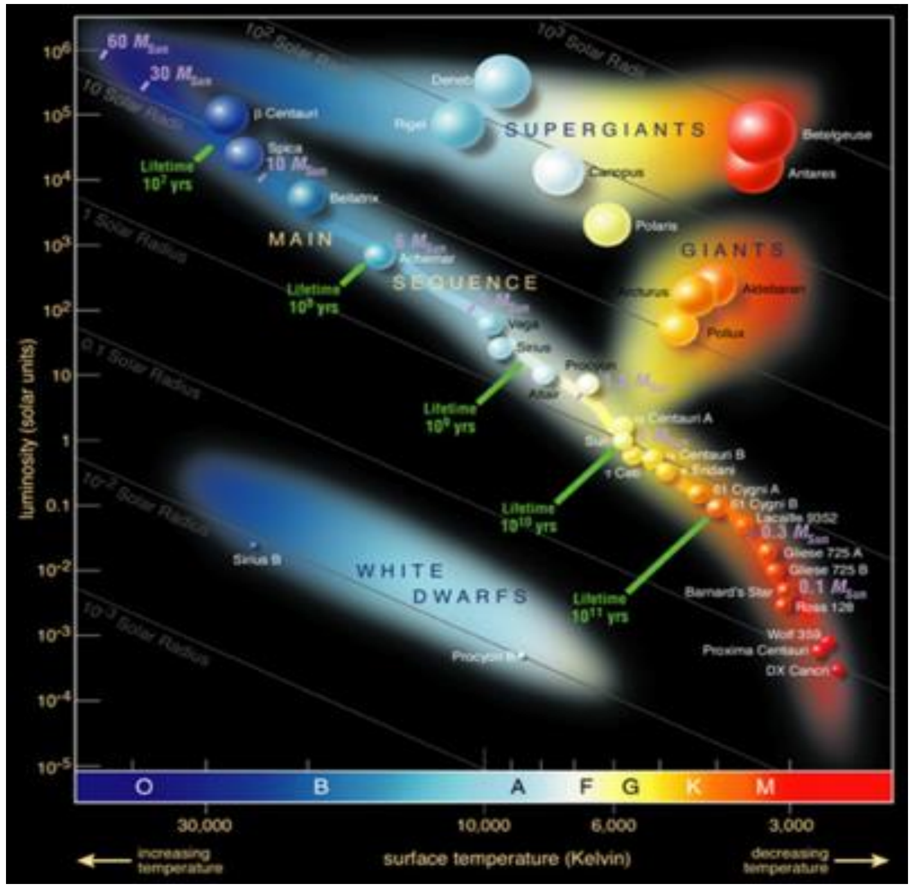

Depends on where in atmosphere light escapes from

Question: Why is this "formation depth" different for different wavebands and diagnostics?

Spectroscopy and Photometry (see part 1)

...gives insight into and understanding of our cosmos

- requires
  - plasma physics, plasma is "normal" state of atmospheres and interstellar matter (plasma diagnostics, line broadening, influence of magnetic fields,...)
  - atomic physics/quantum mechanics, interaction light/matter (micro quantities)
  - radiative transfer, interaction light/matter (macroscopic description)
  - thermodynamics, thermodynamic equilibria: TE, LTE (local), NLTE (non-local)
  - hydrodynamics, atmospheric structure, velocity fields, shockwaves,...

- provides
  - stellar properties, mass, radius, luminosity, energy production, chemical composition, properties of outflows
  - properties of (inter) stellar plasmas, temperature, density, excitation, chemical comp., magnetic fields

- INPUT for stellar, galactic and cosmologic evolution and for stellar and galactic structure

Spectroscopy (see part 1)

UV spectrum of the O4I(f) supergiant ζ Pup

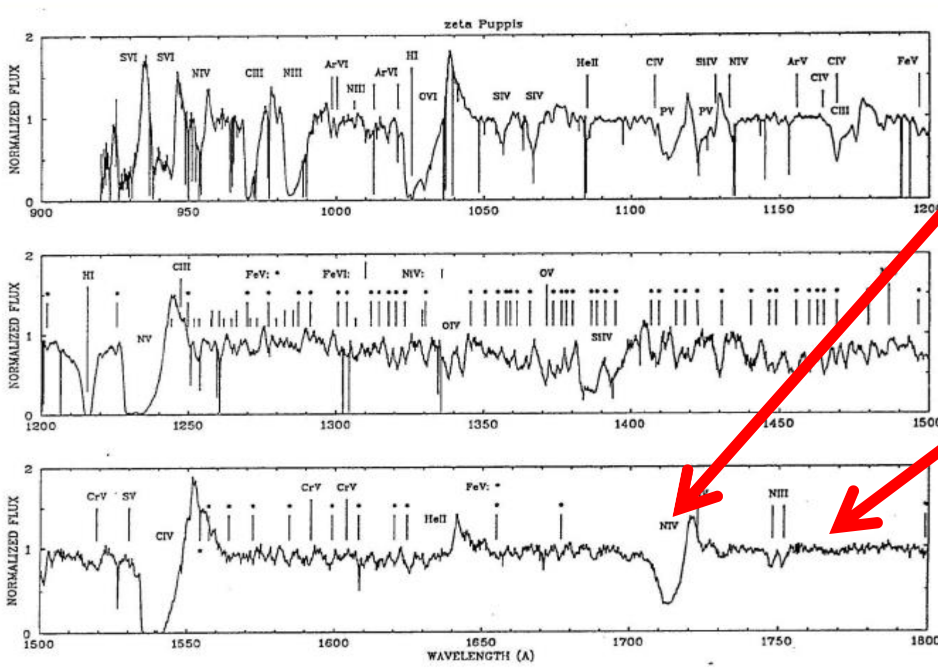

montage of Copernicus (λ < 1500 Å, high res. mode, Δλ ≈ 0.05 Å, Morton & Underhill 1977) and IUE (Δλ ≈ 0.1 Å) observations

31

UV "P-Cygni" lines formed in rapidly accel-erating, hot stellar winds

(quasi-) Continuum formed in (quasi-) hydrostatic photosphere

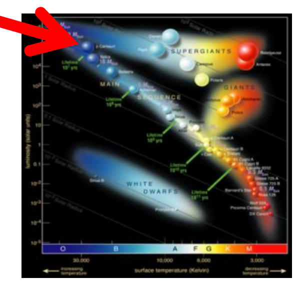

Stellar Atmospheres in practice

Spectroscopy

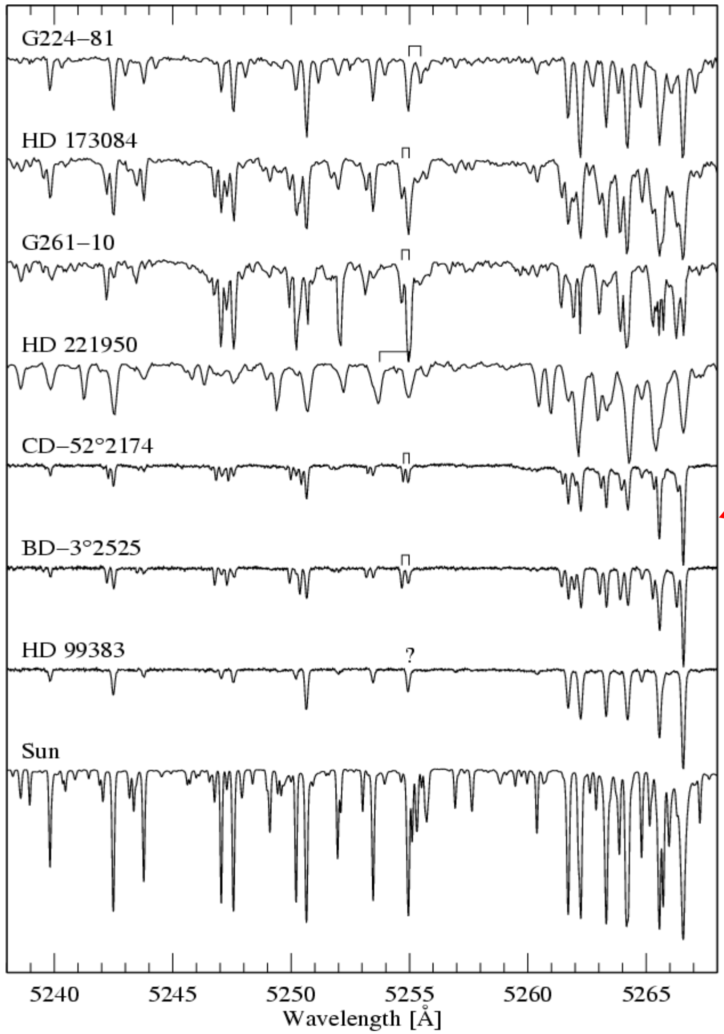

Lines and continuum in the optical around 5200 Å, in cool solar-type stars, formed in the photosphere

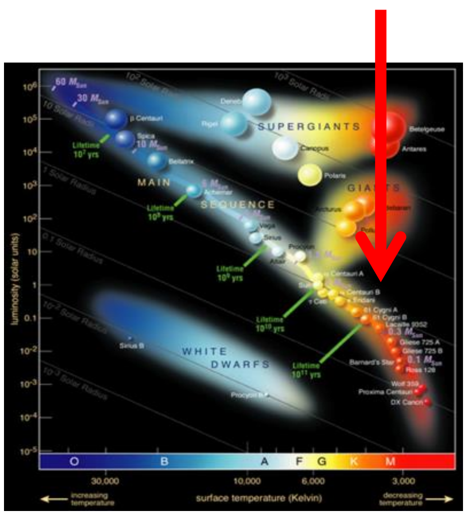

Spectroscopy

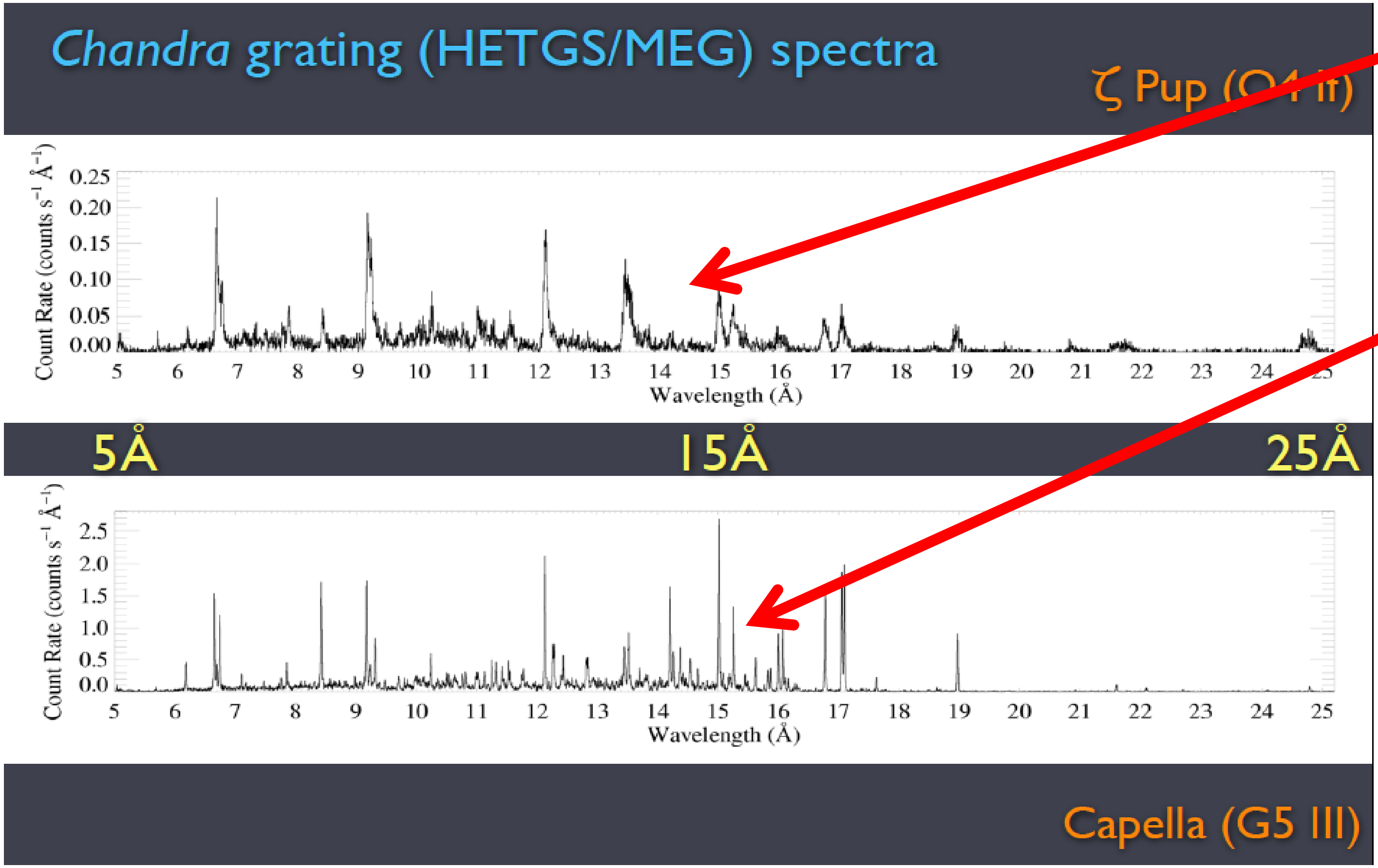

X-rays from hot stars, formed in shocks in stellar wind

X-rays from cool stars, formed in hot corona

A tour de modeling and analysis of stellar atmospheres throughout the HRD

Stellar Winds – 2nd part of course!

KEY QUESTION: What provides the force able to overcome gravity?

$$\dot{M} \approx 10^{-4} \ldots 10^{-8} M_{\odot} / yr$$

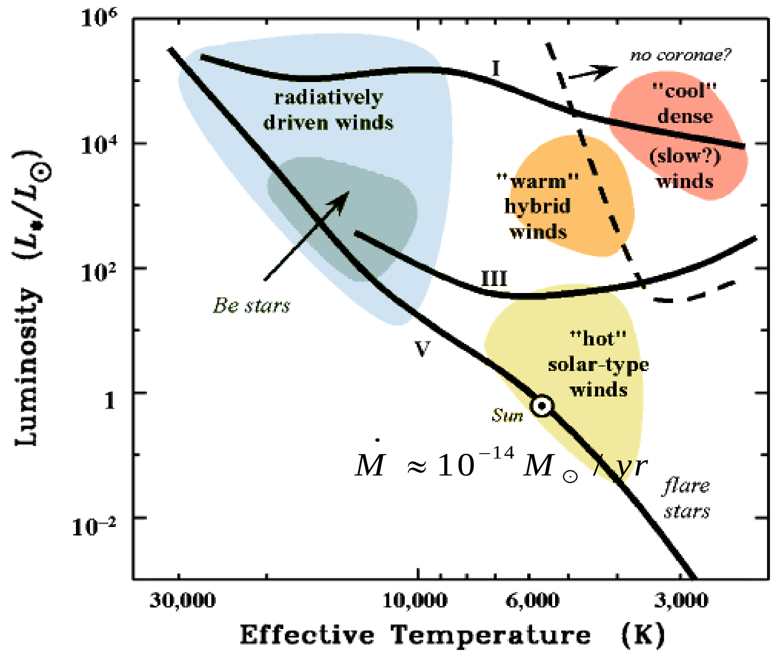

- LTE or NLTE
- Spectral line blocking/blanketing
- (sub-) Surface convection
- Geometry and dimensionality
- Velocity fields and outflows

A tour de modeling and analysis of stellar atmospheres throughout the HRD

KEY QUESTION: What provides the force able to overcome gravity?

Pressure gradient
in hot coronae of solar-type stars

Radiation force:
Dust scattering (in pulsation-levitated material) in cool AGB stars (Höffner and colleagues)

Same mechanism In cool RSGs?

$$\dot{M} \approx 10^{-4} \ldots 10^{-8} M_\odot / yr$$

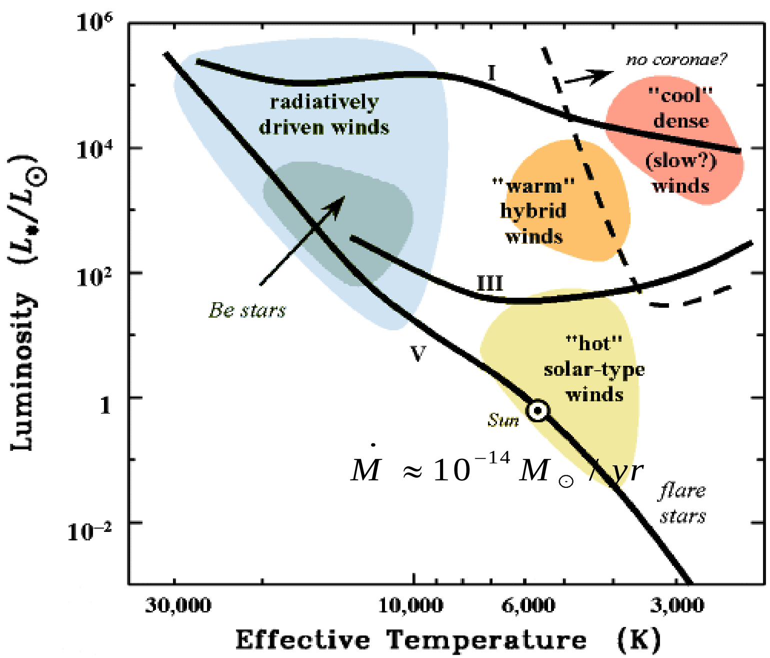

- LTE or NLTE
- Spectral line blocking/blanketing
- (sub-) Surface convection
- Geometry and dimensionality
- Velocity fields and outflows

A tour de modeling and analysis of stellar atmospheres throughout the HRD

KEY QUESTION: What provides the force able to overcome gravity?

Radiation force:
line scattering in hot, luminous stars
→ done here at USM, more to follow in part 2

$$\dot{M} \approx 10^{-4} \ldots 10^{-8} M_{\odot} / yr$$

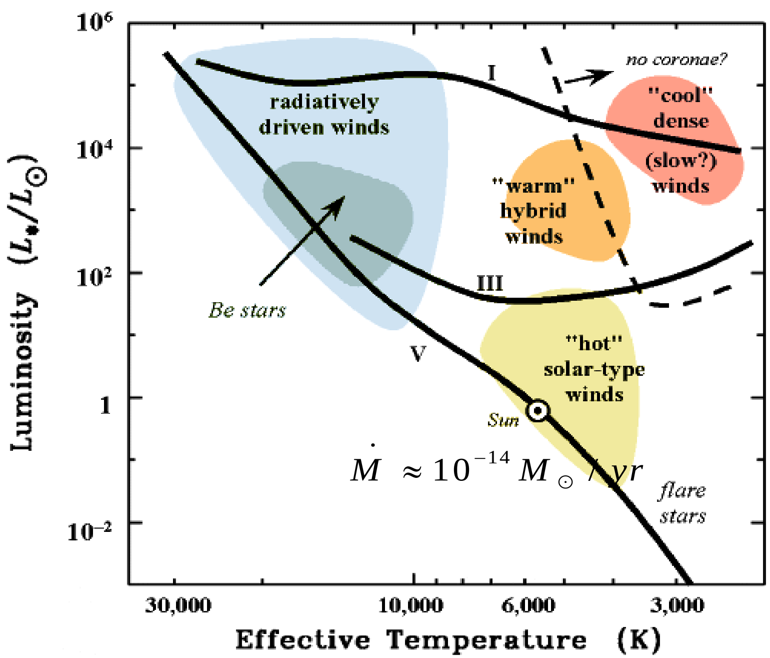

- LTE or NLTE
- Spectral line blocking/blanketing
- (sub-) Surface convection
- Geometry and dimensionality
- Velocity fields and outflows

Question: How do you think the high mass loss of stars with high luminosities affects the evolution of the star and its surroundings?

from introductory slides …

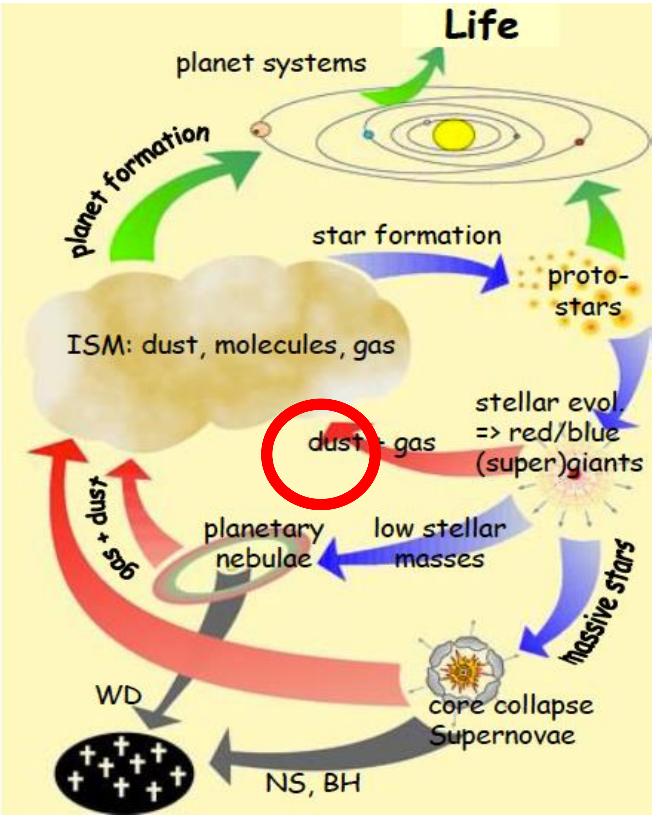

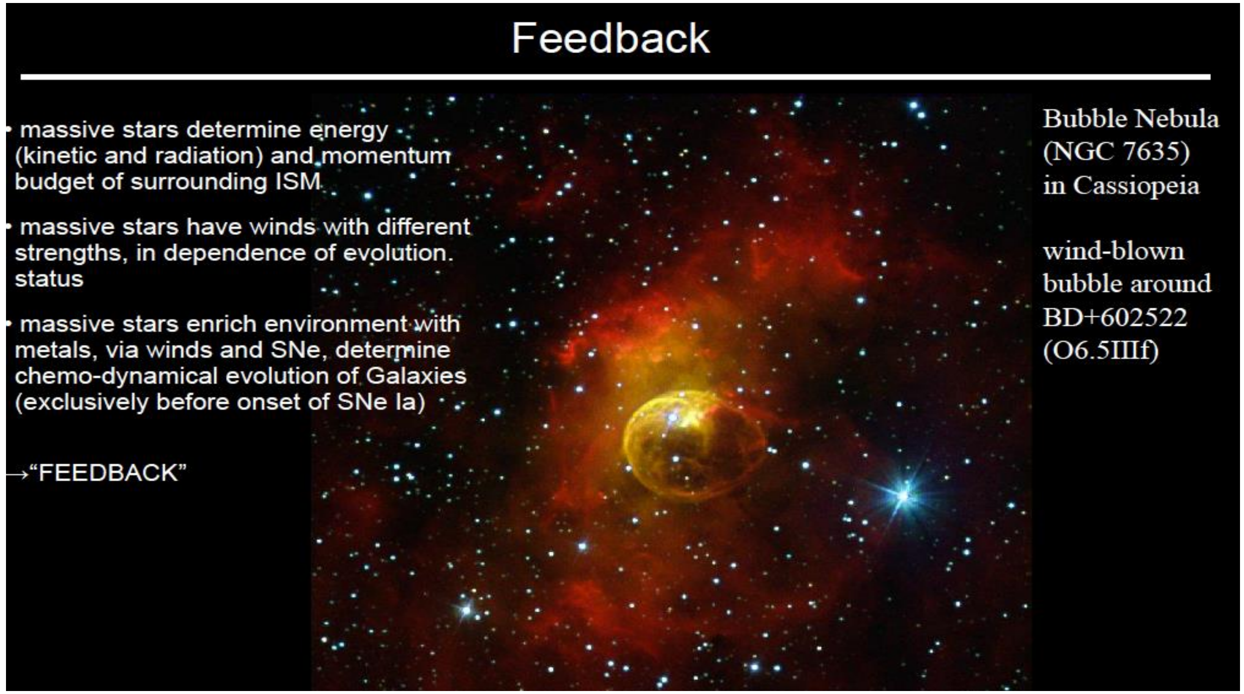

Stellar Winds from evolved hot and cool stars control late evolution, and feed the ISM with nuclear processed material

A tour de modeling and analysis of stellar atmospheres throughout the HRD

In the following,
we focus on stellar
photospheres

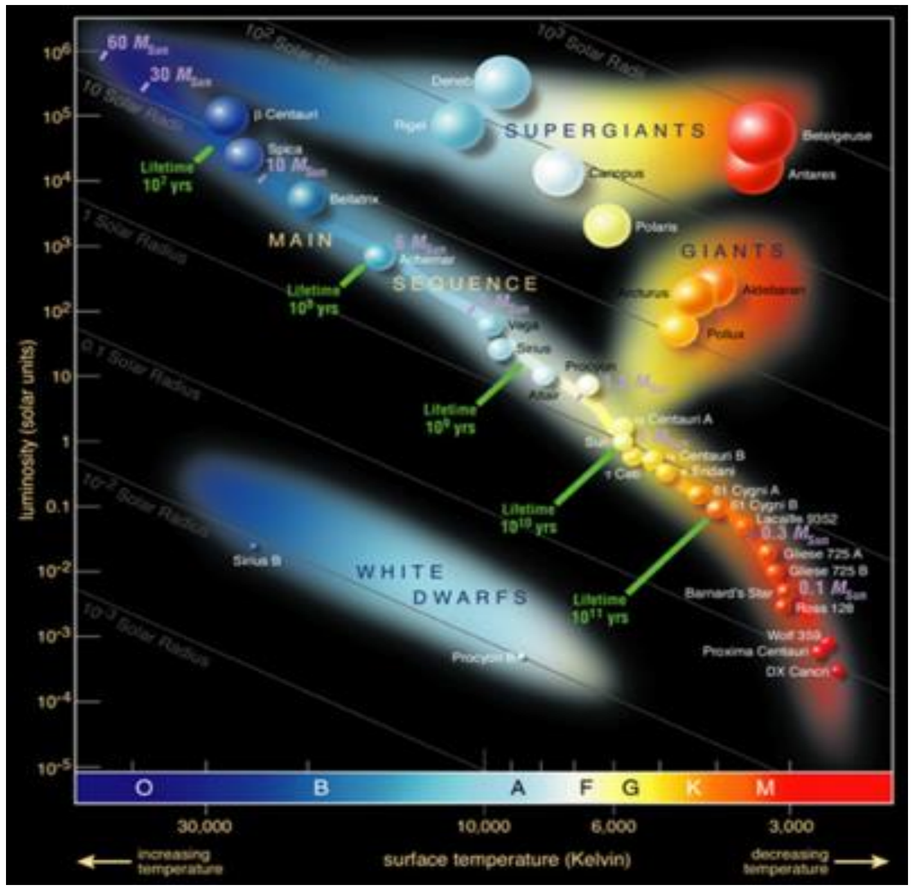

From part 1

Summary: stellar atmospheres - the solution principle

THUS problem of stellar atmospheres solved (in principle, without convection, p-p geometry, static)

Given log g_*, T_{eff}, abundances

(A) hydrostatic equilibrium

$$\frac{dp_{gas}}{dz} = -\rho(g_* - g_{rad}) \; ; \quad g_{rad} = \frac{4\pi}{c\rho}\int_0^\infty \chi_\nu H_\nu d\nu = \frac{4\pi}{c\rho}\left(\sigma^{TH} H(z) + \int_0^\infty \chi_\nu^{rest} H_\nu d\nu\right)$$

$$\Rightarrow \frac{dp_{gas}}{dz} = -\rho g_* + \sigma^{TH}\frac{\sigma_B T_{eff}^4}{c} + \frac{4\pi}{c}\int_0^\infty \chi_\nu^{rest} H_\nu d\nu$$

$$H = \frac{1}{4\pi}\sigma_B T_{eff}^4 \quad \left(= \frac{1}{4\pi}\mathcal{F}\right)$$

(B) equation of rad. transfer

$$\mu\frac{dI_\nu}{dz} = \chi_\nu(S_\nu - I_\nu) \quad \forall \nu,\mu \quad \Rightarrow J_\nu = \frac{1}{2}\int_{-1}^{+1} I_\nu(\mu)d\mu \; ; \quad H_\nu = \frac{1}{2}\int_{-1}^{+1} I_\nu(\mu)\mu d\mu$$

(C) a) radiative equilibrium

scattering terms cancel, since conservative

$$\int_0^\infty(\eta_\nu - \kappa_\nu J_\nu)d\nu = \int_0^\infty\left\{(\sigma^{TH}J_\nu + \chi_\nu^{rest}S_\nu^{rest}) - (\sigma^{TH} + \chi_\nu^{rest})J_\nu\right\}d\nu = \int_0^\infty \chi_\nu^{rest}(S_\nu^{rest} - J_\nu)d\nu \overset{?}{=} 0$$

b) flux-conservation: $4\pi\int_0^\infty H_\nu(z)d\nu = 4\pi H(z) \overset{?}{=} \sigma_B T_{eff}^4$

$\Rightarrow \Delta T(z)$

$\rightarrow \Delta\chi_\nu(z)$ etc

(D) equation of state $p_{gas}(z) = \frac{k_B}{\mu m_H}\rho(z)T(z)$

solution by iteration!

Solution of differential equations A and B by discretization
differential operators => finite differences
all quantities have to be evaluated on suitable grid

Eq. of radiative transfer (B)
usually solved by the so-called
Feautrier and/or Rybicki scheme

- OBSER-
VATIONS!!!

A tour de modeling and analysis of stellar atmospheres throughout the HRD

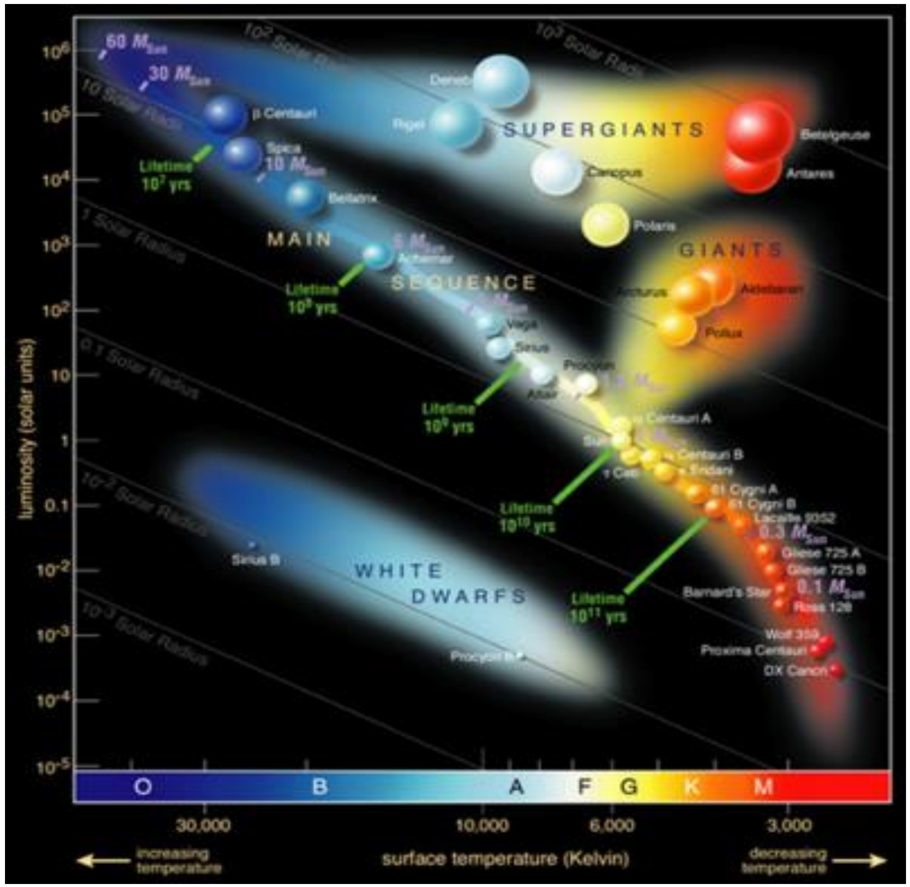

- LTE or NLTE
- Spectral line blocking/blanketing
- (sub-) Surface convection
- Geometry and dimensionality
- Velocity fields and outflows

LTE or NLTE? (see part 1)

When is LTE valid???

roughly: electron collisions >> photoabsorption rates
$\propto n_e T^{1/2}$ $\propto I_\nu(T) \propto T^x$, $x \geq 1$

LTE: T low, n_e high dwarfs (giants), late B and cooler
NLTE: T high, n_e low all supergiants + rest

however: NLTE-effects also in cooler stars, e.g.. iron in sun

HOT STARS:

Complete model atmosphere and synthetic spectrum must be calculated in NLTE

NLTE calculations for various applications (including Supernovae remnants) within the expertise of USM

COOL STARS:

Standard to neglect NLTE-effects on atmospheric structure, might be included when calculating line spectra for individual “trace” elements (typically used for chemical abundance determinations)

BUT: See work by Phoenix-team (Hauschildt et al.)
ALSO: RSGs still somewhat open question

A tour de modeling and analysis of stellar atmospheres throughout the HRD

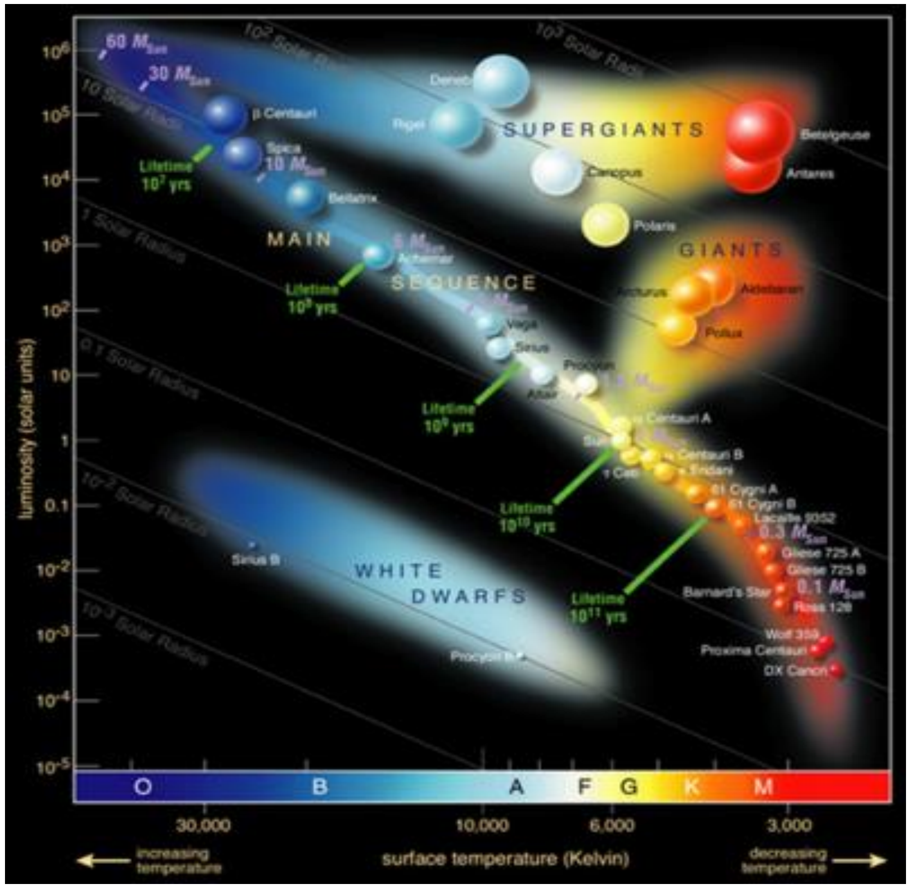

- LTE or NLTE
- Spectral line blocking/blanketing
- (sub-) Surface convection
- Geometry and dimensionality
- Velocity fields and outflows

Spectral line blocking/blanketing

- Effects of numerous -- literally millions -- of (primarily metal) spectral lines upon the atmospheric structure and flux distribution
- Q: Why is this tricky business?

Spectral line blocking/blanketing

- Effects of numerous -- literally millions -- of (primarily metal) spectral lines upon the atmospheric structure and flux distribution
- Q: Why is this tricky business?

- Lots of atomic data required (thus atomic physics and/or experiments)
- LTE or NLTE?
- What lines are relevant?
  (i.e., what ionization stages? Are there molecules present?)

Techniques:

Opacity Distribution Functions
Opacity-Sampling
Direct line by line calculations

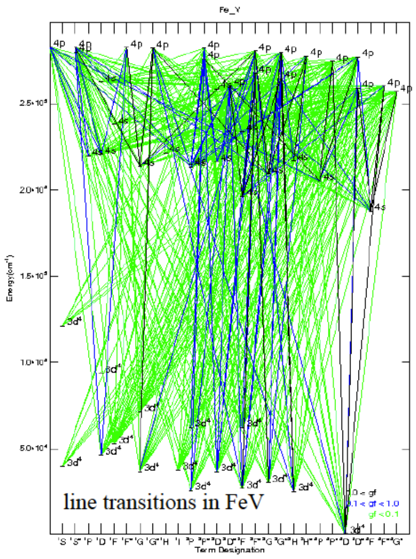

Spectral line blocking/blanketing

Back-warming (and surface-cooling)

- Numerous absorption lines "block" (E)UV radiation flux
- Total flux conservation demands these photons be emitted elsewhere → redistributed to optical/infra-red
- Lines act as "blanket", whereby back-scattered line photons are (partly) thermalized and thus heat up deeper layers

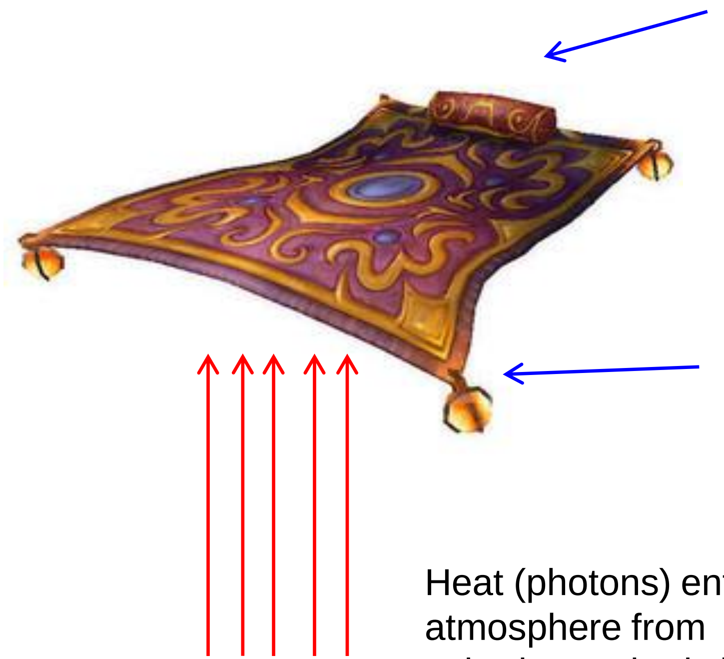

"Blanket" typically cools uppermost layers

"Blanket" warms deep layers

Heat (photons) enters atmosphere from sub-photospheric layers

Spectral line blocking/blanketing

Back-warming and flux redistribution

…occur in stars of all spectral types

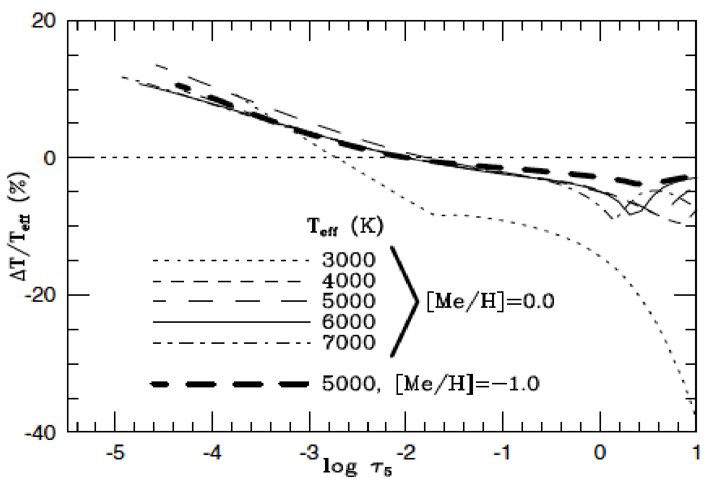

Fig. 4. The effects of switching off line absorption on the temperature structure of a sequence of models with $\log g = 3.0$ and solar metallicity. Note that $\Delta T \equiv T(\text{nolines}) - T(\text{lines})$. It is seen that the blanketing effects are fairly independent of effective temperature for models with $T_{eff} \geq 4000$.

Back warming in cool stars
(from Gustafsson et al. 2008)

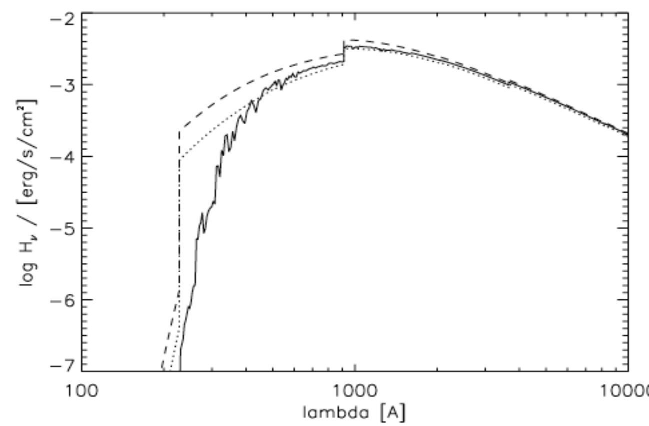

Fig. 10. Emergent Eddington flux H_ν as function of wavelength. Solid line: Current model of HD 15629 (O5V((f)) with parameters from Table 1 ($T_{eff} = 40\,500$ K, $\log g = 3.7$, "model 1"). Dotted: Pure H/He model without line-blocking/blanketing and negligible wind, at same T_{eff} and $\log g$ ("model 2"). Dashed: Pure H/He model, but with $T_{eff} = 45\,000$ K and $\log g = 3.9$ ("model 3").

UV to optical flux redistribution in hot stars
(from Repolust, Puls & Hererro 2004)

Spectral line blocking/blanketing

Back-warming and flux redistribution

…occur in stars of all spectral types

From Puls et al. 2008

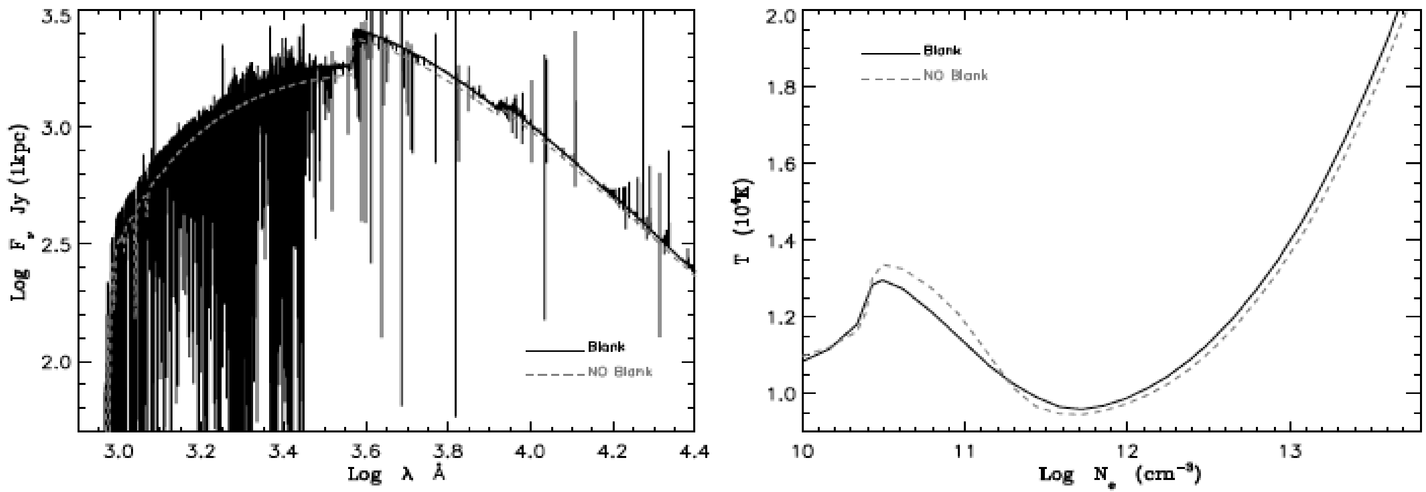

Fig. 9 Effects of line blanketing (solid) vs. unblanketed models (dashed) on the flux distribution ($\log F_\nu$ (Jansky) vs. $\log \lambda$ (Å), left panel) and temperature structure ($T(10^4$ K) vs. $\log n_e$, right panel) in the atmosphere of a late B-hypergiant. Blanketing blocks flux in the UV, redistributes it towards longer wavelengths and causes back-warming.

Spectral line blocking/blanketing

Back-warming – effect on effective temperature

RECALL: T_{eff} -- or total flux (plane-parallel) -- fundamental input parameter in model atmosphere!

From Gustafsson et al. 2008: Estimate effect by assuming a blanketed model with T_{eff} such that the deeper layers correspond to an unblanketed model with effective temperature $T'_{eff} > T_{eff}$

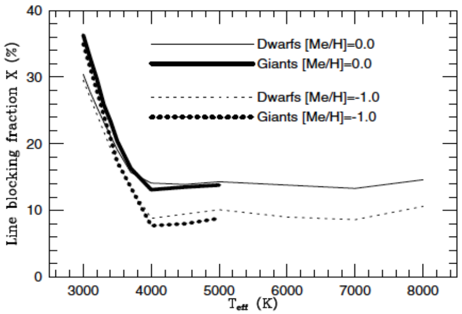

Fig. 3. The blocking fraction X in percent for models in the grid with two different metallicities. The dwarf models all have $\log g = 4.5$ while the giant models have $\log g$ values increasing with temperature, from $\log g = 0.0$ at $T_{eff} = 3000$ K to $\log g = 3.0$ at $T_{eff} = 5000$ K.

Question: Why does the line blocking fraction increase for very cool stars?

$$F = \sigma_B T_{eff}^4$$

$$T'_{eff} = (1 - X)^{-\frac{1}{4}} \cdot T_{eff}, \qquad (35)$$

where X is the fraction of the integrated continuous flux blocked out by spectral lines,

$$X = \frac{\int_0^\infty (F_{cont} - F_\lambda)\mathrm{d}\lambda}{\int_0^\infty F_{cont}\mathrm{d}\lambda}. \qquad (36)$$

T_{eff} in cool stars derived, e.g., by optical photometry

Spectral line blocking/blanketing

Back-warming – effect on effective temperature

RECALL: T_{eff} -- or total flux (plane-parallel) -- fundamental input parameter in model atmosphere!

Previous slide were LTE models. In hot stars, everything has to be done in NLTE…

$$F = \sigma_B T_{eff}^4$$

Question: Why is optical photometry generally NOT well suited to derive Teff in hot stars?

Spectral line blocking/blanketing

Instead, He ionization-balance is typically used
(or N for the very hottest stars, or, e.g., Si for B-stars)

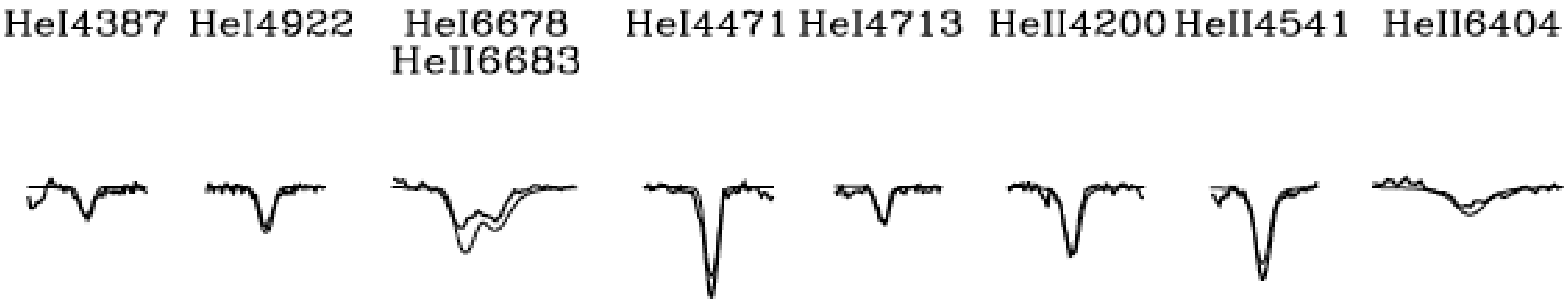

Simultaneous fits to observed HeI and HeII lines
-– from Repolust, Puls, Hererro (2004)

Back-warming shifts ionization balance toward more completely ionized Helium in blanketed models, thus fitting the same observed spectrum requires lower T_{eff} than in unblanketed models

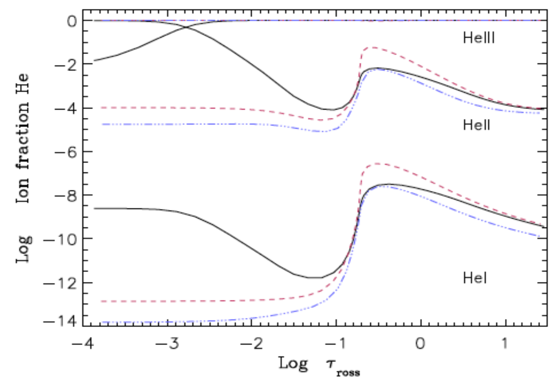

- black – blanketed Teff=45 kK
- red – unblanketed Teff=45 kK
- blue – unblanketed Teff= 50 kK

Spectral line blocking/blanketing

Instead, He ionization-balance is typically used
(or N for the very hottest stars, or, e.g., Si for B-stars)

Result: In hot O-stars with Teff~40,000 K, back-warming can lower the derived T_{eff} as compared to unblanketed models by several thousand degrees! (~ 10 %)

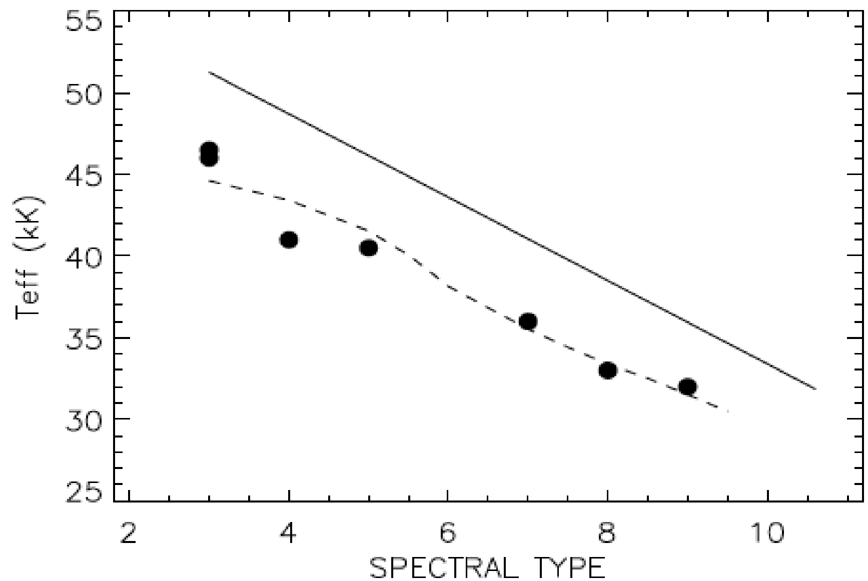

New T_{eff} scale for O-dwarf stars. Solid line – unblanketed models. Dashed – blanketed calibration, dots – observed blanketed values (from Puls et al. 2008)

A tour de modeling and analysis of stellar atmospheres throughout the HRD

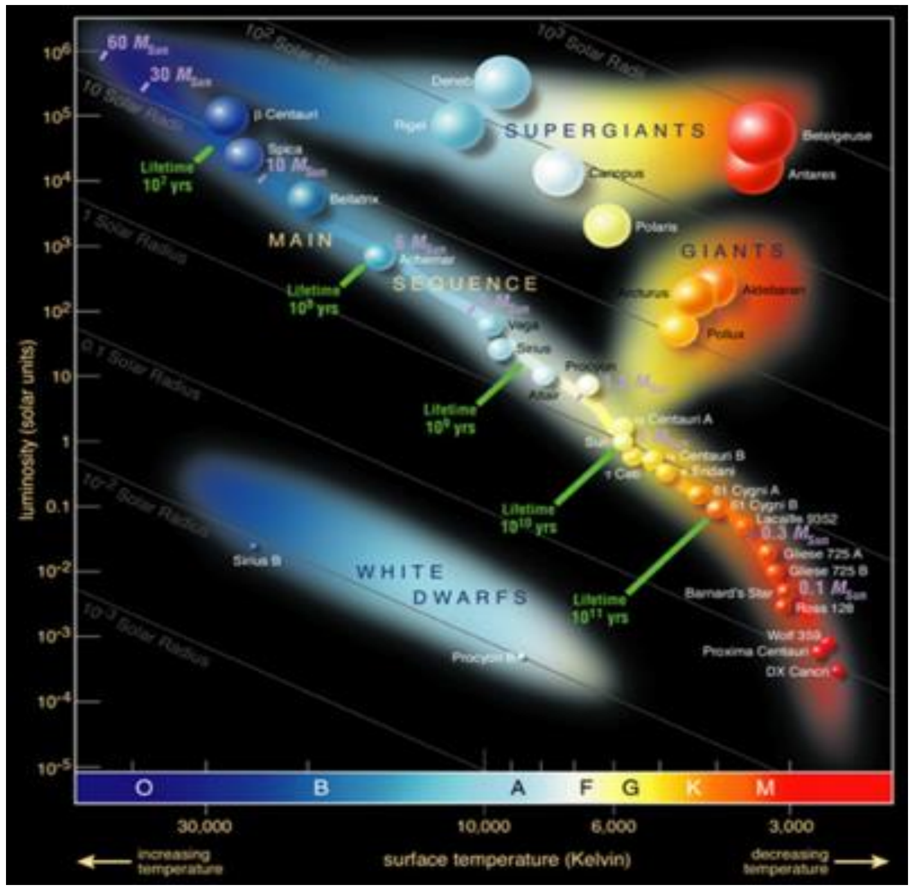

- LTE or NLTE
- Spectral line blocking/blanketing
- (sub-) Surface convection
- Geometry and dimensionality
- Velocity fields and outflows

Surface Convection

from part 1

Convection

energy transport not only by radiation, however also by

- waves
- heat conduction
- convection

} not efficient in typical stellar atmospheres, but ... coronae, chromospheres, white dwarfs

Thus

total flux = const

$$\nabla \cdot \left(\underline{\mathcal{F}}^{\mathrm{rad}} + \underline{\mathcal{F}}^{\mathrm{conv}} \right) = 0$$

(in quasi-hydrostatic atmospheres)

Surface Convection

OBSERVATIONS:
"Sub-surface" convection in layers T~160,000 K (due to iron-opacity peak) currently discussed also in hot stars

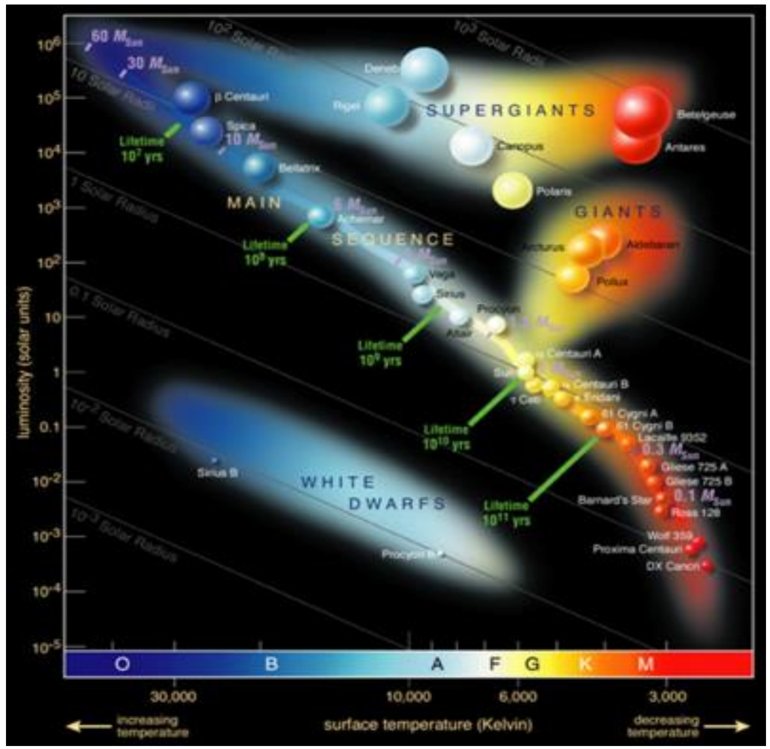

- H/He recombines in atmospheres of cool stars
  → Provides MUCH opacity
  → Convective Energy transport

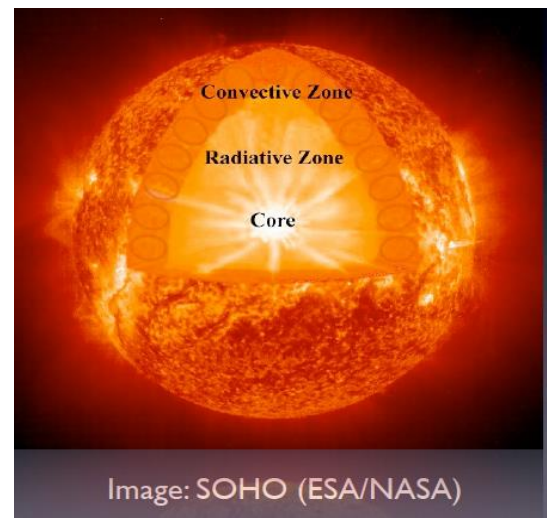

Surface Convection

Traditionally accounted for by rudimentary "mixing-length theory (see part 1) in 1-D atmosphere codes

BUT:
- Solar observations show very dynamic structure
- Granulation and lateral inhomogeneity

→ Need for full 3-D radiation-hydrodynamics simulations in which convective motions occur spontaneously if required conditions fulfilled (all physics of convection 'naturally' included)

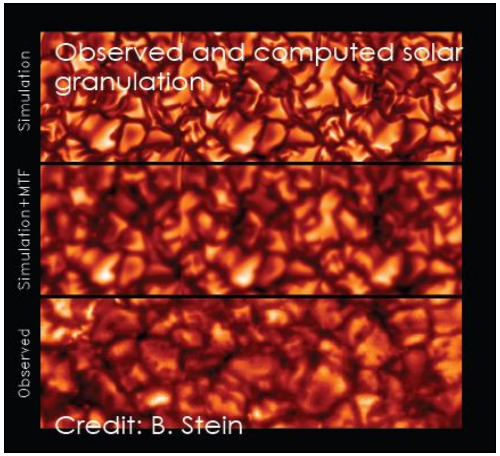

Surface Convection

Solar-type stars:
Photospheric extent << stellar radius
Small granulation patterns

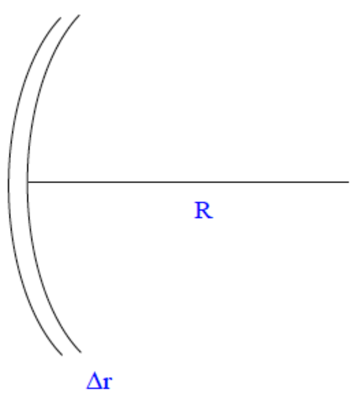

example: the sun

$R_{sun} \approx$ 700,000 km
Δr (photo) $\approx$ 300 km

=> $\Delta r / R \approx 4\ 10^{-4}$

BUT corona
$\Delta r / R$ (corona) ≈ 3

as long as $\Delta r / R << 1$ => plane-parallel symmetry

light ray through atmosphere

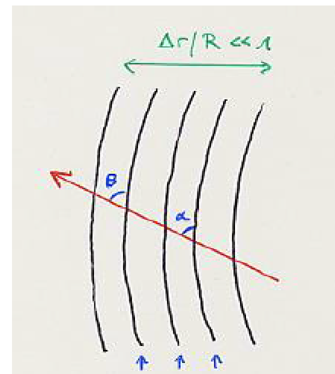

lines of constant temperature and density (isocontours)

curvature of atmosphere insignificant for photons' path : $\alpha = \beta$

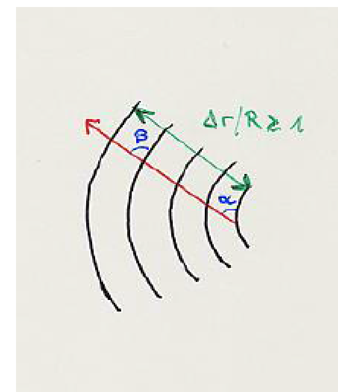

significant curvature : $\alpha \neq \beta$, spherical symmetry

examples

solar photosphere / cromosphere	solar corona
atmospheres of	atmospheres of
main sequence stars	supergiants
white dwarfs	expanding envelopes (stellar winds)
giants (partly)	of OBA stars, M-giants and supergiants

from part 1

Surface Convection

Solar-type stars:
Atmospheric extent << stellar radius
Small granulation patterns

→

Box-in-a-star Simulations

(cmp. plane-parallel approximation)

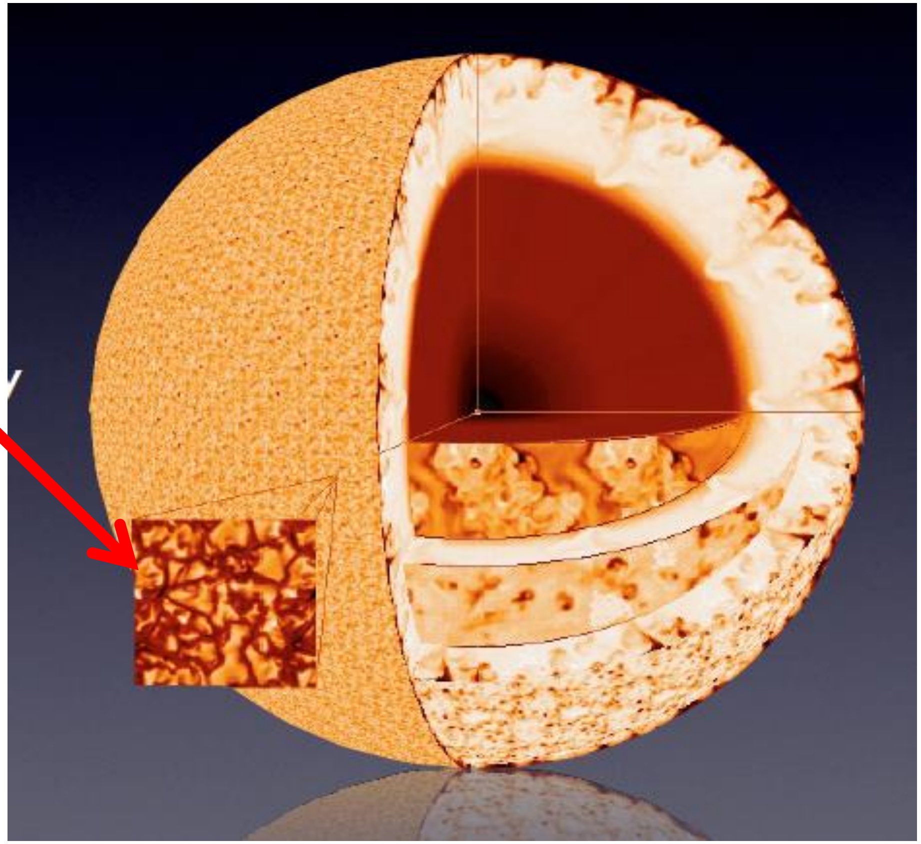

From Wolfgang Hayek

Surface Convection

Approach
(teams by Nordlund, Steffen):

Solve radiation-hydrodynamical conservation equations of mass, momentum, and energy (closed by equation of state).

3-D radiative transfer included to calculate net radiative heating/cooling q_{rad} in energy equation, typically assuming LTE and a very simplified treatment of line-blanketing

$$q_{\mathrm{rad}} = 4\pi\rho \int_\lambda \kappa_\lambda (J_\lambda - S_\lambda)\, d\lambda,$$

(= 0 in case of radiative equilibrium)

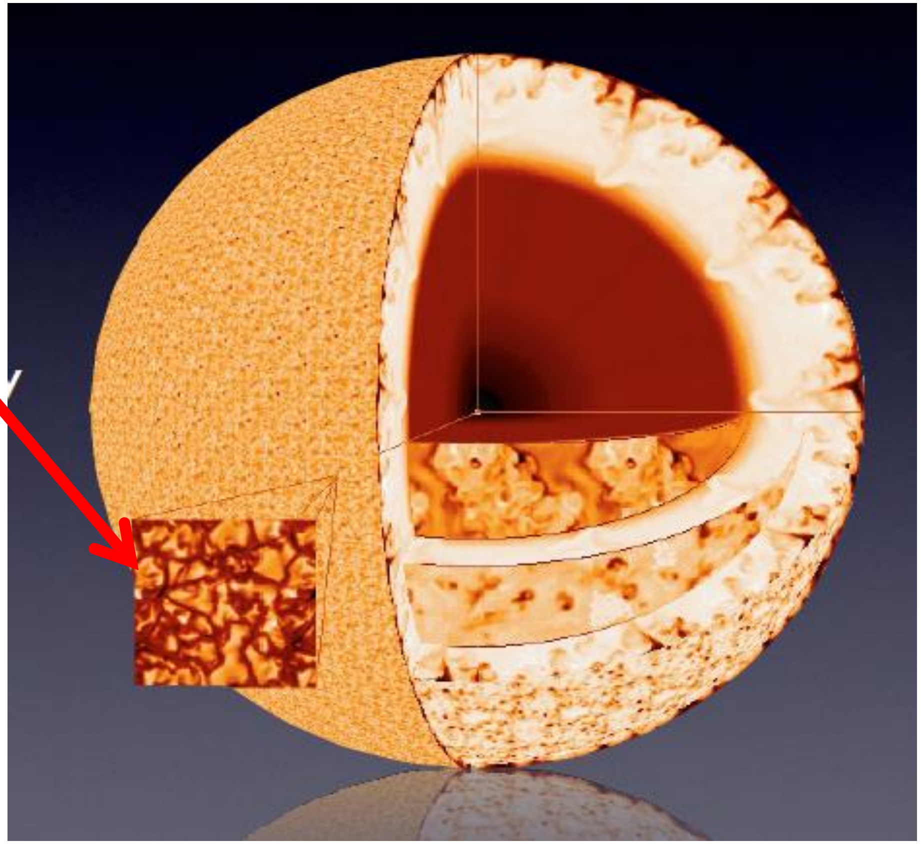

From Wolfgang Hayek

Surface Convection

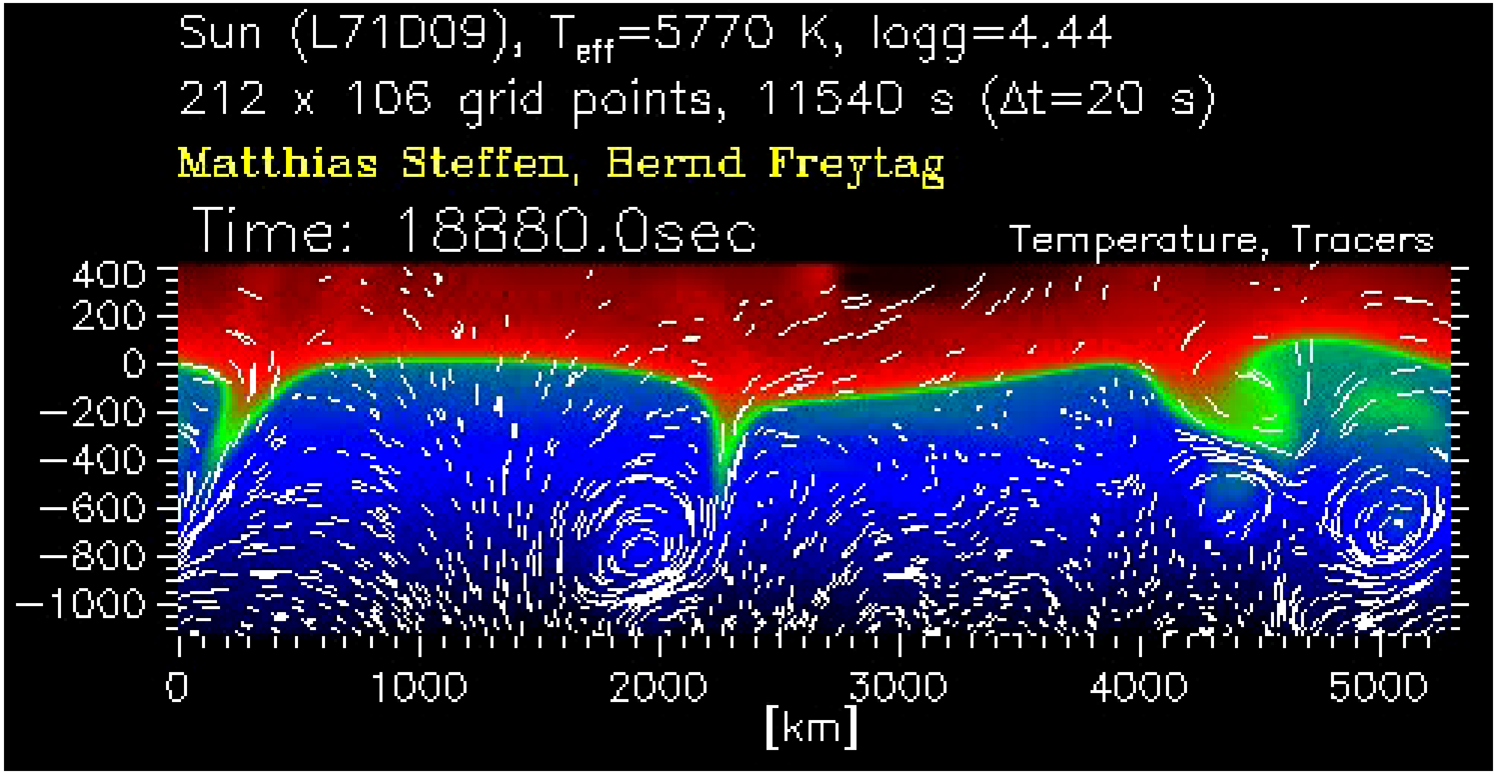

From Berndt Freytag's homepage: http://www.astro.uu.se/~bf/

Surface Convection

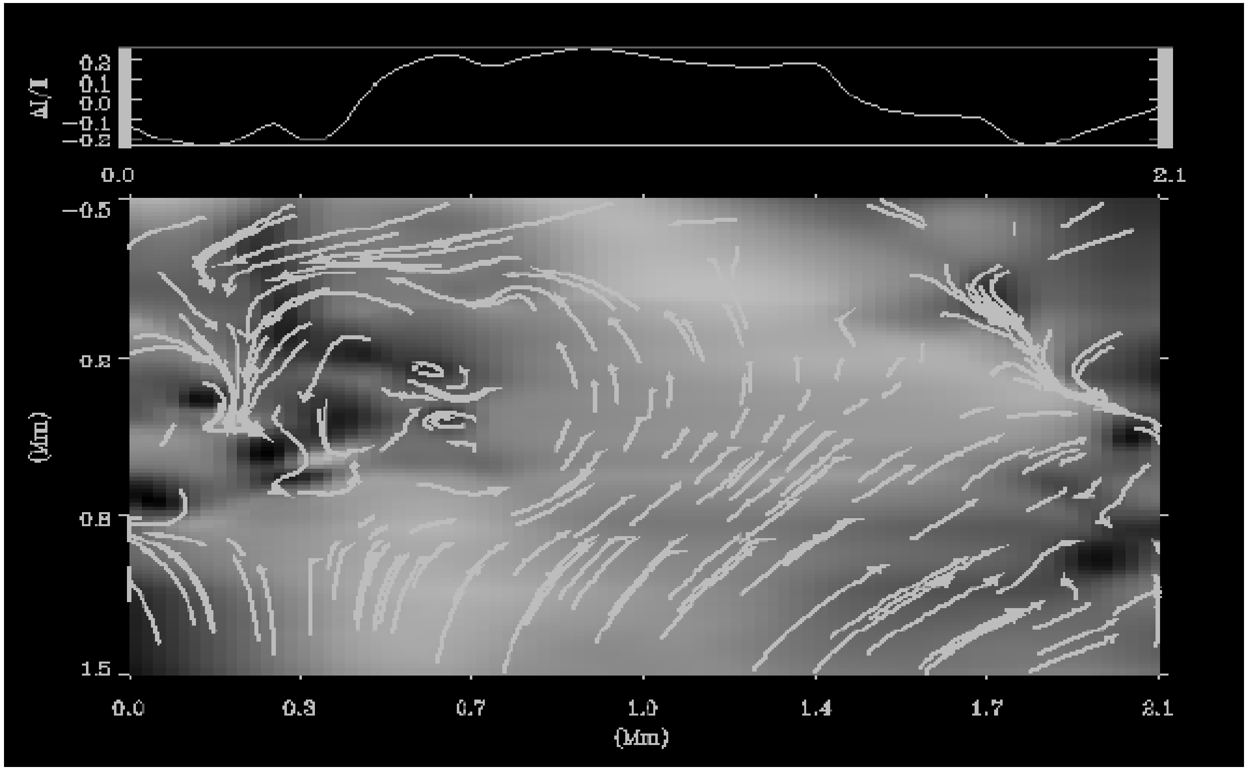

FIG. 4.—Pressure fluctuations about the mean hydrostatic equilibrium and the velocity field in an xz slice through a granule. The pressure is high above the centers of granules, which decelerates the warm upflowing fluid and diverts it horizontally. High pressure also occurs in the intergranular lanes where the horizontal motions are halted and gravity pulls the now cool, dense fluid down into the intergranular lanes. Horizontal rolls of high vorticity occur at the edges of the intergranular lanes. The emergent intensity profile across the slice is shown at the top.

From Stein & Nordlund (1998)

Surface Convection

Some key features:

Slow, broad upward motions, and faster, thinner downward motions
Non-thermal velocity fields
Overshooting from zone where convection is efficient according to stability criteria (see part 1)
Energy balance in upper layers not only controlled by radiative heating/cooling, but also by cooling from adiabatic expansion

See Stein & Nordlund (1998); Collet et al. (2006), etc

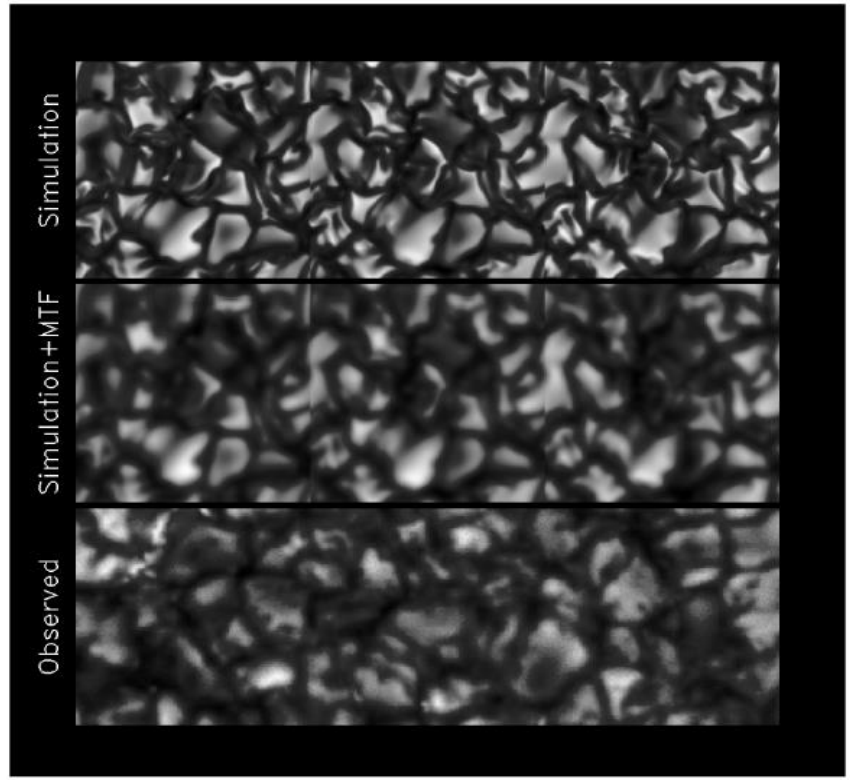

FIG. 19.—Comparison of granulation as seen in the emergent intensity from the simulations and as observed by the Swedish Vacuum Solar Telescope on La Palma. The top row shows three simulation images at 1 minute intervals, which together make a composite image 18 × 6 Mm in extent. The middle row shows this image smoothed by an Airy plus exponential point-spread function. The bottom row shows an 18 × 6 Mm white-light image from La Palma. Note the similar appearance of the smoothed simulation image and the observed granulation. The common edge brightening in the simulation is reduced when smoothed. Images by (Title 1996, private communication) taken in the CH G-band have much more contrast than white light and clearly reveal the edge brightening of granules.

Question: This does not look much like the traditional 1-D models we've discussed during the previous lecture! – Do you think we should throw them in the garbage?

Surface Convection

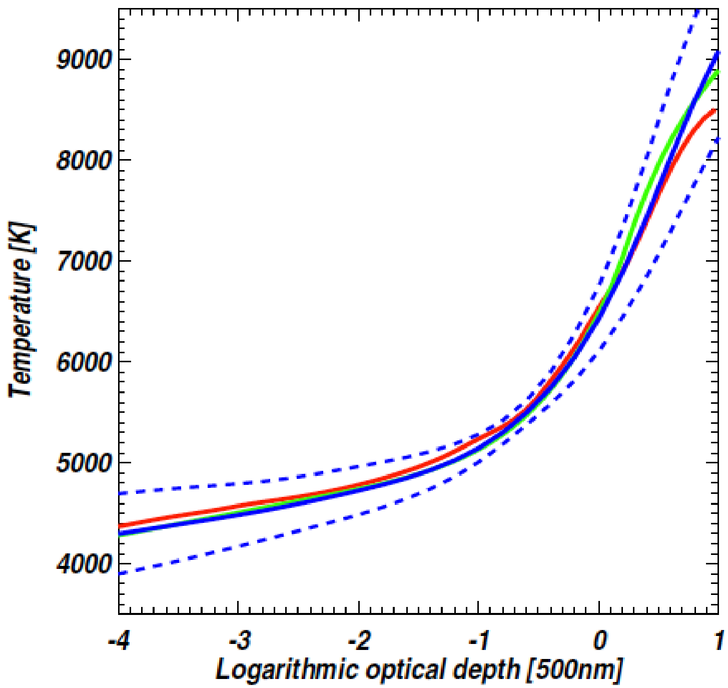

Figure 1: The mean temperature structure of the 3D hydrodynamical model of Trampedach et al. (2009) is shown as a function of optical depth at 500 nm (blue solid line). The blue dashed lines correspond to the spatial and temporal rms variations of the 3D model, while the red and green curves denote the 1D semi-empirical Holweger & Müller (1974) and the 1D theoretical MARCS (Gustafsson et al. 2008) model atmospheres, respectively.

In many (though not all) cases, AVERAGE properties still quite OK:

Convection in energy balance approximated by "mixing-length theory"
Non-thermal velocity fields due to convective motions included by means of so-called "micro-" and "macro-turbulence"

BUT quantitatively we always need to ask:
To what extent can average properties be modeled by traditional 1-D codes?

Unfortunately, a general answer very difficult to give, need to be considered case by case

Surface Convection

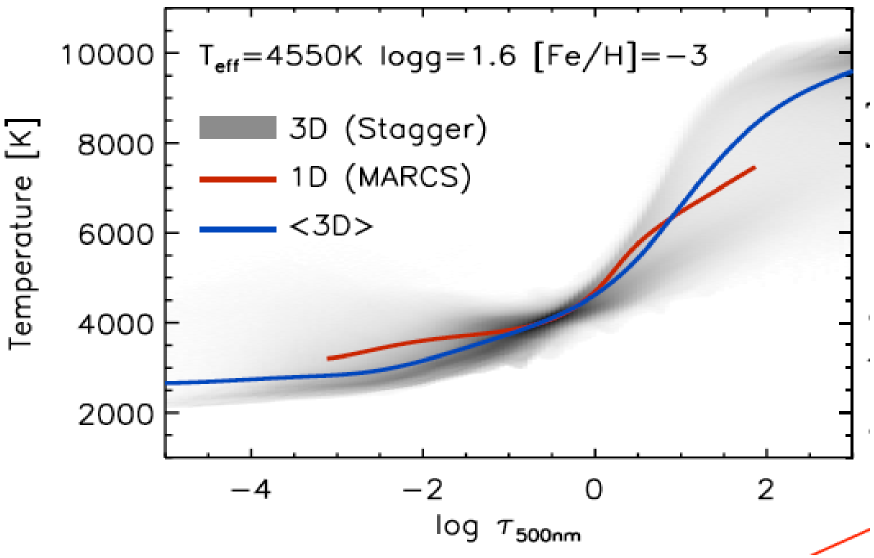

Metal-poor red giant, simulation by Remo Collet, figure from talk by M. Bergemann

For example:

In metal-poor cool stars spectral lines are scarce (Question: Why?), and energy balance in upper photosphere controlled to a higher degree by adiabatic expansion of convectively overshot material.

In classical 1-D models though, these layers are convectively stable, and energy balance controlled only by radiation (radiative equilibrium, see part1).

Surface Convection

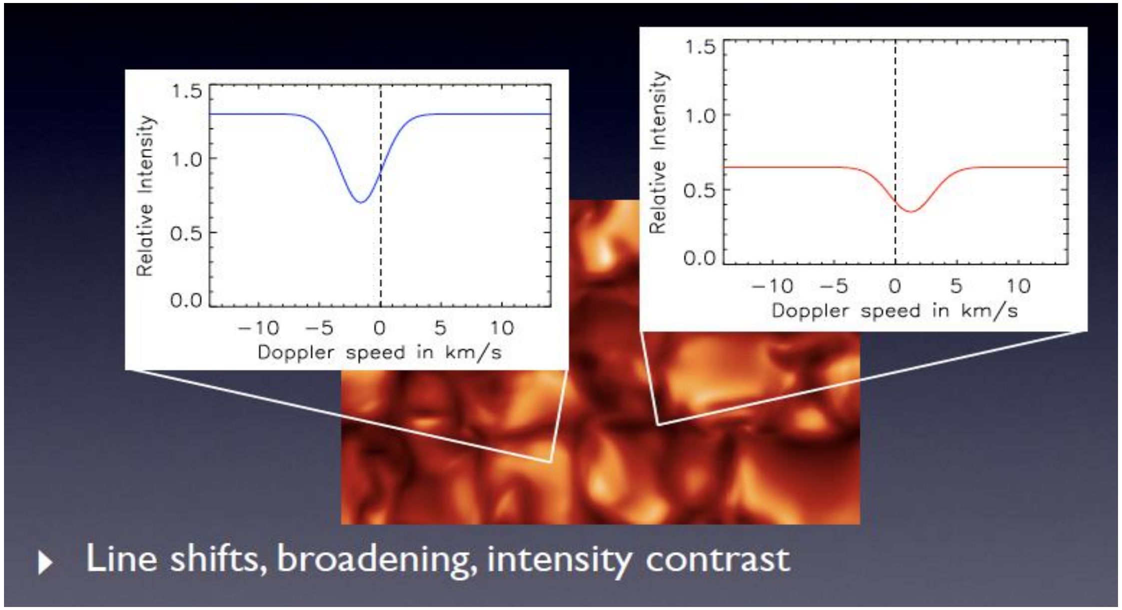

From talk by Hayek

3-D radiation-hydro models successful in reproducing many solar features (see overview in Asplund et al. 2009), e.g:

Center-to-limb intensity variation

Line profiles and their shifts and variations (without micro/macroturbulence)

Observed granulation patterns

Surface Convection

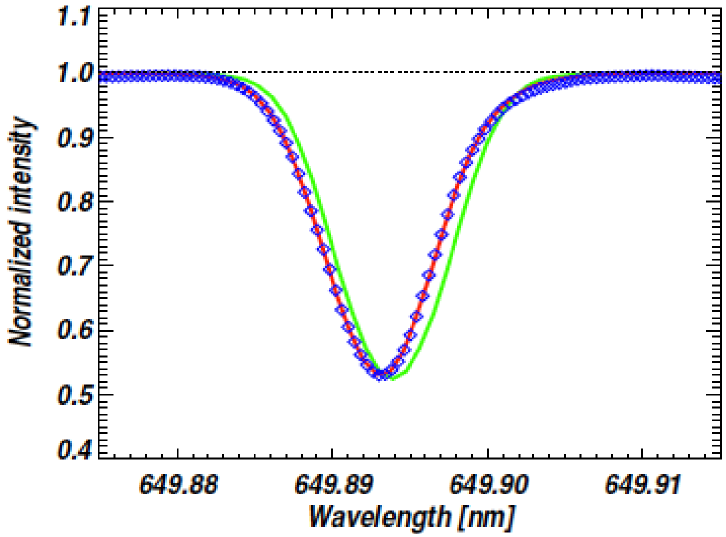

Figure 3: The predicted spectral line profile of a typical Fe I line from the 3D hydrodynamical solar model (red solid line) compared with the observations (blue rhombs). The agreement is clearly very satisfactory, which is the result of the Doppler shifts arising from the self-consistently computed convective motions that broaden, shift and skew the theoretical profile. For comparison purposes also the predicted profile from a 1D model atmosphere (here Holweger & Müller 1974) is shown; the 1D profile has been computed with a microturbulence of 1 km s^{-1} and a tuned macroturbulence to obtain the right overall linewidth. Note that even with these two free parameters the 1D profile can neither predict the shift nor the asymmetry of the line.

affects chemical abundance (determined by means of line profile fitting to observations)

One MAJOR result:
Effects on line formation has led to a downward revision of the CNO solar abundances and the solar metallicity, and thus to a revision of the *standard cosmic chemical abundance scale*

Fig. from Asplund et al. (2009) – "The Chemical Composition of the Sun"

Surface Convection

Also potentially critical for Galactic archeology…

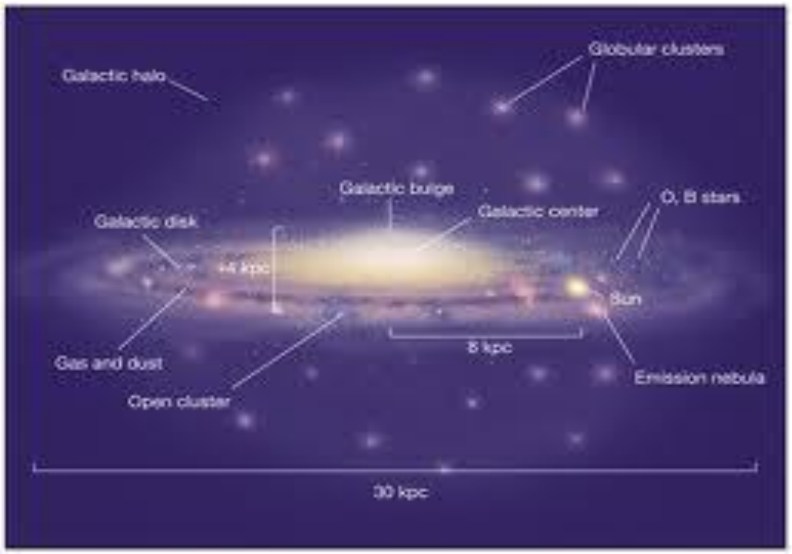

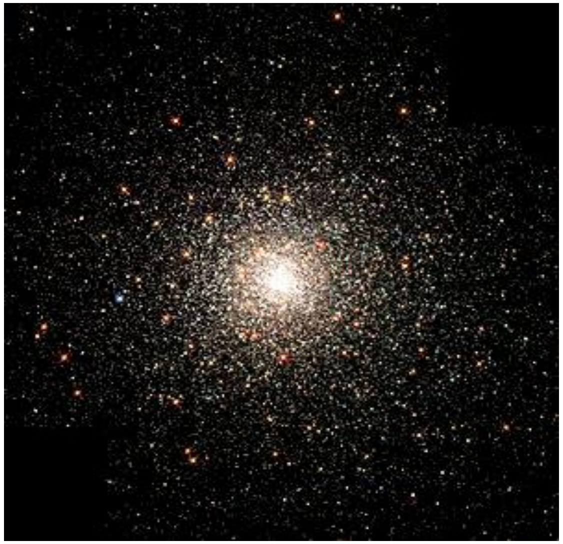

…which traces the chemical evolution of the Universe by analyzing VERY old, metal-poor Globular Cluster stars –- relics from the early epochs (e.g. Anna Frebel and collaborators)

Surface Convection

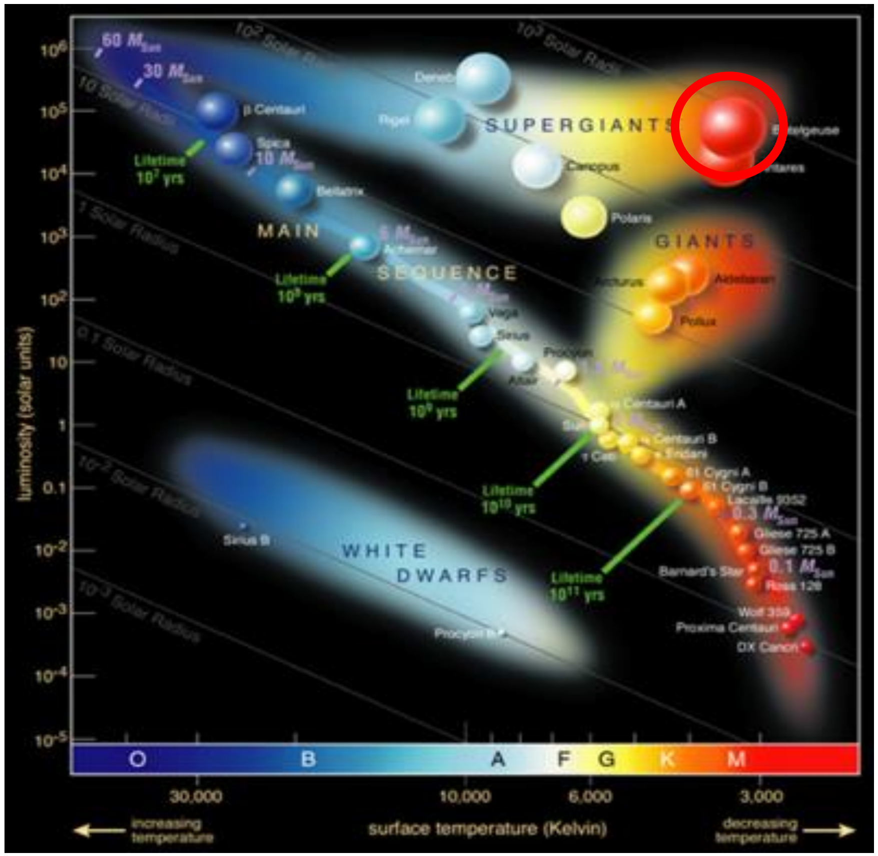

- Giant Convection Cells in the low-gravity, extended atmospheres of Red Supergiants
- Question: Why extended?

$H = a^2 / g$ (with a the isothermal speed of sound)

$a^2_{RSG} / a^2_{sun} \approx T_{RSG} / T_{sun} = 0.5 \ldots 0.6$

$g_{RSG} / g_{sun} \approx 10^{-4}$!

(see part 1)

Out to Jupiter…

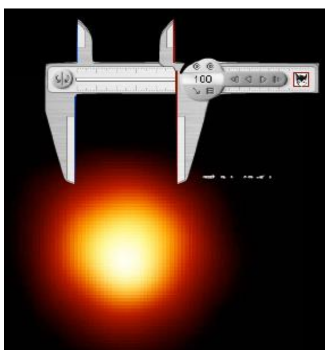

Betelgeuse (HST)
Gilliland & Dupree 1996

Surface Convection

Supergiants (or models including a stellar wind):
Atmospheric extent > stellar radius:

Box-in-a-star → Star-in-a-box

(1D: Plane-parallel → Spherical symmetry, see part 1)

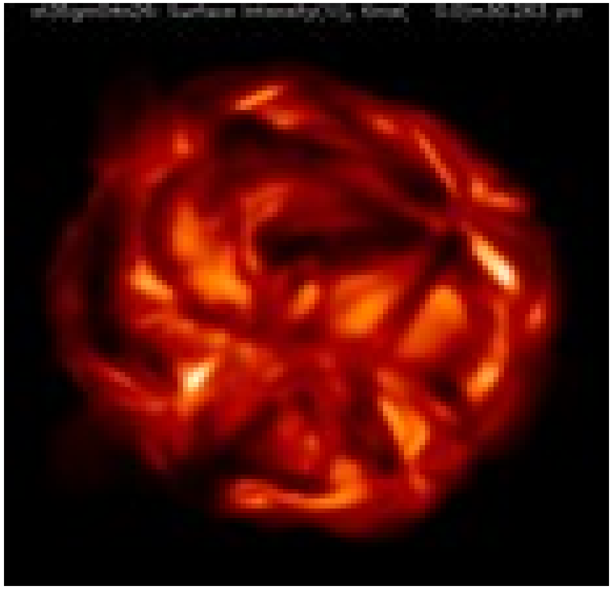

Star to model: Betelgeuse
Mass: 5 solar masses
Radius: 600 Rsun
Luminosity: 41400 Lsun
Grid: Cartesian cubical grid with 171^3 points
Edge length of box 1674 solar radii

Model by Berndt Freytag, note the HUGE convective cells visible in the emergent intensity map!!

Surface Convection

Star to model: Betelgeuse
Mass: 5 solar masses
Radius: 600 Rsun
Luminosity: 41400 Lsun
Grid: Cartesian cubical grid with 171^3 points
Edge length of box 1674 solar radii
Movie time span: 7.5 years

http://www.astro.uu.se/~bf/movie/dst35gm04n26/movie.html

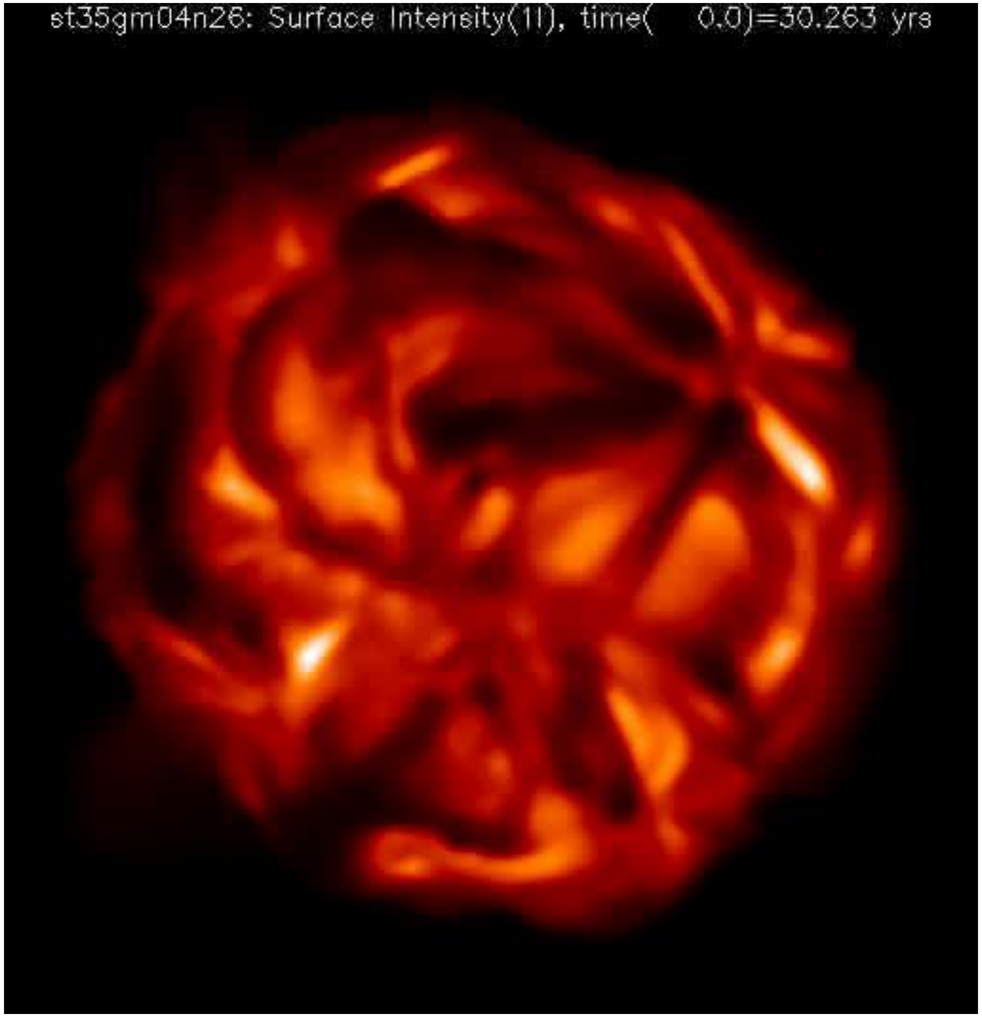

Surface Convection

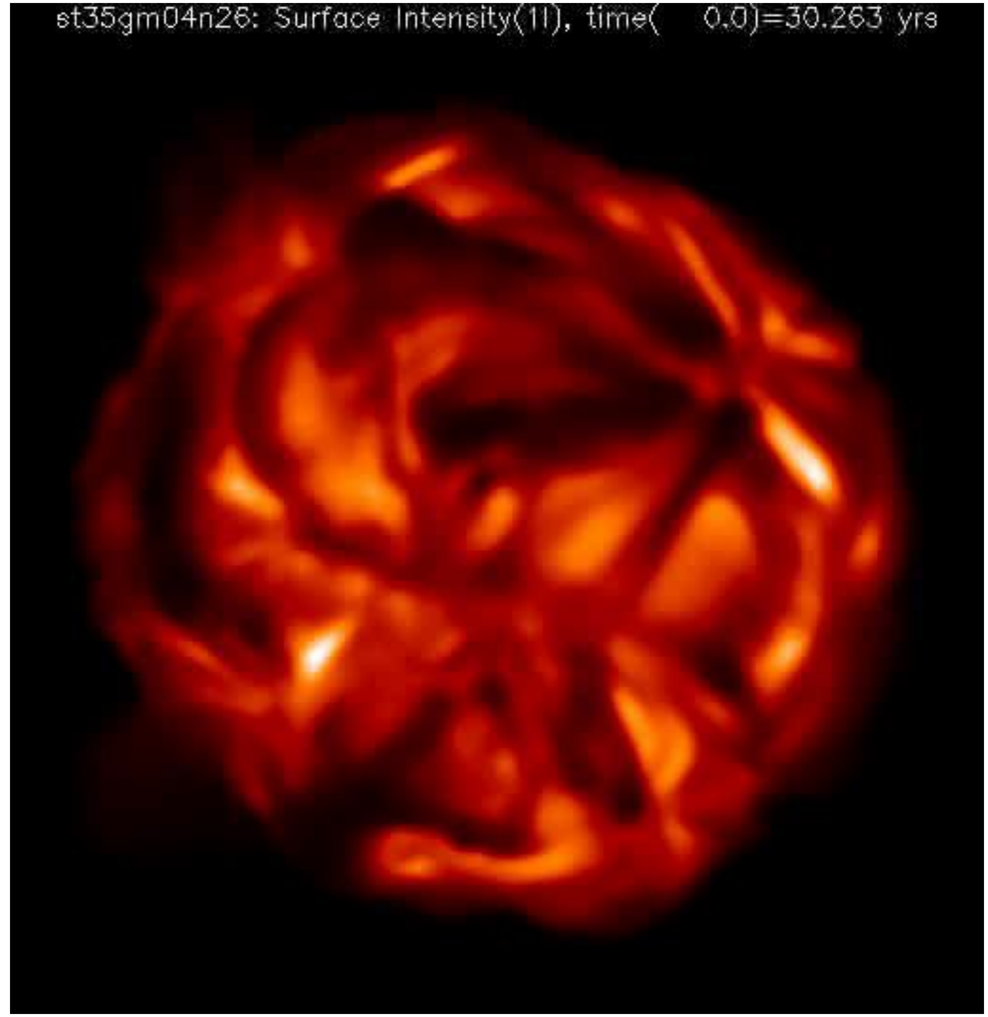

Extremely challenging,
models still in their infancies.
LOTS of exciting physics to explore, like

Pulsations
Convection
Numerical radiation-hydrodynamics
Role of magnetic fields
Stellar wind mechanisms

Also, to what extent can main effects be captured by 1-D models?
For quantitative applications like….

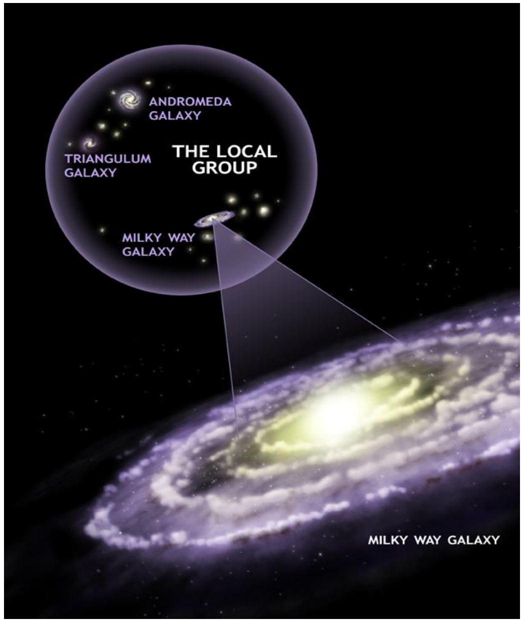

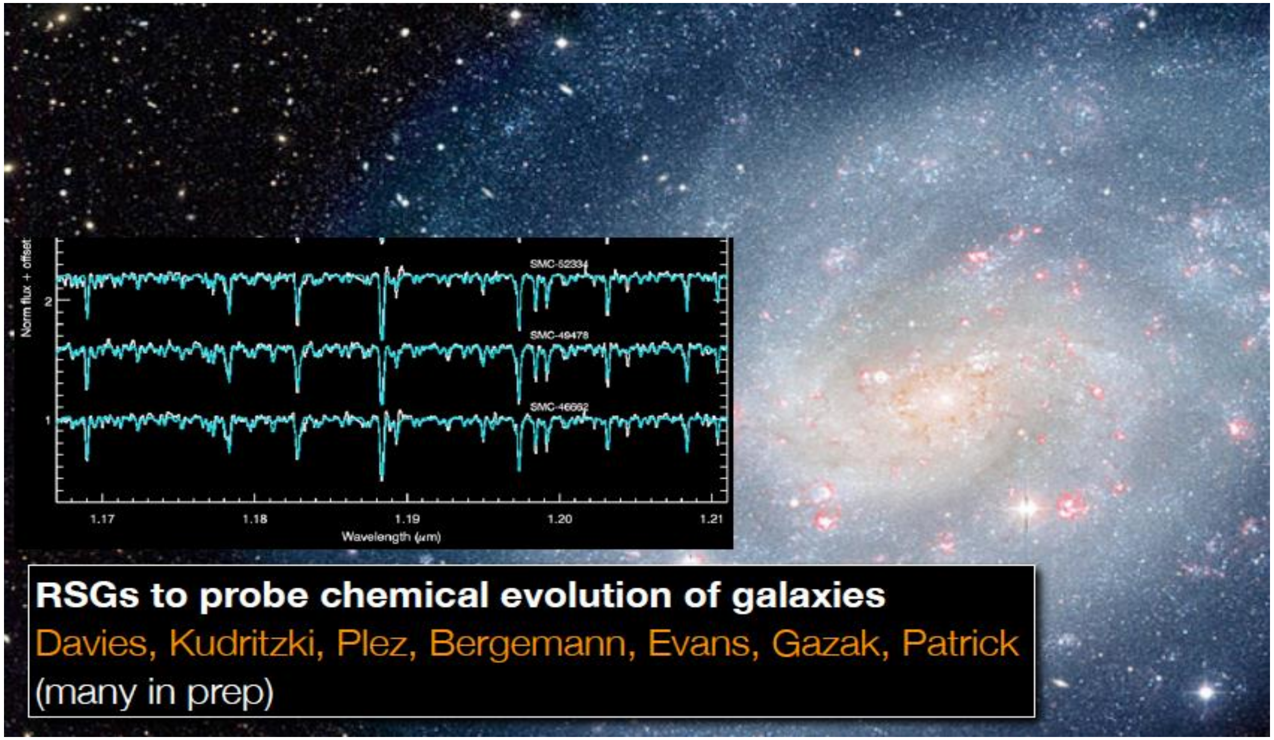

Question: Why are RSGs ideal for
extragalactic observational stellar astrophysics
using new generations of extremely large infra-red telescopes?

important codes and their features ….

Codes	FASTWIND CMFGEN PoWR	WM-basic	TLUSTY Detail/Surface	Phoenix	MARCS Atlas	CO5BOLD STAGGER
geometry	1-D spherical	1-D spherical	1-D plane-parallel	1-D/3-D spherical/ plane-parallel	1-D plane-parallel (MARCS also spherical)	3-D Cartesian
LTE/NLTE	NLTE	NLTE	NLTE	NLTE/LTE	LTE	LTE simplified
dynamics	quasi-static photosphere + prescribed supersonic outflow	time-independent hydrodynamics	hydrostatic	hydrostatic or allowing for supersonic outflows	hydrostatic	hydrodynamic
stellar wind	yes	yes	no	yes	no	no
major application	hot stars with winds	hot stars with dense winds, ion. fluxes, SNRs	hot stars with negligible winds	cool stars, brown dwarfs, SNRs	cool stars	cool stars
comments	CMFGEN also for SNRs; FASTWIND using approx. line-blocking	line-transfer in Sobolev approx. (see part 2)	Detail/Surface with LTE-blanketing	convection via mixing-length theory	convection via mixing-length theory	very long execution times, but model grids start to emerge

And then there are, e.g.,

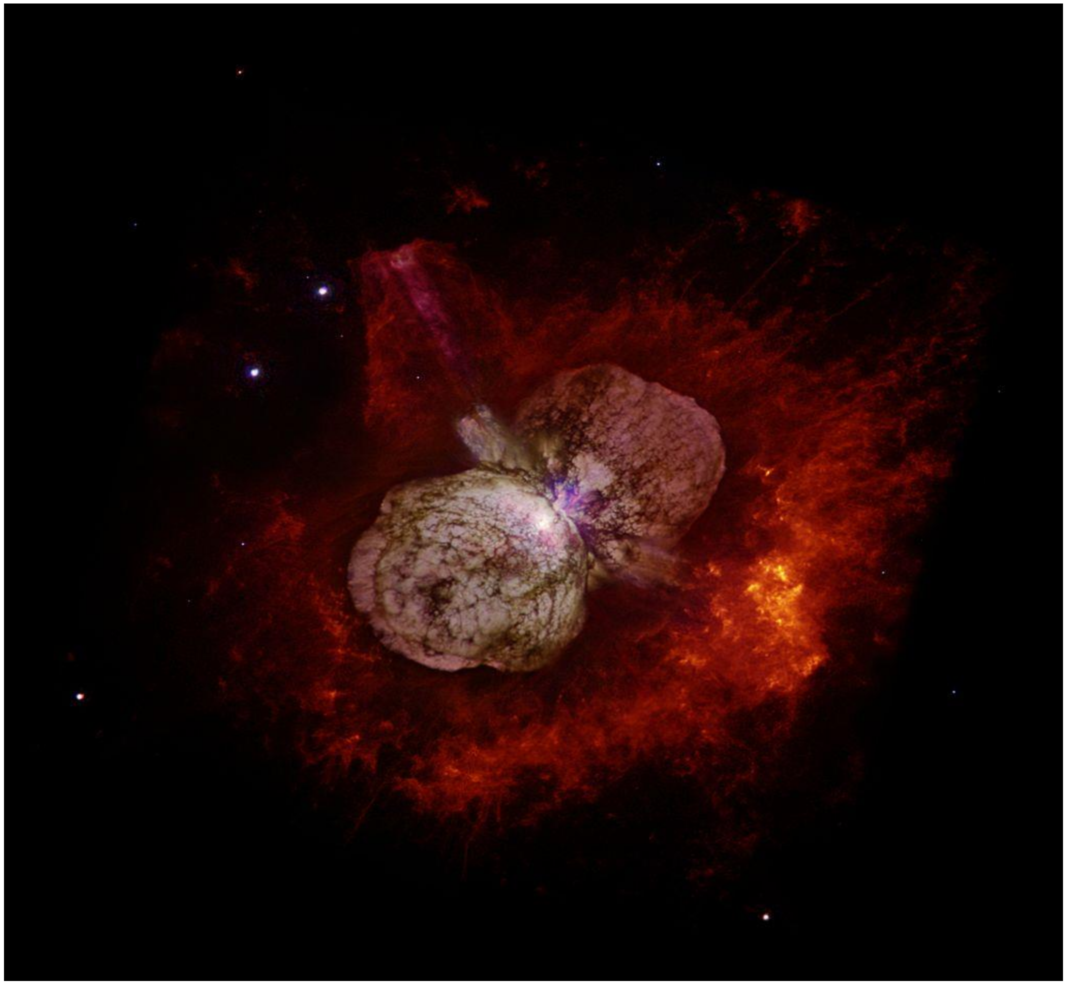

- Luminous Blue Variables (LBVs) like Eta Carina,
- Wolf-Rayet Stars (WRs)
- Planetary Nebulae (and their Central Stars)
- Be-stars with disks
- Brown Dwarfs
- Pre main-sequence T-Tauri and Herbig stars

…and many other interesting objects

Stellar astronomy alive and kicking! Very rich in both

Physics
Observational applications

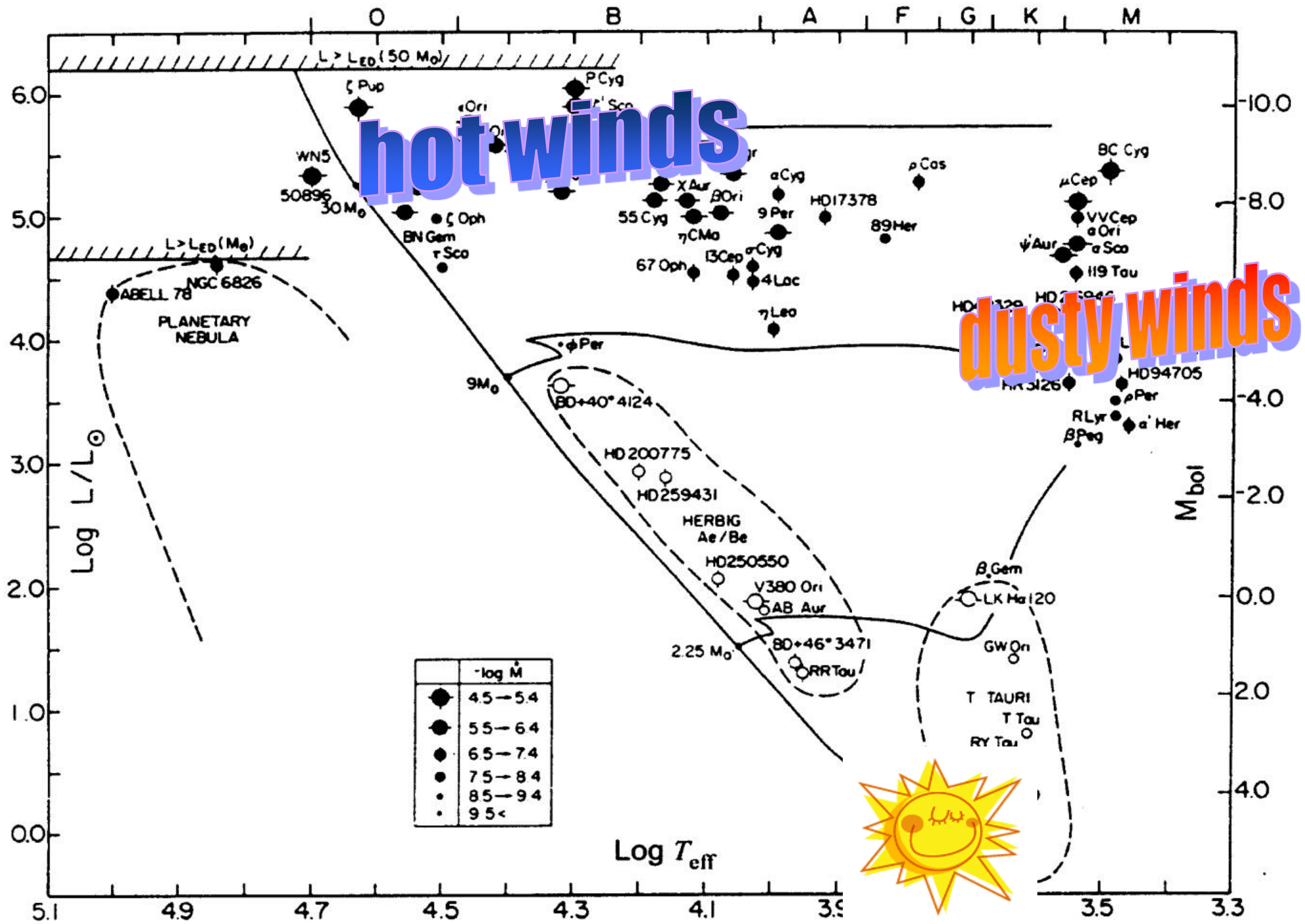

ubiquitous phenomenon

- solar type stars (incl. the sun)
- red supergiants/AGB-stars ("normal" + Mira Variables)
- hot stars (OBA supergiants, Luminous Blue Variables, OB-dwarfs, Central Stars of PN, sdO, sdB, Wolf-Rayet stars)
- T-Tauri stars
- and many more

The solar wind – a suspicion

comet Halley,
with „kink“ in
tail

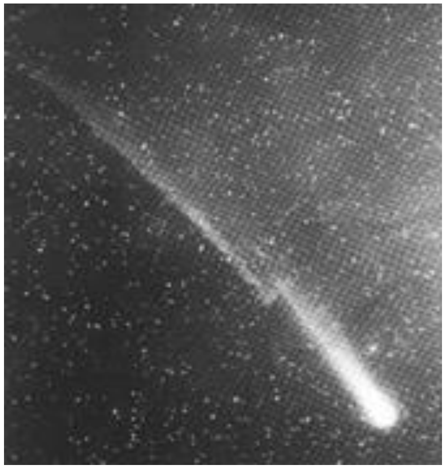

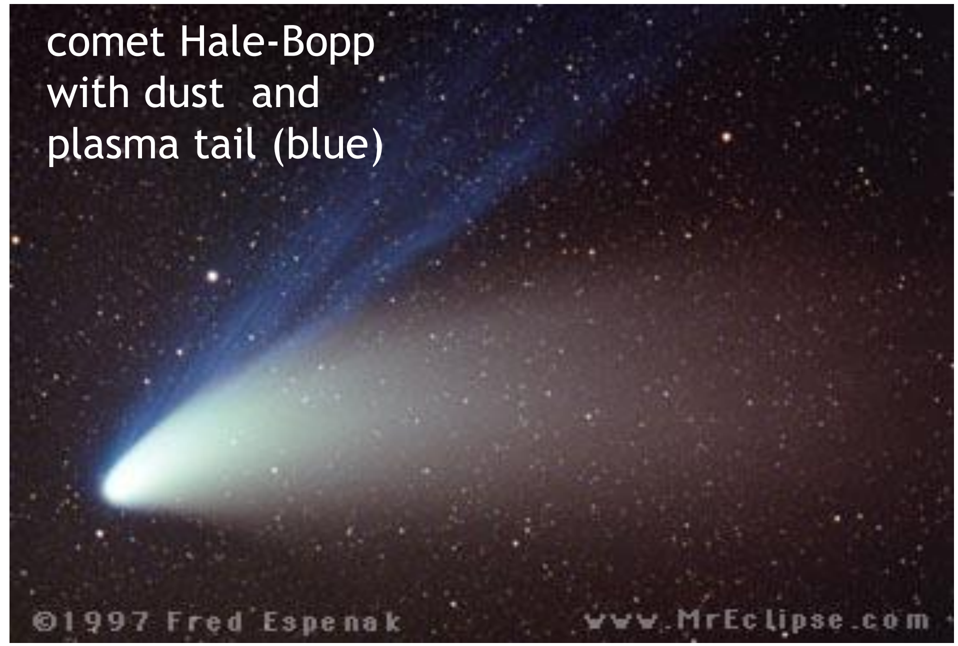

comet Hale-Bopp
with dust and
plasma tail (blue)

- comet tails *directed away from the sun*
- **Kepler:** influence of solar radiation pressure (-> radiation driven winds)
- *Ionic tail*: emits own radiation, sometimes different direction
- **Hoffmeister** (1943, subsequently Biermann): *solar particle radiation* different direction, since **v** (particle) comparable to **v** (comet)

The solar wind – the discovery

- **Eugene Parker (1958):** theoretical(!) investigation of coronal equilibrium:
  high temperature leads to (solar) wind (more detailed later on)
- **confirmed by**
  - Soviet measurements (Lunik2/3) with “ion-traps” (1959)
  - Explorer 10 (1961)
  - Mariner II (1962): measurement of fast and slow flows
    (27 day cycle -> co-rotating, related “coronal holes” and sun spots)

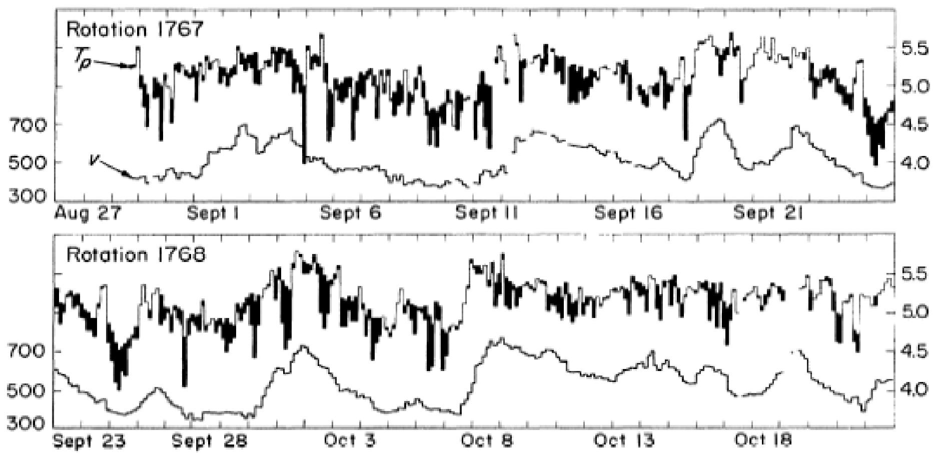

The solar wind – Ulysses ...

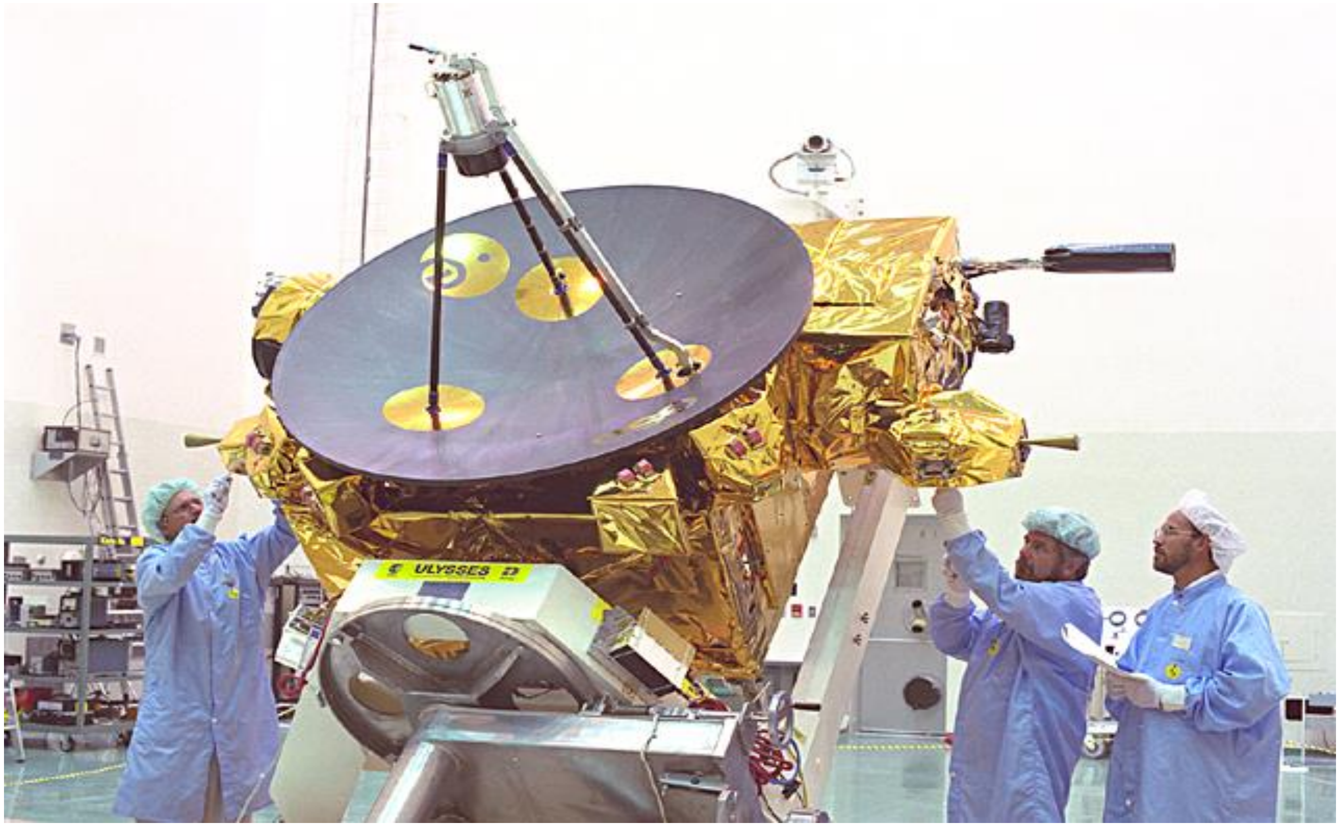

… surveying the polar regions

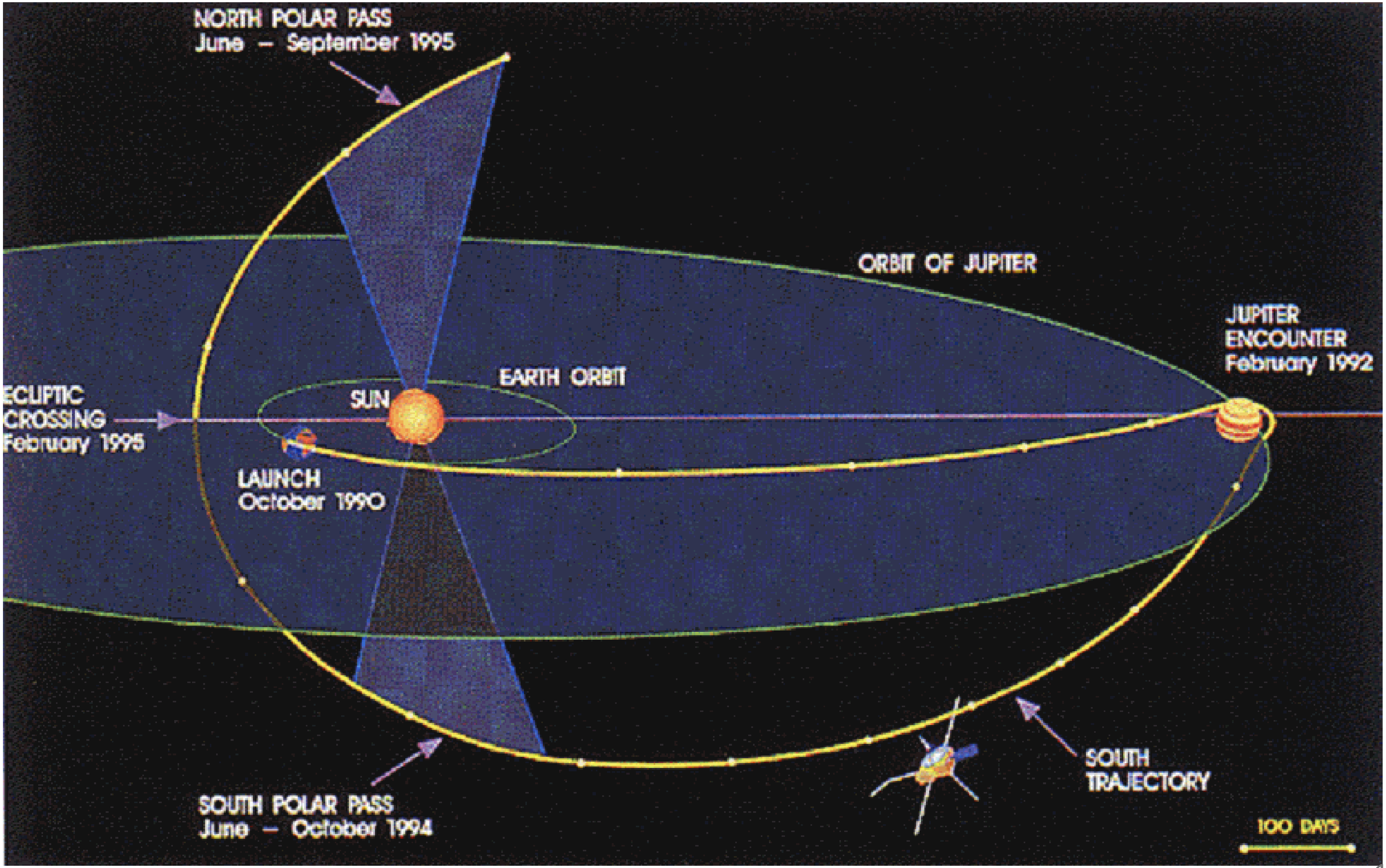

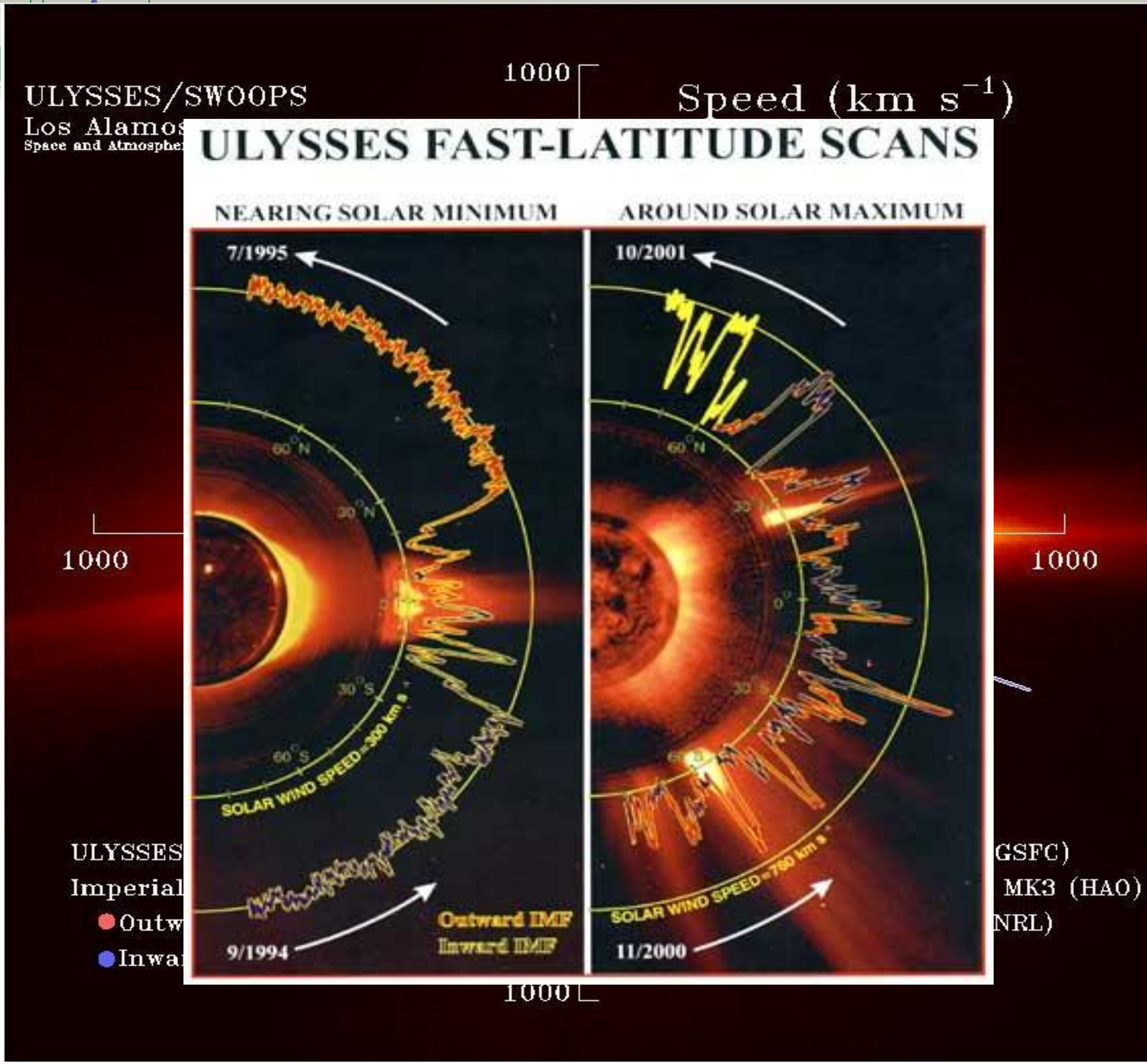

polar wind:
fast and thin

equatorial wind:
slow and dense

The solar wind – coronal holes

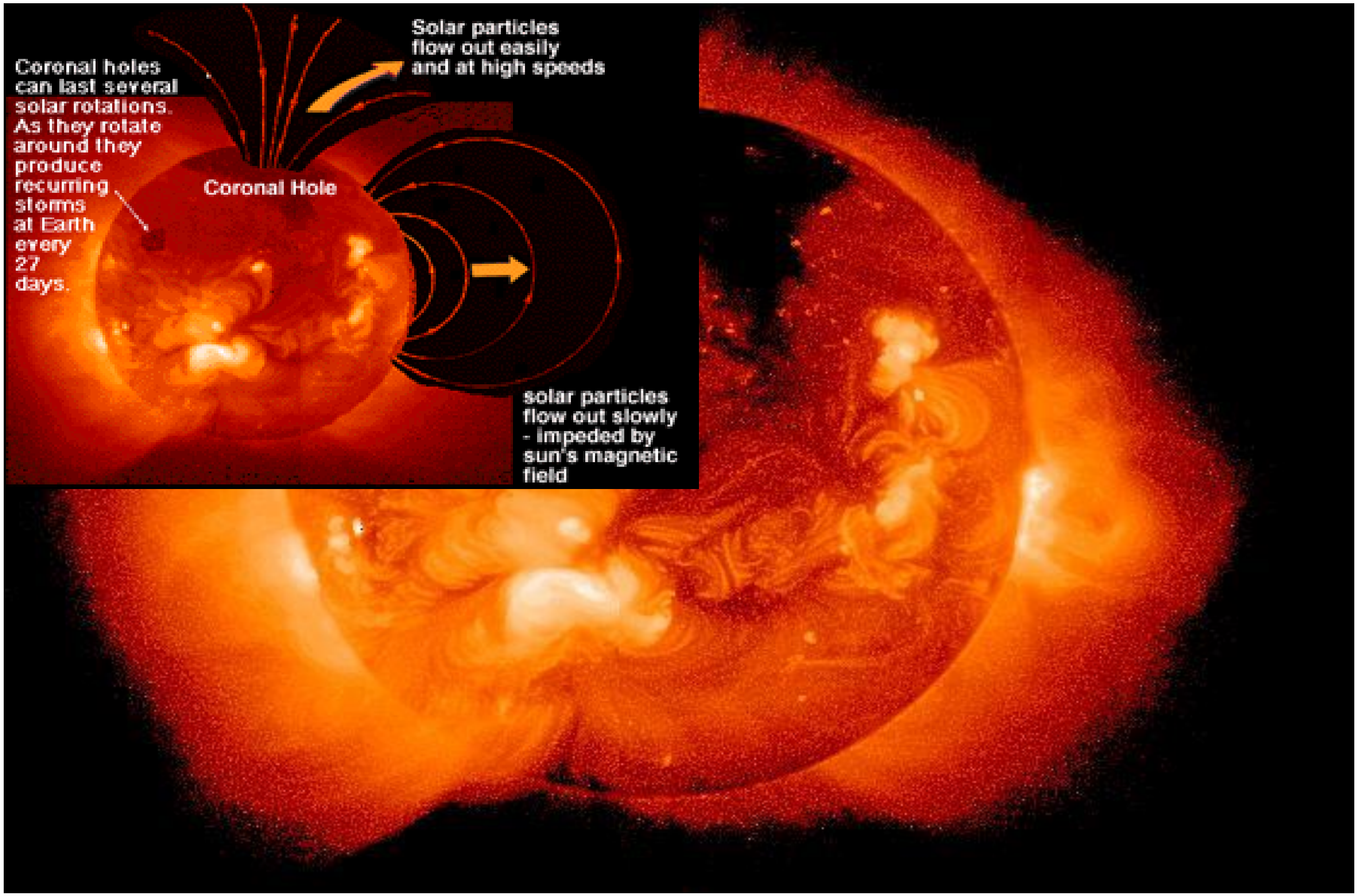

fast wind:
over coronal holes (dark corona, "open" field lines, e.g., in polar regions)

coronal X-ray emission

⇒

very high temperatures

(Yohkoh Mission)

The sun and its wind: mean properties

The sun

radius = 695,990 km = 109 terrestrial radii
mass = 1.989 10^{30} kg = 333,000 terrestrial masses
luminosity = 3.85 10^{33} erg/s = 3.85 10^{20} MW ≈ 10^{18} nuclear power plants
effective temperature = 5770 °K
central temperature = 15,600,000 °K
life time approx. 10 10^9 years
age = 4.57 10^9 years
distance sun earth approx. 150 10^6 km ≈ 400 times earth-moon

The solar wind

temperature when leaving the corona: approx.1 10^6 K
average speed approx. 400-500 km/s (travel time sun-earth approx. 4 days)
particle density close to earth: approx. 6 cm^{-3}
temperature close to earth: $\lesssim 10^5$ K
mass-loss rate: approx 10^{12} g/s (1 Megaton/s) ≈ 10^{-14} solar masses/year
≈ one Great-Salt-Lake-mass/day ≈ one Baltic-sea-mass/year
⇒ no consequence for solar evolution, since only 0.01% of total mass lost over total life time

Stellar winds – hydrodynamic description

Need mechanism which accelerates material beyond escape velocity:

- **pressure** driven winds
- **radiation** driven winds

Note: red giant winds still not understood,
only scaling relations available ("Reimers-formula")

remember equation of motion (conservation of momentum + stationarity, cf. Chap. 6, p. 84)

$$v\frac{dv}{dr} = -\frac{1}{\rho}\frac{dp}{dr} + g^{ext} \quad \text{(in spherical symmetry)}$$

$\Rightarrow$ With mass-loss rate $\dot{M}$, radius r, density ρ and velocity v

$$\dot{M} = 4\pi r^2 \rho v,$$

equation of continuity:
conservation of mass

and with isothermal sound-speed a

$$\left(1-\frac{a^2}{v^2}\right)v\frac{dv}{dr} = -\frac{GM}{r^2} + g_{rad} + \frac{2a^2}{r} - \frac{da^2}{dr}$$

equation of motion:
from conservation of momentum

vel. field	grav. accel.	radiative accel.	(part of) accel. by pressure gradient
positive for v > a **negative** for v < a	inwards	outwards	outwards

Pressure driven winds

$$\left(1-\frac{a^2}{v^2}\right)v\frac{dv}{dr} = -\frac{GM}{r^2} + \cancel{g_{rad}} + \frac{2a^2}{r} - \cancel{\frac{da^2}{dr}}$$

vel. field — grav. accel. — radiative accel. — pressure

The solar wind as a proto-type for pressure driven winds

- present in stars which have an (extremely) hot corona ($T \approx 10^6$ K)
- with $g_{rad} \approx 0$ and $T \approx$ const, the rhs of the equation of motion changes sign at

$$r_c = \frac{GM}{2a^2}; \quad \text{with } a\,(T=1.5\cdot 10^6\ \text{K}) \approx 160\ \text{km/s},$$

we find for the sun $r_c \approx 3.9\,R_{sun}$

and obtain four possible solutions for v/v_c ("c" = critical point)

- only one (the "transonic") solution compatible with observations
- pressure driven winds as described here rely on the presence of a hot corona (large value of a!)
- Mass-loss rate $\dot{M} \approx 10^{-14}\ M_{sun}$ / yr, terminal velocity $v_\infty \approx 500$ km/s
- has to be heated (dissipation of acoustic and magneto-hydrodynamic waves)
- not completely understood so far

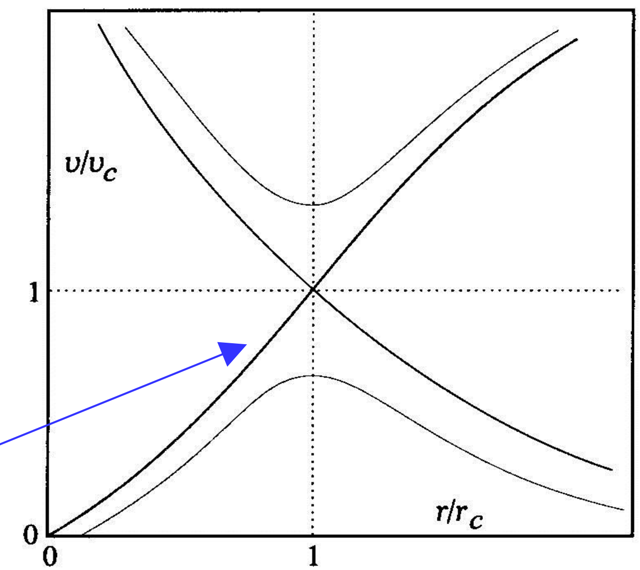

Radiation driven winds

accelerated by radiation pressure:

$$\left(1-\frac{a^2}{v^2}\right)v\frac{dv}{dr} = -\frac{GM}{r^2} + g_{rad} + \underbrace{\frac{2a^2}{r}-\frac{da^2}{dr}}_{\text{important only in lowermost wind}}$$

pressure terms only of secondary order
(a ≈ 20 km/s for hot stars,
≈ 3 km/s for cool stars)

- cool stars (AGB): major contribution from **dust** absorption;
  coupling to "gas" by viscous drag force (gas – grain collisions)

  $\dot{M} \approx 10^{-6} \mathrm{M_{sun}/yr}, \mathrm{v}_\infty \approx 20 \mathrm{~km/s}$

- hot stars: major contribution from **metal line** absorption;
  coupling to bulk matter (H/He) by Coulomb collisions

  $\dot{M} \approx 10^{-6} \ldots 10^{-5} \mathrm{M_{sun}/yr}, \mathrm{v}_\infty \approx 2{,}000 \mathrm{~km/s}$

dusty winds

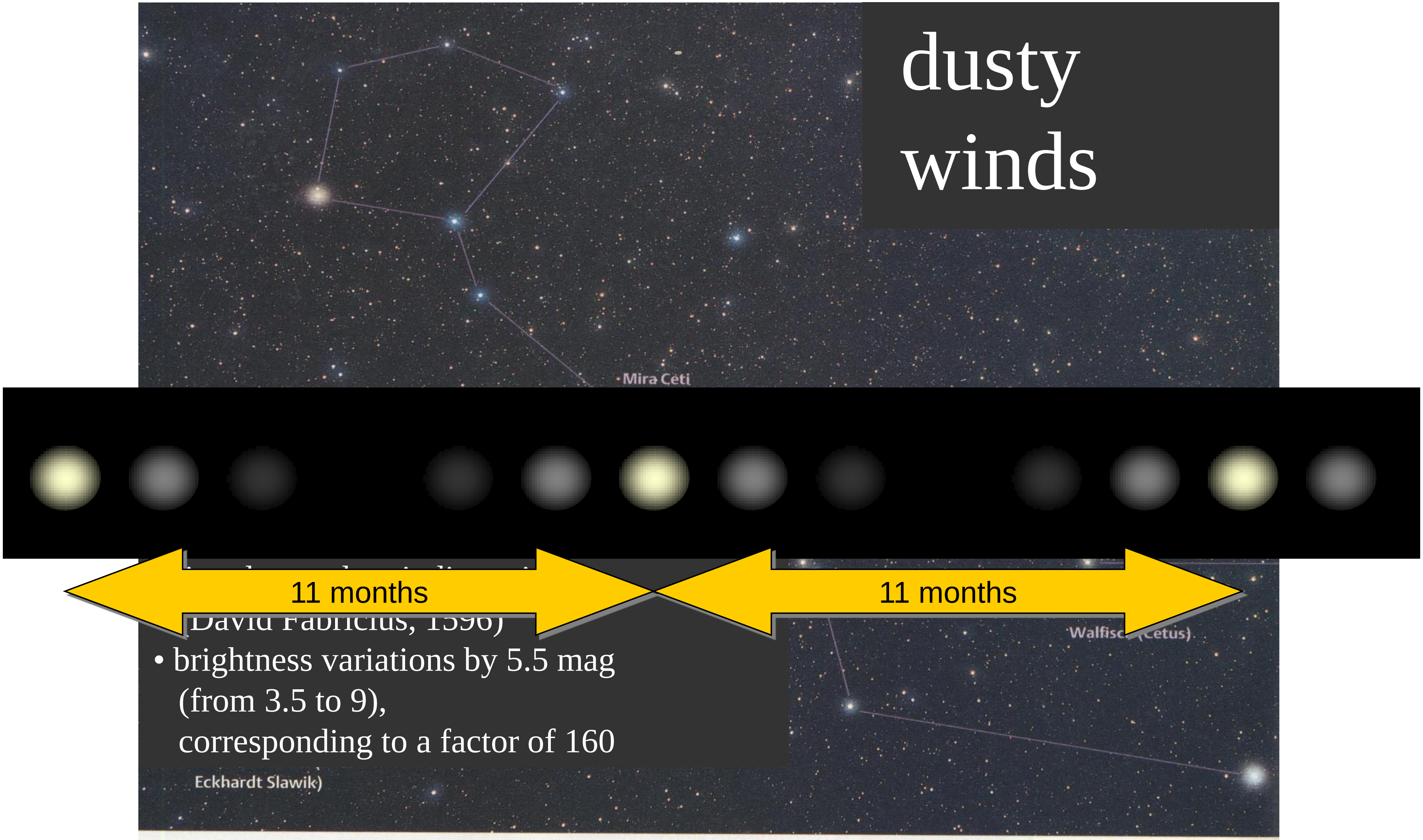

(David Fabricius, 1596)

- brightness variations by 5.5 mag (from 3.5 to 9), corresponding to a factor of 160

Cool supergiants: The dust-factories of our Universe

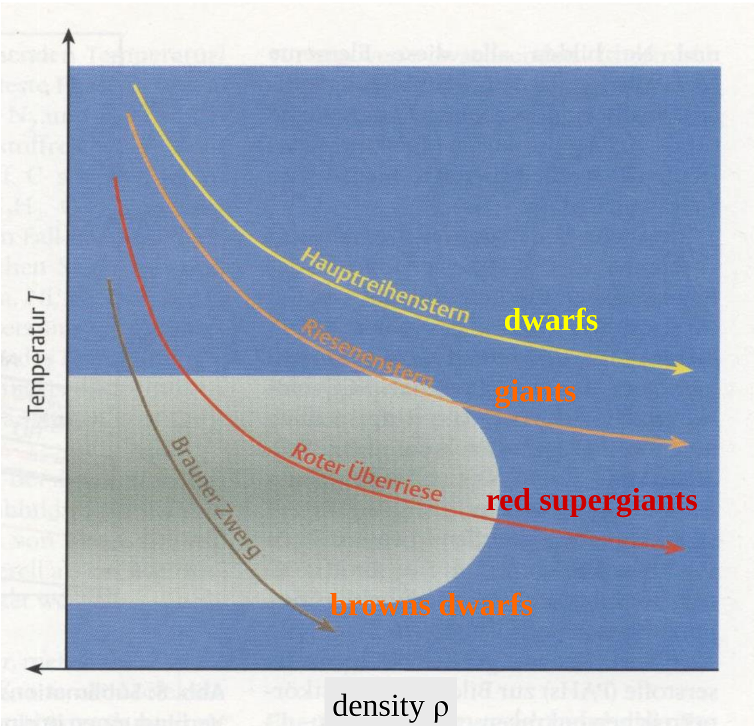

Material on this and following pages from Chr. Helling, *Sterne und Weltraum*, Feb/March 2002

dust: approx. 1% of ISM, 70% of this fraction formed in the winds of AGB-stars (cool, low-mass supergiants)

Red supergiants are located in dust-forming "window"

transition from gaseous phase to solid state possible only in **narrow range of temperature and density:**

gas density must be high enough and temperature low enough to allow for the chemical reactions:

- sufficient number of dust forming molecules required
- the dust particles formed have to be thermally stable

Growth of dust in matter outflow

- decrease of density and temperature
- more and more complex structures are forming
- dust: macroscopic, solid state body, approx. 10^{-7} m (1000 Angstrom), 10^9 atoms

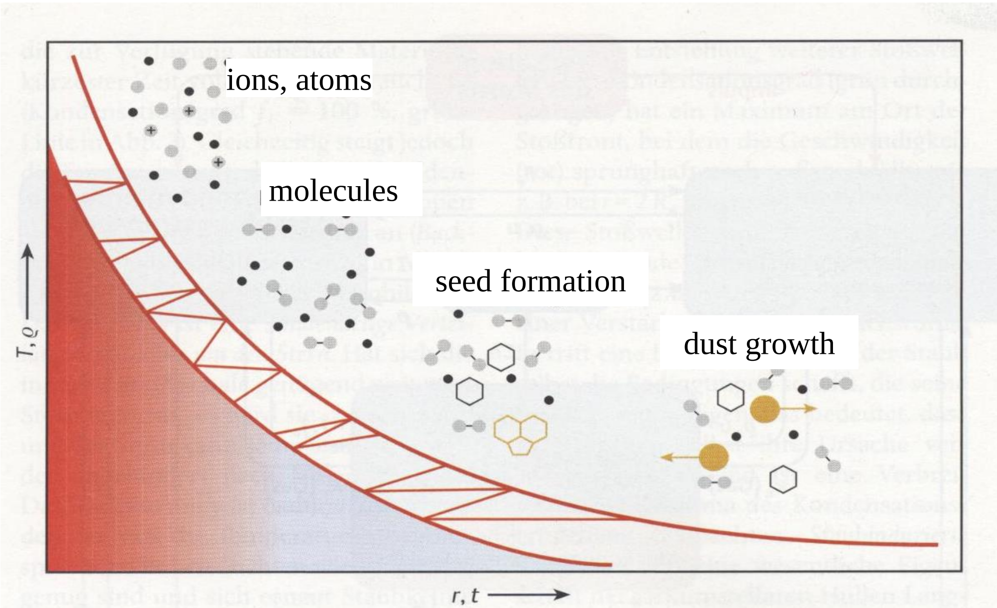

terrestrial, macroscopic rutile crystal (TiO_2, yellowish)

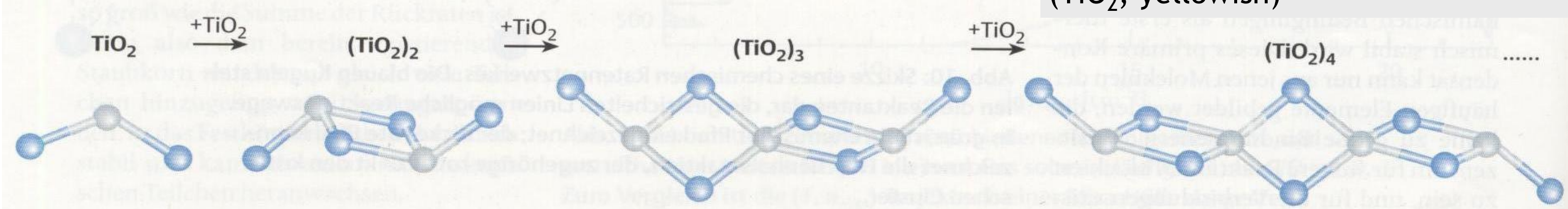

first steps of a linear reaction chain, forming the seed of $(TiO_2)_N$

Dust-driven winds: the principle

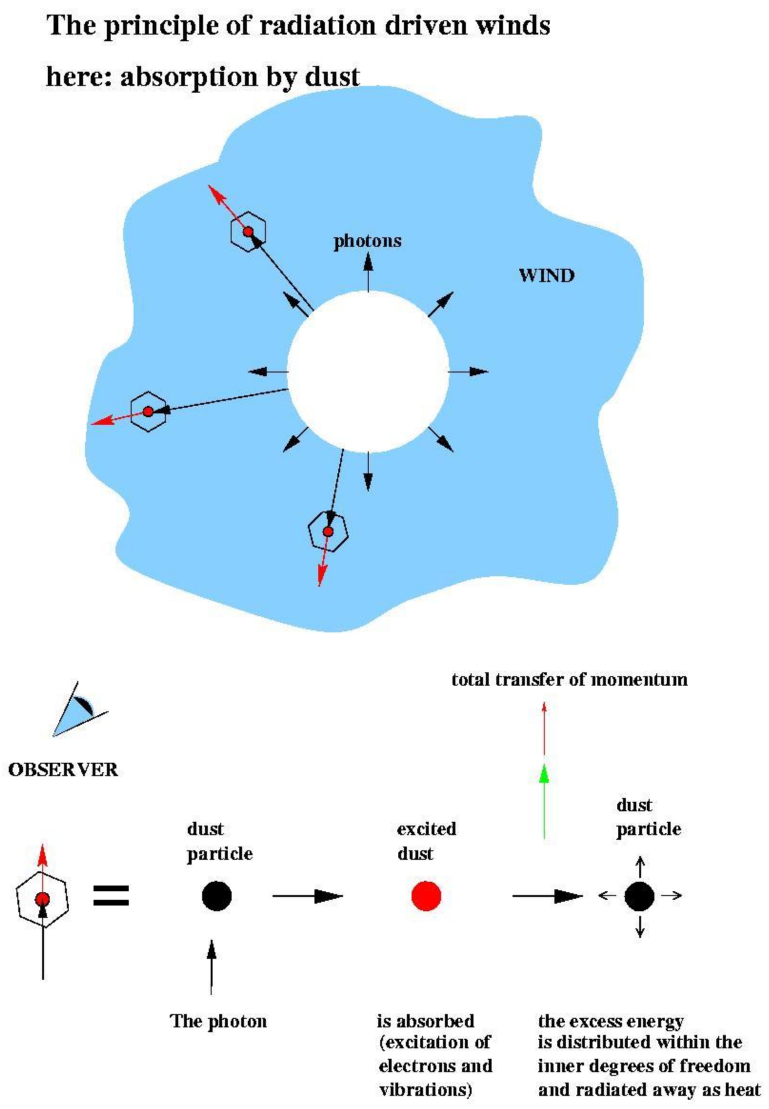

- star emits photons
- photons absorbed by dust
- momentum transfer accelerates dust
- gas accelerated by viscous drag force due to gas-dust collisions

acceleration
proportional to number of photons, i.e.,
proportional to *stellar luminosity* ***L***

$\Rightarrow$ mass-loss rate $\propto$ ***L***

dust driven winds at tip of AGB responsible for ejection of envelope
$\Rightarrow$ Planetary Nebulae

winds from massive red supergiants still not explained, but probably similar mechanism

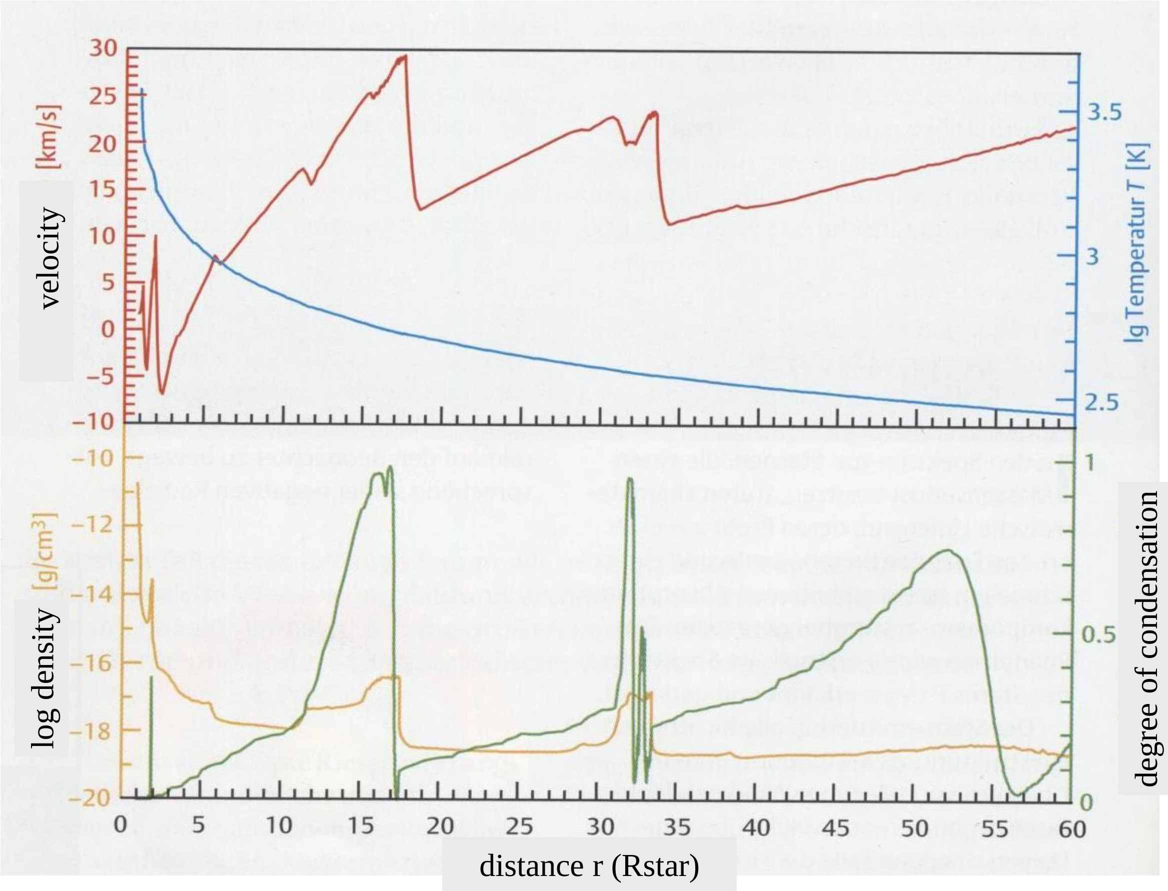

snapshot of a time-dependent hydro-simulation of a carbon-rich circumstellar envelope of an AGB-star. Model parameters similar to next slide.

- star ("surface") pulsates,
- sound waves are created,
- steepen into shocks;
- matter is compressed,
- dust is formed
- and accelerated by radiation pressure

dust shells are blown away, following the pulsational cycle

$\Rightarrow$ periodic darkening of stellar disc
$\Rightarrow$ **brightness variations**

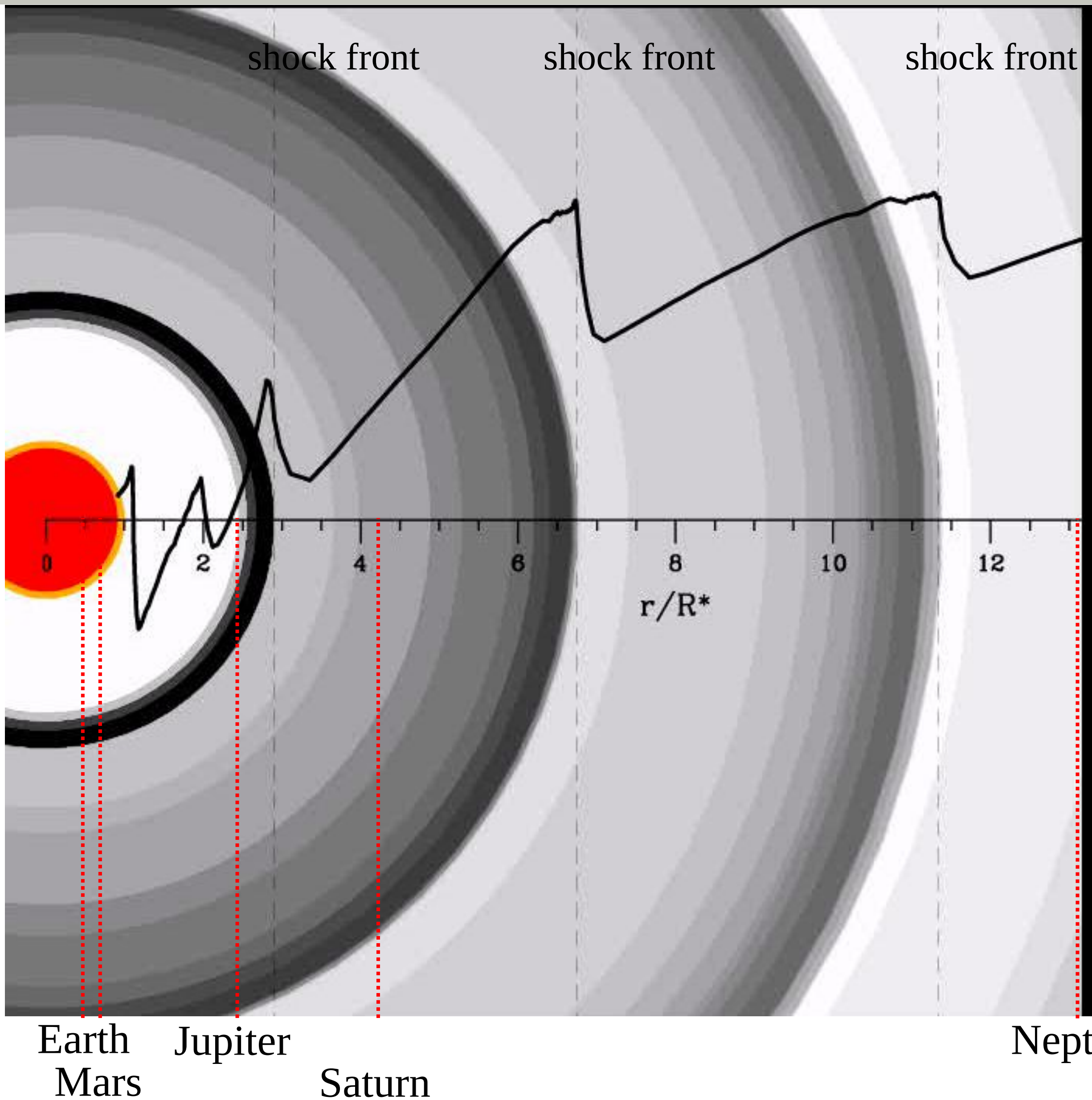

dark colors: dust shells

velocity

simulation of a
dust-driven wind
(*working group E. Sedlmayr, TU Berlin*)

T = 2600 K, L = 10^4 L_{sun},
M = 1 M_{sun}, Δv = 2 km/s

Stars and their winds – typical parameters

	The sun	Red AGB-stars	Blue supergiants
mass $[M_\odot]$	1	1 ... 3	10...100
luminosity $[L_\odot]$	1	10^4	$10^5...10^6$
stellar radius $[R_\odot]$	1	400	10...200
effective temperature [K]	5570	2500	$10^4...5\cdot10^4$
wind temperature [K]	10^6	1000	8000...40000
mass loss rate $[M_\odot/yr]$	10^{-14}	$10^{-6}...10^{-4}$	10^{-6} ... few 10^{-5}
terminal velocity [km/s]	500	30	200...3000
life time [yr]	10^{10}	10^5	10^7
total mass loss $[M_\odot]$	10^{-4}	$\gtrsim 0.5$	up to 90% of total mass

Massive stars determine energy (kinetic and radiation) and momentum budget of surrounding ISM

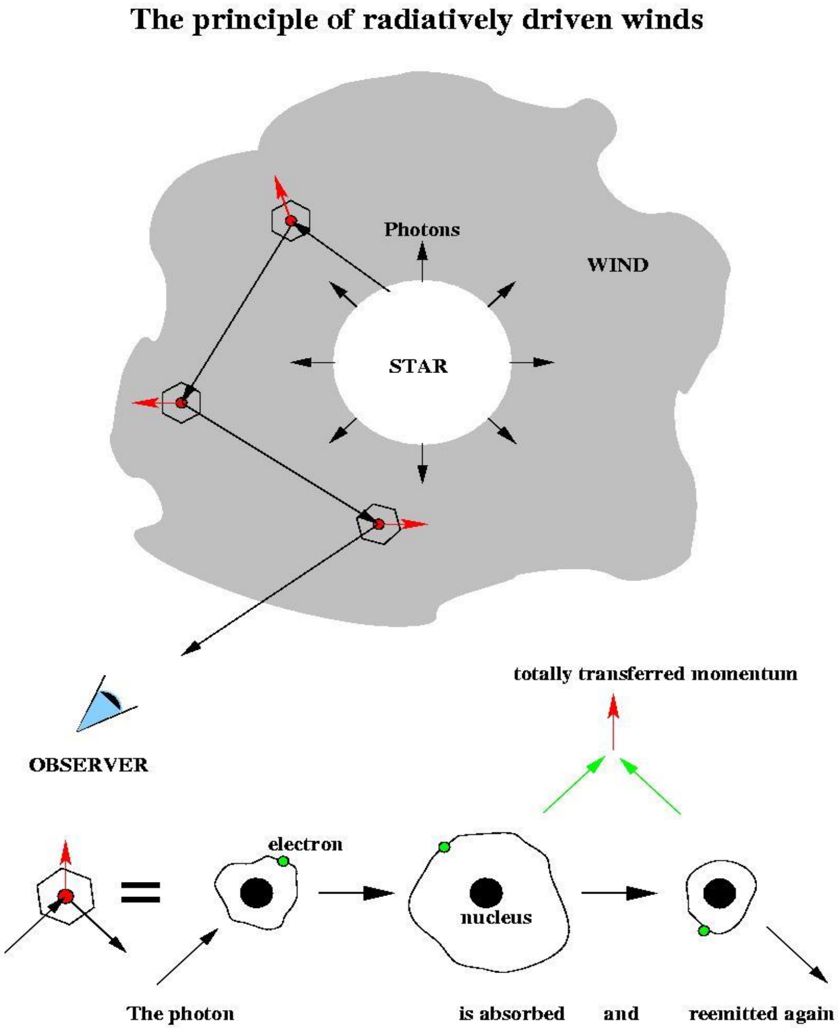

- accelerated by radiation pressure in **lines**
  $\dot{M} \approx 10^{-7} ... 10^{-5}\ M_{\rm sun}/{\rm yr},\ v_\infty \approx 200\ ...\ 3{,}000\ {\rm km/s}$
- momentum transfer from accelerated species (ions) to bulk matter (H/He) via Coulomb collisions

Prerequesites for radiative driving

- large number of photons => high luminosity
  $L \propto R_*^2\ T_{\rm eff}^4$ => supergiants or hot dwarfs
- line driving:
  large number of lines close to flux maximum
  (typically some $10^4...10^5$ lines relevant)
  with high interaction probability
  (=> mass-loss dependent on metal abundances)

- line driven winds important for chemical evolution of (spiral) Galaxies, in particular for starbursts
- transfer of momentum (=> induces *star formation*, hot stars mostly in *associations)*, energy and nuclear processed material to surrounding environment
- dramatic impact on stellar evolution of massive stars (mass-loss rate vs. life time!)

pioneering investigations by
Lucy & Solomon, 1970, ApJ 159
Castor, Abbott & Klein, 1975, ApJ 195 (CAK)

reviews by Kudritzki & Puls, 2000, ARAA 38
Puls et al. 2008 A&ARv 16, issue 3

9.1 Radiative line driving and line-statistics

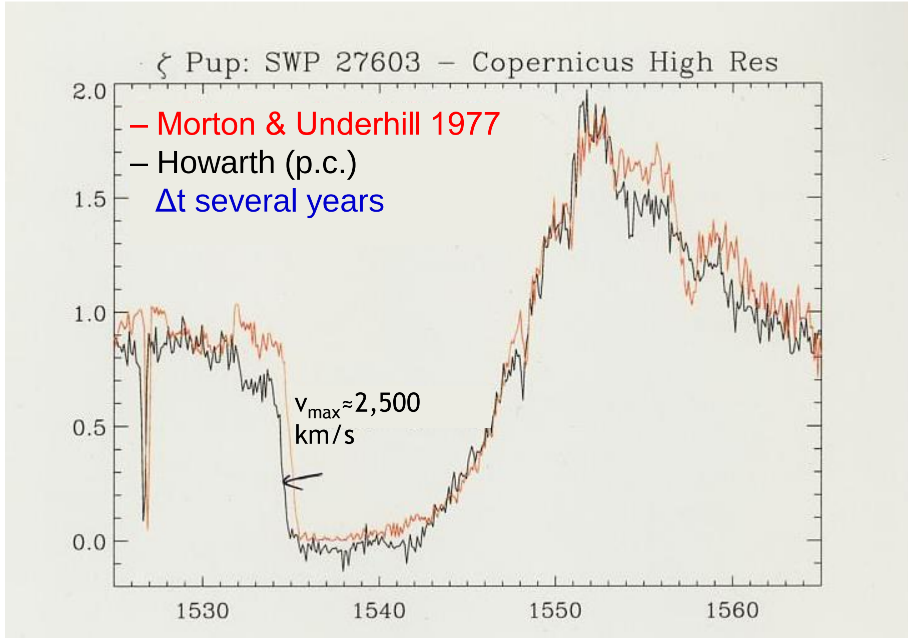

- Observational findings:
  massive star have outflows, at least quasi-stationary
- only small, in NO WAY dominant variability of global quantities $(\dot{M}, v_\infty)$
- $\dot{M}, v_\infty, v(r)$ have to be explained
- diagnostic tools have to be developed
- predictions have to be given

Hydro-equations

$$\frac{\partial}{\partial t}\rho + \nabla\cdot(\rho\mathbf{v}) = 0$$ continuity equation

$$\frac{\partial}{\partial t}(\rho\mathbf{v}) + \nabla\cdot(\rho\mathbf{v}\mathbf{v}) = -\nabla p + \rho\mathbf{a}^{\mathrm{ext}}$$ momentum equation

$\Rightarrow$ (use continuity equation)

$$\frac{\partial}{\partial t}\mathbf{v} + (\mathbf{v}\cdot\nabla)\mathbf{v} = -\frac{1}{\rho}\nabla p + \mathbf{a}^{\mathrm{ext}}$$ equation of motion

$\Rightarrow$ (with $\frac{\partial}{\partial t} = 0$, 1-D spherically symmetric)

$$\boxed{4\pi r^2\rho(r)\mathrm{v}(r) = \mathrm{const} = \dot{M}}$$ mass-loss rate

$$\mathrm{v}\frac{d\mathrm{v}}{dr} = -\frac{1}{\rho(r)}\frac{dp}{dr} + a^{\mathrm{ext}}(r)$$

$$p = NkT \quad \text{(equation of state)} \quad = \frac{kT}{\mu m_{\mathrm{H}}}\rho = \mathrm{v}_{\mathrm{s}}^2\rho$$

v_{s} isothermal sound speed, μ mean molecular weight

$$\Rightarrow \quad \boxed{\mathrm{v}\left(1-\frac{\mathrm{v}_{\mathrm{s}}^2}{\mathrm{v}^2}\right)\frac{d\mathrm{v}}{dr} = \frac{2\mathrm{v}_{\mathrm{s}}^2}{\mathrm{r}} - \frac{d\mathrm{v}_{\mathrm{s}}^2}{dr} + a^{\mathrm{ext}}}$$

(assumption here: $\mathrm{v}_{\mathrm{s}}^2 \sim T$ known)

$$\boxed{a^{\mathrm{ext}}(r) = -\frac{GM}{r^2}(1-\Gamma) + g_{\mathrm{Rad}}^{\mathrm{true\ cont}}(r) + g_{\mathrm{Rad}}^{\mathrm{line}}(r)}$$

$$\Gamma = \frac{g_{\mathrm{Rad}}^{\mathrm{Thomson}}(r)}{g_{\mathrm{grav}}(r)} = \mathrm{const} \text{ is Eddington factor,}$$

corrects for radiative acceleration due to Thomson scattering

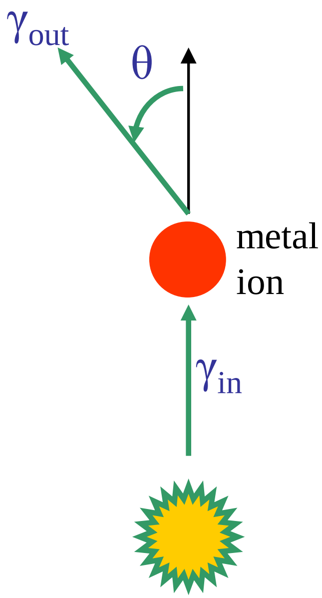

$$
\left.\begin{array}{l} \cos\theta_{\rm in} \approx 1 \\ \text{isotropic reemission} \\ \langle \cos\theta_{\rm out} \rangle = 0 \end{array}\right\} \quad \langle \Delta P \rangle = \frac{h\nu_{\rm in}}{c}
$$

$$
\Rightarrow g_{\rm rad} = \frac{\langle \Delta P \rangle_{\rm tot}}{\Delta t \, \Delta m} = \frac{\sum_{\text{all lines}} \langle \Delta P \rangle_i}{\Delta t \, \Delta m}
$$

a) scattering of continuum light in resonance lines

$$
\Delta P_{\rm radial} = P_{\rm in} - P_{\rm out}
$$

$$
= \frac{h}{c}(\nu_{\rm in} \cos\theta_{\rm in} - \nu_{\rm out} \cos\theta_{\rm out})
$$

absorption reemission

b) momentum transfer from metal ions (fraction 10^{-3}) to bulk plasma (H/He) via Coulomb collisions (see Springmann & Pauldrach 1992)

- velocity drift of ions w.r.t. H/He is compensated by frictional force as long as $v_D/v_{th} < 1$ (linear regime, “Stokes” law)

$$R_{ij}^{\text{fric}} \sim G(x_{ij}) \qquad x_{ij} = \sqrt{A_{ij}}\,\frac{|\mathrm{v}_i - \mathrm{v}_j|}{\mathrm{v}_{\text{th}}(\text{prot})} \qquad A_{ij} \text{ is reduced mass}$$

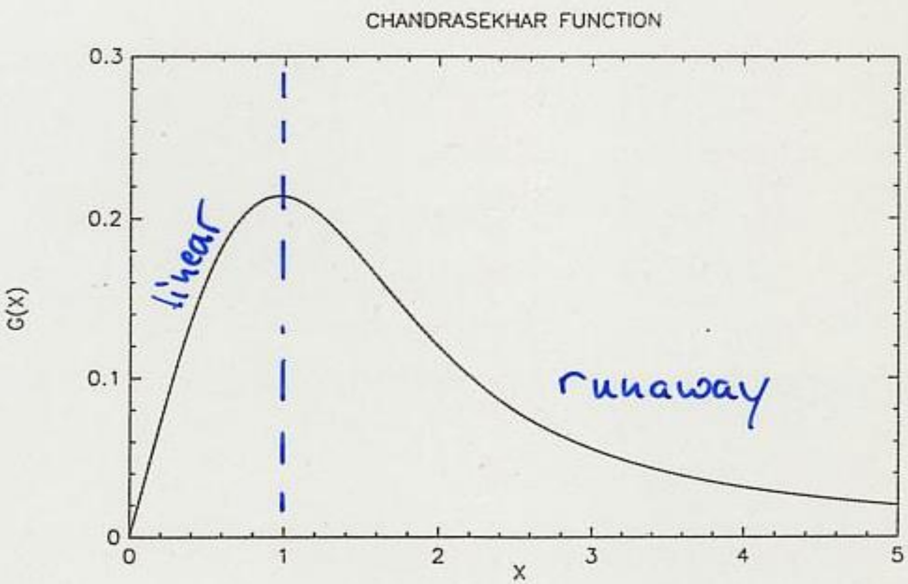

Fig. 1. The Chandrasekhar function $G(x)$ which gives the frictional force on test particles by field particles of unit density for an inverse square law of Coulomb interaction. The variable x is essentially the ratio of the velocity of the test particles in the rest frame of the field particles to the thermal velocity of the field particles (see text). The limiting cases are $G(x) \sim x$ for $x \ll 1$ and $G(x) \sim x^{-2}$ for $x \gg 1$

from Springmann & Pauldrach (1992, A&A 262)
see also Owocki & Puls (2002, ApJ 568)

approximate description (supersonic regime) by linear diffusion equation

$$\mathrm{v}_{\text{ion}} \frac{d}{dr}\mathrm{v}_{\text{ion}} = g_{\text{Rad}}^{\text{ion}} - \frac{GM}{r^2} - \frac{w}{\tau_{ib}} \qquad w \text{ drift velocity}$$

$$\mathrm{v}_{\text{bulk}} \frac{d}{dr}\mathrm{v}_{\text{bulk}} = -\frac{GM}{r^2} + \frac{w}{\tau_{bi}} \qquad \text{bulk} \approx \text{H/He},$$

τ relaxation time between collisions

in order to obtain one-component fluid,

$$\mathrm{v}_{\text{ion}} \frac{d\mathrm{v}_{\text{ion}}}{dr} = \mathrm{v}_{\text{bulk}} \frac{d\mathrm{v}_{\text{bulk}}}{dr}$$

$$\Rightarrow w = g_{\text{Rad}}^{\text{ion}} \left(\frac{1}{\tau_{ib}} + \frac{1}{\tau_{bi}}\right)^{-1} \approx g_{\text{Rad}}^{\text{tot}} \frac{\rho_{\text{tot}}}{\rho_{\text{ion}}} \cdot \tau \sim g_{\text{Rad}}^{\text{tot}} \frac{1}{Z}\frac{1}{\rho}$$

tot = bulk + ion, Z is metallicity

for low $\rho \sim \frac{\dot{M}}{V}$ and/or low Z $\rightarrow$ drift large $\rightarrow$ runaway

e.g., winds of A-dwarfs, Babel et al. 1995, A&A 301

9.1.3 The single scattering limit/multi-line scattering

$$\mathrm{v}\left(1-\frac{\mathrm{v}_s^2}{\mathrm{v}^2}\right)\frac{d\mathrm{v}}{dr}=\frac{2\mathrm{v}_s^2}{\mathrm{r}}-\frac{d\mathrm{v}_s^2}{dr}-\frac{GM}{r^2}(1-\Gamma)+g_{\mathrm{Rad}}^{\mathrm{line}}$$

supersonic approx., $\mathrm{v} > \mathrm{v}_s$, pressure forces negligible

$$\mathrm{v}\frac{d\mathrm{v}}{dr}+\frac{GM}{r^2}(1-\Gamma)=g_{\mathrm{Rad}}^{\mathrm{line}} \quad \Big|4\pi r^2\rho$$

$$\dot{M}\frac{d\mathrm{v}}{dr}+4\pi GM\,(1-\Gamma)\rho=4\pi r^2\rho\, g_{\mathrm{Rad}}^{\mathrm{line}} \quad \Big|\int_{R_s}^{\infty} dr$$

$$\dot{M}\,(\mathrm{v}_\infty-\cancel{\mathrm{v}_s})+\frac{4\pi GM\,(1-\Gamma)}{s_e}\underbrace{\int_{R_s}^{\infty} s_e\rho\, dr}_{\tau_{\mathrm{TH}}}=\int_{\mathrm{wind}} g_{\mathrm{Rad}}^{\mathrm{line}}\, dm$$

$$s_e=\sigma_{\mathrm{TH}}/\rho,\quad \Gamma=s_e\frac{L}{4\pi cGM},\quad g_{\mathrm{Rad}}^{\mathrm{line}}=\frac{\sum\Delta P}{\Delta m\,\Delta t}$$

$$\dot{M}\mathrm{v}_\infty+\frac{L}{c}\frac{1-\Gamma}{\Gamma}\tau_{\mathrm{TH}}=\frac{\sum\Delta P}{\Delta t}$$

$$\frac{\dot{M}\mathrm{v}_\infty}{L/c}+\frac{1-\Gamma}{\Gamma}\tau_{\mathrm{TH}}=\frac{c}{L}\frac{\sum\Delta P}{\Delta t} \quad \leftarrow \text{momentum loss of radiation field}$$

Now so-called S(ingle) S(cattering) L(imit), SSL

assume that each photon is scattered once somewhere in the wind, with $\Delta P=\frac{h\nu_{\mathrm{in}}}{c}$

number of photons per time and $d\nu$ is $\frac{L(\nu)}{h\nu}d\nu$

$$\Rightarrow \frac{c}{L}\frac{\sum\Delta P}{\Delta t}=\frac{c}{L}\int\frac{L(\nu)}{h\nu}\frac{h\nu}{c}d\nu=1!$$

"performance number" or wind efficiency

$$\boxed{\eta=\frac{\dot{M}\mathrm{v}_\infty}{L/c}\overset{\mathrm{SSL}}{=}1-\frac{1-\Gamma}{\Gamma}\tau_{\mathrm{TH}}}$$

momentum rate
needed to support
wind against gravity

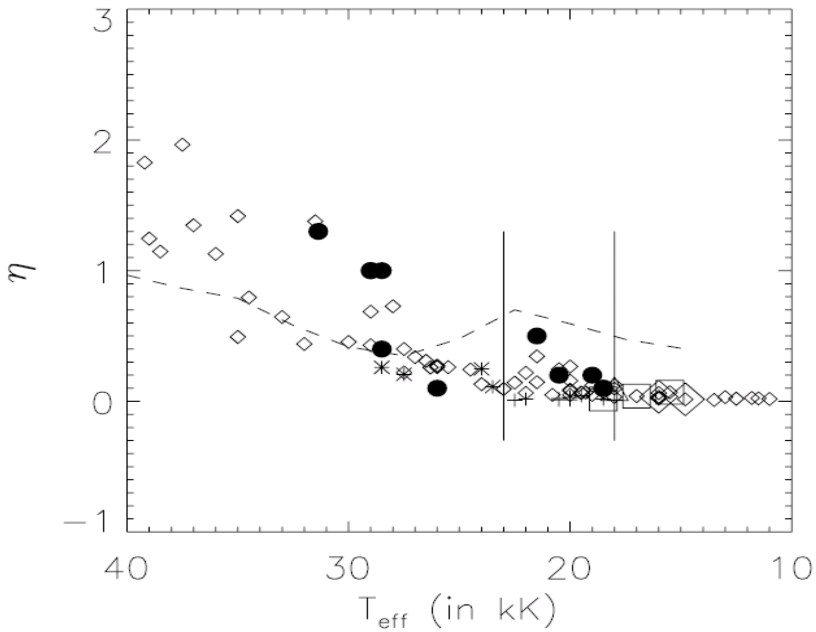

Wind efficiencies for Galactic OBA supergiants. The actual efficiency might be smaller, due to neglected wind clumping.
From Markova & Puls 2008

NOTE: Wolf-Rayet stars have much larger wind-efficiencies (η = O(10)), due to higher Mdot (and also Γ and τ are larger).

→ Single-scattering not sufficient to provide enough radiative acceleration

Multi-line scattering

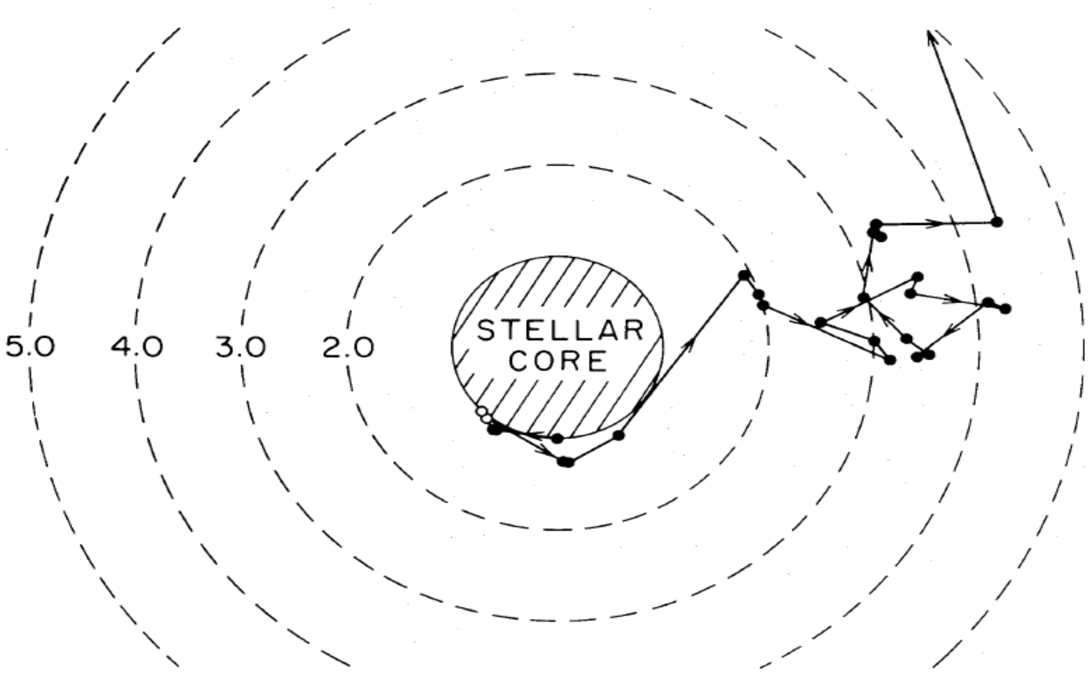

from Abbott & Lucy (1985)

Friend & Castor (1983)
Abbott & Lucy (1985)
→ Monte Carlo Method
Puls (1987)
not very efficient in OB-star winds
Lucy & Abbott (1993)
explain large wind-efficiencies of WR winds due to multi-line scattering in stratified ionization equilibrium
Springmann (1994)
Gayley et al. (1995)

Throughout following slides WR case not considered

- assume that each line can be treated separately, i.e.,

$$\Delta P^{tot} = \sum_{\text{lines i}} \Delta P^{i} / \text{line}$$

$\boxed{\text{no interaction between different lines}}$

- don't misinterpret this assumption ("single-line approximation") with SSL!!!
- η(SL) > η(SSL) !!!

The photon-tiring limit

What is the maximum mass-loss rate that can be accelerated???

- mechanical luminosity in wind at infinity is

$$L_{\rm wind} = \dot M \left(\frac{v_\infty^2}{2} + \frac{GM}{R} \right) = \dot M \left(\frac{v_\infty^2}{2} + \frac{v_{\rm esc}^2}{2} \right) \quad \text{with } v_{\rm esc} = \sqrt{\frac{2GM}{R}}$$

- maximum mass loss, if $L_{\rm wind} = L_*$ $\Rightarrow$ $L(\infty) = 0$, star becomes invisible

$$\dot M_{\rm max} = \frac{2L_*}{v_\infty^2 + v_{\rm esc}^2}$$

$$\Rightarrow \eta_{\rm max} = \frac{\dot M_{\rm max} v_\infty}{L/c} = \frac{2c}{v_\infty \left(1 + \left(\frac{v_{\rm esc}}{v_\infty} \right)^2 \right)}$$

typical values: $v_\infty \approx 2000...3000$ km/s $\approx 0.01c$, $v_{\rm esc}/v_\infty \approx 1/3$ $\rightarrow \eta_{\rm max} \approx 200$

$\dot M_{\rm tir}$ (Owocki & Gayley 1997) is maximum mass-loss rate when wind just escapes the gravitational potential, with $v_\infty \rightarrow 0$

$$\boxed{\dot M_{\rm tir} = \frac{2L_*}{v_{\rm esc}^2} = 0.032 \frac{M_\odot}{\rm yr} \frac{L_*}{10^6 L_\odot} \frac{R}{R_\odot} \frac{M_\odot}{M} = 0.0012 \frac{M_\odot}{\rm yr} \Gamma_e \frac{R}{R_\odot}}$$

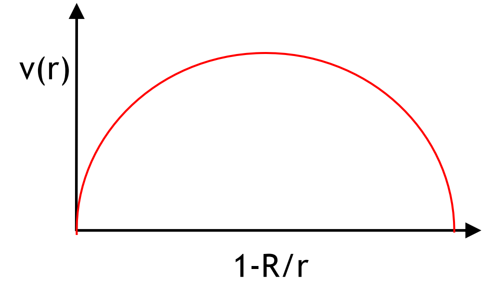

9.1.4 Calculation of the line force

crucial point of the problem

$$g_{\mathrm{Rad}}^{\mathrm{line}} = \frac{4\pi}{c\rho}\frac{1}{2}\int_0^\infty d\nu \int_{-1}^{1} \mu\, d\mu \left[\chi_\nu^{\mathrm{line}}(r,\mu) I_\nu(r,\mu) - \cancel{\eta_\nu^{\mathrm{line}}(r,\mu)}\right]$$

absorbed emitted

$\rightarrow$ (in single-line approximation)

$$g_{\mathrm{Rad}}^{\mathrm{line}} = \frac{2\pi}{c\rho}\sum_{\mathrm{lines\ i}} \int_{\mathrm{line}} d\nu \int_{-1}^{1} \mu\, d\mu\ \chi_\nu^{\mathrm{i}}(r,\mu) I_\nu^{i}(r,\mu)$$

- two quantities to be known
  - force/line in response to χ_ν
  - distribution of lines with χ_ν and ν

The force per line

- super-simplified
- simplified: Sobolev approximation
- “exact”:
  - comoving frame, special cases
  - observer’s frame, instability

Super-simplified theory

interaction with line at ν_0, when comoving frame frequency of photon starting at R_* with ν_{obs} is equal to ν_0

(finite profile width neglected, interaction probability = 1)

$$\nu_{\text{CMF}} = \nu_{\text{obs}} - \frac{\nu_0 \text{v}(r)}{c} =: \nu_0 \quad \text{(Doppler shift, radial photons, } \mu{=}1\text{, assumed)}$$

$$\left.\begin{aligned} \nu_0 &= \nu_1^{\text{obs}} - \frac{\nu_0}{c}\text{v}_1(r) \\ \nu_0 &= \nu_2^{\text{obs}} - \frac{\nu_0}{c}\text{v}_2(r) \end{aligned}\right\} \text{ scattering at larger v requires 'bluer' photons}$$

$$\Rightarrow \Delta\nu_{\text{obs}} = \frac{\nu_0}{c}\Delta\text{v}$$

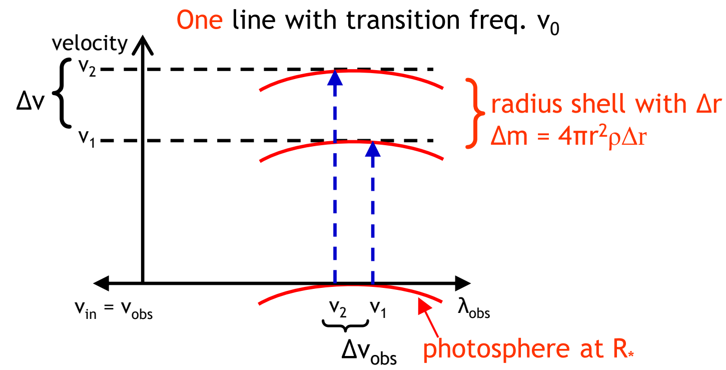

Number of photons in interval $\left[\nu_1^{\text{obs}}, \nu_2^{\text{obs}} = \nu_1^{\text{obs}} + \Delta\nu_{\text{obs}}\right]$ per unit time

$$\frac{N_\nu \Delta\nu}{\Delta t} = \frac{L_\nu \Delta\nu}{h\nu_{\text{obs}}} \quad \Rightarrow \quad \left(g_{\text{Rad}} = \frac{\Delta P}{\Delta t \Delta m}\right)$$

$$g_{\text{Rad}} = \frac{h\nu_{\text{obs}}}{\text{c}} \cdot \frac{L_\nu \Delta\nu}{h\nu_{\text{obs}}} \cdot \frac{1}{\Delta m} = \qquad \left(\Delta\nu = \frac{\nu_0}{c}\Delta\text{v}\right)$$

$$= \frac{L_\nu \nu_0}{c^2} \frac{\Delta\text{v}}{\Delta r} \frac{1}{4\pi r^2 \rho} \propto \boxed{\frac{d\text{v}}{dr}} \frac{1}{r^2 \rho}$$

Why $g_{rad} \propto dv/dr$?

shell of matter with spatial extent Δr,

and velocity $v_0 + \left(\frac{dv}{dr}\right)_1 \Delta r$

absorption of photons at $\nu_0 \pm \delta\nu$

in frame of matter

photons must start at higher (stellar)

frequencies, are "seen" at $\nu_0 \pm \delta\nu$

in frame of matter because of Doppler-effect.

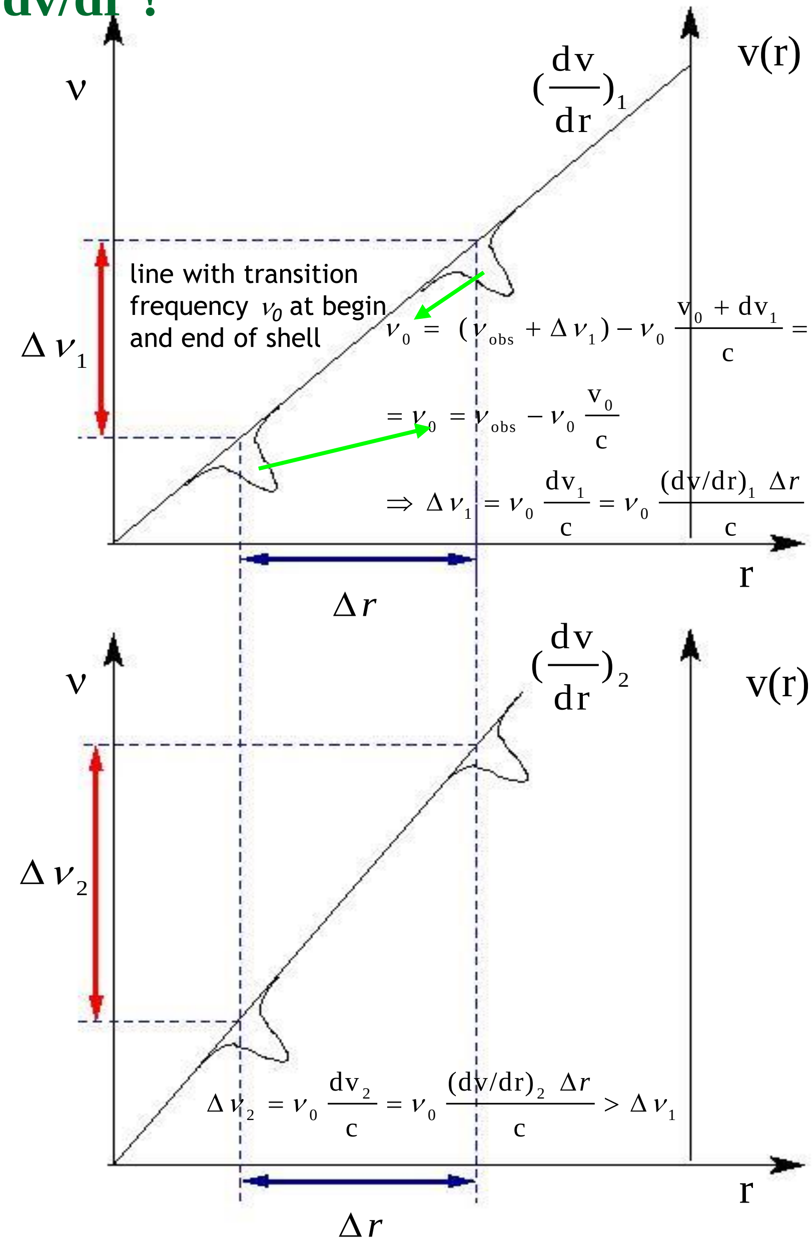

Let $\Delta\nu$ be frequency band contributing to

acceleration of matter in Δr

The larger $\frac{dv}{dr}$,

- the larger $\Delta\nu$
- the more photons can be absorbed
- the larger the acceleration

$$\boxed{g_{rad} \propto \frac{dv}{dr}}$$

(assuming that each photon is absorbed,
i.e., acceleration from optically thick lines)

$$\boxed{g_{\text{rad}}(\text{one line at } \nu_0) = \frac{L_\nu \nu_0}{c^2} \frac{\Delta \text{v}}{\Delta r} \frac{1}{4\pi r^2}}$$

Assumption was: each photon is scattered

Then: g_{rad} independent of cross-sections, occuption numbers etc.

only dependent on hydro-structure and flux distribution

What happens if interaction probability < 1?

interaction probability = $1 - e^{-\tau}$, with optical depth τ

$\tau \gg 1$ prob = 1

$\tau \ll 1$ prob = τ

Now: division in two classes

optically thick lines, $\tau \geq 1$ $\xrightarrow{\approx}$ prob = 1 (saturation, independent of τ)

optically thin lines $\tau < 1$ $\xrightarrow{\approx}$ prob = τ

$\Rightarrow$ $\boxed{g_{\text{rad}}(\text{optically thin line}) = \tau \cdot g_{\text{rad}}(\text{optically thick line})}$

Calculating the optical depth: The Sobolev-approximation (SA)

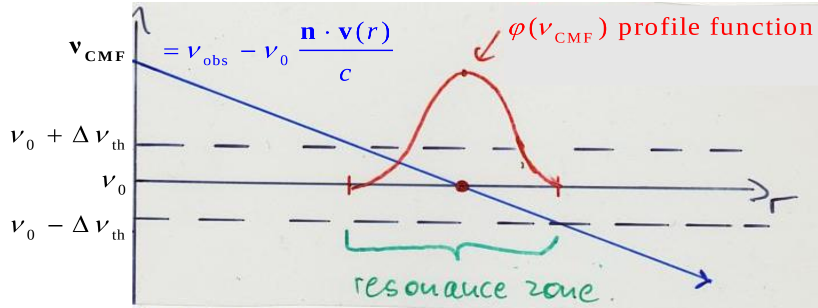

Note: 'first' interaction at highest CMF-freq., 'blue' edge
'last' interaction (final reemission) at 'red' edge

TRICK of Sobolev approximation (Sobolev, 1960; developed around 1945)

- in the resonance zone (width ~ 2 times 3 v_{th}), assume 'macro'-quantities such as opacity, source-function and density to be constant or perform Taylor expansion
- account at least for v and dv/dr
- then, all integrals of radiative transfer can be performed analytically and are exact within the assumptions

The validity of the SA can be checked by comparing the scale-length of the macro-quantities with the co-called Sobolev length, which is the scale length associated to the line-profile:
From dv/dr $L_S = v_{th}$, we find $L_S = [d(v/v_{th}) / dr]^{-1}$
Note: always required: $v > v_{th} \approx v_{sound}/\sqrt{m}$; m mass of absorbing ion

general definition

$$\tau_{\nu_{\rm obs}} = \int_{R_*}^{\infty} \bar{\chi}_{\rm L}(r)\cdot\varphi\left(\nu_{\rm obs} - \nu_0 \frac{\mu v(r)}{c}\right) dr \qquad \left(\rightarrow \int_{\substack{\text{res.}\\ \text{zone}}} \chi_\nu \, dr\right)$$

first assumption: $\bar{\chi}_{\rm L}(r) = $ const in resonance zone at r_0

$$\Rightarrow \tau_{\nu_{\rm obs}} = \bar{\chi}_{\rm L}(r_0)\int_{R_*}^{\infty} \varphi\left(\nu_{\rm obs} - \nu_0 \frac{\mu v(r)}{c}\right) dr$$

$$\nu' = \nu_{\rm obs} - \nu_0 \frac{\mu v(r)}{c}$$

2nd assumption: $\dfrac{d(\mu v)}{dr} = $ const in resonance zone

$$\Rightarrow d\nu' = -\frac{\nu_0}{c}\frac{d(\mu v)}{dr}\bigg|_{r_0} dr$$ replace spatial by frequenntial integral!

$$\tau^{\rm S}_{\nu_{\rm obs}} = \bar{\chi}_{\rm L}(r_0)\int_{-\infty}^{\infty} \varphi(\nu')\frac{c}{\left[\nu_0 \dfrac{d(\mu v)}{dr}\right]} d\nu' \; = \frac{\bar{\chi}_{\rm L}(r_0)\lambda_0}{\dfrac{d(\mu v)}{dr}\bigg|_{r_0}}\int_{-\infty}^{\infty}\varphi(\nu')d\nu'$$

$$\boxed{\tau^{\rm S}_{\nu_{\rm obs}} = \frac{\bar{\chi}_{\rm L}(r_0)\lambda_0}{\dfrac{d(\mu v)}{dr}\bigg|_{r_0}}}$$ optical depth in Sobolev theory,

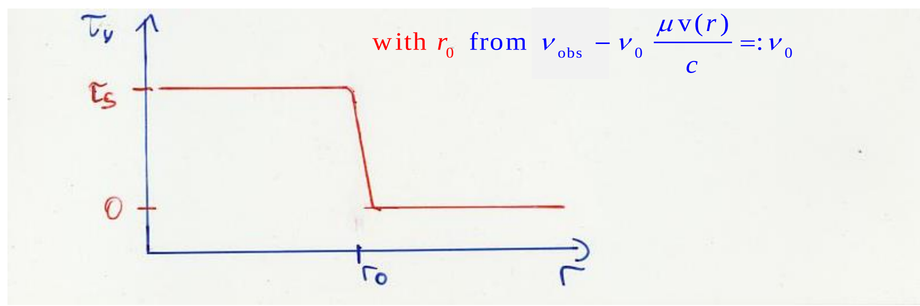

Within Sobolev theory, all radiation field related quantities can be calculated, e.g.,

$\bar{J} = \int J_\nu \phi(\nu) d\nu, \quad \bar{H} = \int H_\nu \phi(\nu) d\nu$ and

$$g_{\rm Rad}(r) = \frac{4\pi}{c} \frac{\bar{\chi}(r)}{\rho(r)} \bar{H}(r).$$

After a number of intelligent manipulation, one finds (see, e.g., Rybicki & Hummer 1978, ApJ 219)

$$g_{\rm Rad} = \frac{4\pi}{c} \frac{\bar{\chi}(r)}{\rho(r)} \frac{1}{2} \int_{\mu_*}^{1} \mu d\mu \frac{\left(1-\exp(-\tau^{\rm S}(\mu,r))\right)}{\tau^{\rm S}(\mu,r)} I_{\rm c}(\mu)$$

with cone-angle $\mu_* = \sqrt{1-\left(\frac{R_*}{r}\right)^2}$, core intensity $I_{\rm c}(\mu)$,

and $\tau^{\rm S}(\mu,r) = \dfrac{\bar{\chi}_{\rm L}(r)\lambda_0}{\frac{d(\mu {\rm v})}{dr}} = \dfrac{\bar{\chi}_{\rm L}(r)\lambda_0}{\left[\mu^2 d{\rm v}/dr + (1-\mu^2){\rm v}/r\right]}$

For r >>R$_*$ (i.e., $\mu_* \approx 1$), this is the same as derived from super-simplified theory (incl. interaction probability),

$$g_{\rm Rad} \approx \frac{4\pi}{c} \frac{\bar{\chi}(r)}{\rho(r)} \frac{\left(1-\exp(-\tau^{\rm S}(1,r))\right)}{\tau^{\rm S}(1,r)} \frac{1}{2} \int_{\mu_*}^{1} \mu d\mu I_{\rm c}(\mu) =$$

$$= \frac{4\pi}{c} \frac{\bar{\chi}(r)}{\rho(r)} \frac{\left(1-\exp(-\tau^{\rm S}(r))\right)}{\tau^{\rm S}(r)} H_\nu =$$

$$= \frac{4\pi}{c} \frac{\bar{\chi}(r)}{\rho(r)} \frac{\frac{d{\rm v}}{dr}\left(1-\exp(-\tau^{\rm S}(r))\right)}{\bar{\chi}_{\rm L}(r)\lambda_0} \frac{L_\nu}{16\pi^2 r^2}$$

$\Rightarrow$

$$g_{\rm Rad} = \frac{L_\nu \nu_0}{c^2} \frac{d{\rm v}}{dr} \frac{1}{4\pi r^2 \rho} \times \left(1-\exp(-\tau^{\rm S}(r))\right)$$

$$\approx \frac{1}{4\pi r^2 c^2} L_\nu \nu_0 \frac{d{\rm v}}{dr} \begin{cases} \dfrac{1}{\rho} & \text{optically thick lines, } \tau > 1 \\[2ex] \dfrac{\tau^{\rm S}}{\rho} & \text{optically thin lines, } \tau < 1 \end{cases}$$

and $\tau^{\rm S}(r) = \dfrac{\bar{\chi}_{\rm L}(r)\lambda_0}{d{\rm v}/dr}$

To calculate the total line acceleration, we have to sum over all contributing lines!

Line acceleration from a line ensemble

$$g_{\mathrm{Rad}}^{\mathrm{tot}}(r) = \sum_{\mathrm{thick}} g_{\mathrm{Rad}}^{\mathrm{i}}(r) + \sum_{\mathrm{thin}} g_{\mathrm{Rad}}^{\mathrm{j}}(r) =$$

$$= \frac{1}{4\pi r^2 c^2}\left(\sum_{\mathrm{thick}} L_\nu \nu_{\mathrm{i}} \underbrace{\frac{d\mathrm{v}}{dr}\frac{1}{\rho}}_{k_1} + \sum_{\mathrm{thin}} L_\nu \nu_{\mathrm{i}} \underbrace{\frac{d\mathrm{v}}{dr}\frac{\tau_i}{\rho}}_{k_{\mathrm{i}}} \right)$$

$$\tau_{\mathrm{i}} = \frac{\bar{\chi}_{\mathrm{Li}}\lambda_{\mathrm{i}}}{d\mathrm{v}/dr} =: \frac{k_{\mathrm{i}}\rho(r)}{d\mathrm{v}/dr} \qquad \left(\text{precisely: } k_{\mathrm{i}} = \frac{\bar{\chi}_{\mathrm{Li}}\lambda_{\mathrm{i}}}{\rho s_{\mathrm{e}} \mathrm{v}_{\mathrm{th}}} \right)$$

$\uparrow$ optical depth of line in Sobolev theory

k_{i} is line strength $\sim \dfrac{\sigma_{\mathrm{i}} n_{\mathrm{i}}(r)\lambda_{\mathrm{i}}}{\rho(r)}$ $\quad \sigma_{\mathrm{i}}$ cross section,

n_{i} lower occup. number of line transition

k_{i} roughly constant in wind!!!

Which line strength corresponds to 'border' $\tau_{\mathrm{i}} = 1$?

$$1 = \frac{k_1 \rho}{d\mathrm{v}/dr} \qquad \Rightarrow \qquad k_1 = \frac{d\mathrm{v}/dr}{\rho}$$

$$\Rightarrow \quad g_{\mathrm{Rad}}^{\mathrm{tot}}(r) = \frac{1}{4\pi r^2 c^2}\left(k_1 \sum_{k_{\mathrm{i}} > k_1} L_\nu \nu_{\mathrm{i}} + \sum_{k_{\mathrm{i}} < k_1} L_\nu \nu_{\mathrm{i}} k_{\mathrm{i}} \right)$$

optically thick $\quad$ optically thin

depends on hydrostruct. $\quad$ depends on line-strength

Millions of lines ....

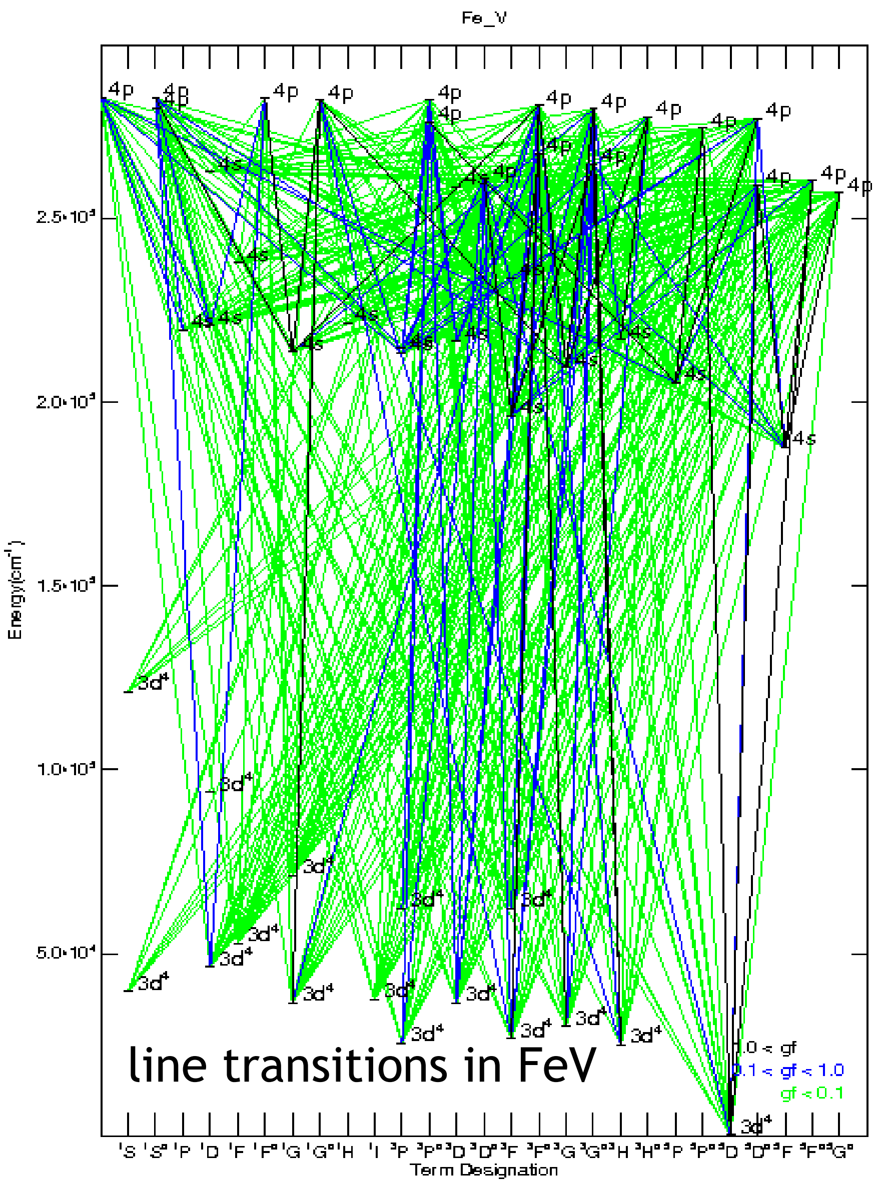

... are present
... and needed!

$$g^{\text{tot}}_{\text{Rad}} = \sum_{\text{all lines}} g^{\text{i}}_{\text{Rad}},$$

$$g^{\text{thin}}_{\text{Rad}} = L^{\text{i}}_{\nu}\nu_{\text{i}}\, k_{\text{i}}, \qquad k_{\text{i}} \propto \frac{\bar{\chi}_{\text{i}}\lambda_{\text{i}}}{\rho} \quad \text{(line-strength)}$$

$$g^{\text{thick}}_{\text{Rad}} = L^{\text{i}}_{\nu}\nu_{\text{i}}\frac{d\text{v}/dr}{\rho} \propto L^{\text{i}}_{\nu}\nu_{\text{i}} k_{1}$$

The line distribution function

- pioneering work by **Castor, Abbott & Klein** (CAK, 1975):
  - from glance at CIII atom in LTE, they suggested that ALL line-strengths follow a power-law distribution
- first realistic line-strength distribution function by Kudritzki et al. (1988)
- NOW: couple of Ml (Mega lines), 150 ionization stages (H – Zn), NLTE

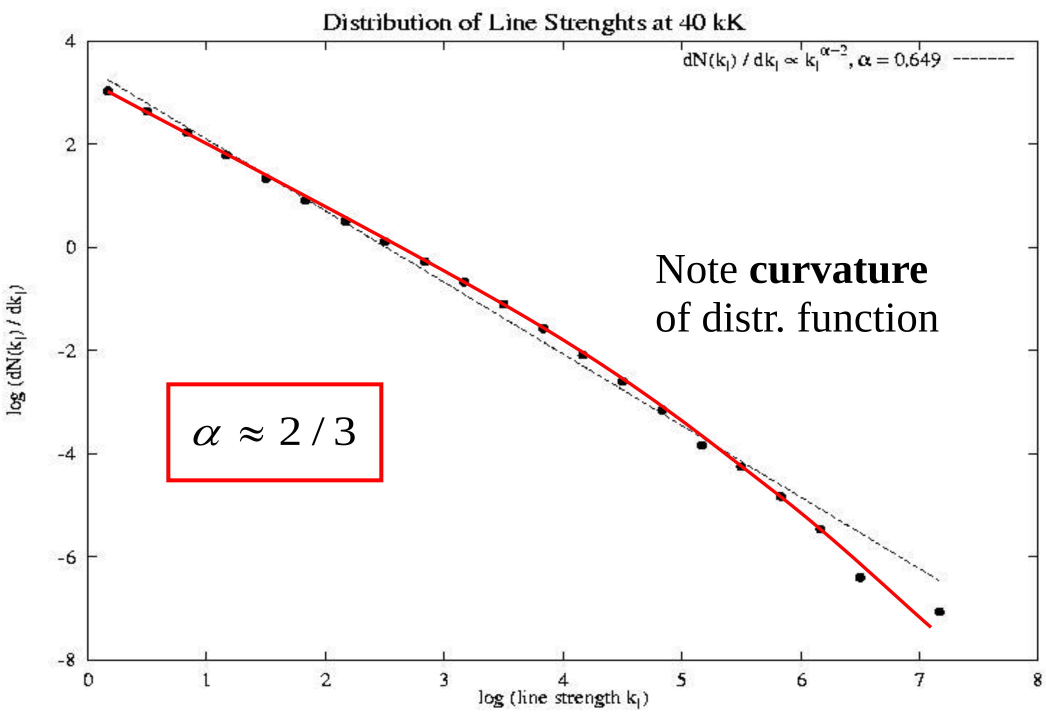

$$\frac{dN(k)}{dk} = k^{\alpha-2}, \quad \alpha \approx 0.6...0.7$$

+ 2nd empirical finding: valid in *each* frequential subinterval

$$dN(k,\nu) = -N_0 f(\nu) d\nu \; k^{\alpha-2} dk$$

Logarithmic plot of line-strength distribution function for an O-type wind at 40,000 K and corresponding power-law fit (see Puls et al. 2000, A&AS 141)

Force/line + line-strength distribution

$$\Rightarrow g_{\mathrm{Rad}}^{\mathrm{tot}}(r) = \frac{1}{4\pi r^2 c^2}\left(k_1 \sum_{k_i > k_1} L_\nu \nu_i + \sum_{k_i < k_1} L_\nu \nu_i k_i \right) \rightarrow$$

$$\rightarrow \frac{1}{4\pi r^2 c^2}\left(\int_0^\infty k_1 \int_{k_{\max}}^{k_1} L(\nu)\nu \, dN(k,\nu) + \int_0^\infty \int_{k_1}^0 L(\nu)\nu k \, dN(k,\nu) \right) =$$

$$= \frac{N_0 \int L(\nu)\nu f(\nu) d\nu}{4\pi r^2 c^2}\left(\underbrace{\underbrace{k_1 \int_{k_1}^{k_{\max}} k^{\alpha-2} dk}_{k_1 \frac{1}{1-a} k_1^{\alpha-1}} + \underbrace{\int_0^{k_1} k \cdot k^{\alpha-2} dk}_{\frac{1}{\alpha} k_1^{\alpha}}}_{\frac{1}{\alpha(1-\alpha)} k_1^{\alpha}} \right)$$

$\Rightarrow$ final result

$$\boxed{g_{\mathrm{Rad}}^{\mathrm{tot}}(r) = \frac{\mathrm{const}}{4\pi \mathrm{r}^2} k_1^{\alpha}}$$

very ‘strange’ acceleration, non-linear in dv/dr

$$k_1 = \frac{d\mathrm{v}/dr}{\rho} = \frac{4\pi}{\dot{M}} r^2 \mathrm{v} \frac{d\mathrm{v}}{dr}; \quad \mathrm{const} = \frac{N_0 \int L(\nu)\nu f(\nu) d\nu}{c^2 \alpha(1-\alpha)}$$

The force-multiplier concept

- neglected so far
  - non-radial photons (μ ≈ 1 justified only for r >> R)
  - ionization effects (have assumed that n_i/ρ = const throughout wind)
- line-force expressed in terms of Thomson acceleration

$$\frac{g_{\mathrm{Rad}}}{g_{\mathrm{grav}}} = \Gamma M(t) \quad \text{with "force-multiplier"}$$

$$M(t) = k_{\mathrm{CAK}} \underbrace{\left(\frac{s_{\mathrm{e}} \mathrm{v}_{\mathrm{th}} \rho}{\mathrm{dv}/\mathrm{d}r}\right)}_{t}^{-\alpha} \left(\frac{n_{\mathrm{E}}}{\mathrm{W}}\right)^{\delta} CF(r, v, \frac{\mathrm{dv}}{\mathrm{d}r}) = k_{\mathrm{CAK}} t^{-\alpha} \left(\frac{n_{\mathrm{E}}}{\mathrm{W}}\right)^{\delta} CF = k_{\mathrm{CAK}} k_1^{\alpha} \left(\frac{n_{\mathrm{E}}}{\mathrm{W}}\right)^{\delta} CF$$

Abbott 1982

Pauldrach, Puls & Kudritzki 1986

CAK 1975

$k_{\mathrm{CAK}}, \alpha, \delta$ "force-multiplier parameter", with δ ionization parameter, O(0.1) under O-star conditions

$t = k_1^{-1}$ optical depth in Sobolev-approx., if line-strength identical with strength of Thomson-scattering ($=s_{\mathrm{e}}$) [correctly normalized]

n_{E} electron density in units of 10^{11} cm^{-3}

$W = 0.5(1 - \mu_*)$ dilution factor of radiation field

CF "finite cone angle correction factor", correction for non-radial photons

$$k_{CAK} = \frac{\int_0^\infty L(\nu)\nu f(\nu) d\nu}{L} \frac{v_{th}}{c} \frac{N_o}{\alpha(1-\alpha)},$$

if everything has been correctly normalized.

- for O-stars, k_{CAK} is of order 0.1
- k_{CAK} can be interpreted as the fraction of photospheric flux which would be blocked if ALL lines were optically thick, divided by α.
- a different parameterization has been suggested by Gayley (1995). Both parameterizations are consistent though.
- for line-driving in hot, pure H/He winds (first stars) one can show that $\alpha + \delta = 1$, i.e., $\delta \approx 0.33$.
- for all subtleties and further discussion, see Puls et al. 2000, A&ASS 141.

9.2 Theoretical predictions for line-driven winds

first hydro-solution developed by CAK 1975, ApJ 195, improved for non-radial photons and ionization effects by Pauldrach, Puls & Kudritzki 1986, A&A 164 and Friend & Abbott 1986, ApJ 311

had equation of motion

$$\mathrm{v}\left(1-\frac{\mathrm{v}_s^2}{\mathrm{v}^2}\right)\frac{d\mathrm{v}}{dr}=\frac{2\mathrm{v}_s^2}{\mathrm{r}}-\frac{d\mathrm{v}_s^2}{dr}+a^{\mathrm{ext}}(r)$$

$$a^{\mathrm{ext}}(r)=-\frac{GM}{r^2}(1-\Gamma)+\cancel{g_{\mathrm{Rad}}^{\mathrm{true\ cont}}}(r)+g_{\mathrm{Rad}}^{\mathrm{line}}(r)$$

for ‘normal’ winds

$$g_{\mathrm{Rad}}^{\mathrm{line}}(r)=f\cdot\frac{L}{r^2}k_1^{\alpha}$$

$$k_1=\frac{r^2\mathrm{v}d\mathrm{v}/dr}{\dot{M}/(4\pi)} \qquad f=f(r,\mathrm{v},\frac{d\mathrm{v}}{\mathrm{dr}},\dot{M}) \text{ if all subtleties included}$$

All together

$$\mathrm{v}\left(1-\frac{\mathrm{v}_s^2}{\mathrm{v}^2}\right)\frac{d\mathrm{v}}{dr}=-\frac{GM}{r^2}(1-\Gamma)+\frac{2\mathrm{v}_s^2}{\mathrm{r}}-\frac{d\mathrm{v}_s^2}{dr}+\frac{f\cdot L}{r^2}\left(\frac{\dot{M}}{4\pi}\right)^{-\alpha}\left(r^2\mathrm{v}\frac{d\mathrm{v}}{dr}\right)^{\alpha}$$

- non-linear differential equation
- has ‘singular point’ in analogy to solar wind
- $\mathrm{v}_{crit} \gg \mathrm{v}_s$ (100… 200 km/s)
- solution: iteration of singular point location/velocity, integration inwards and outwards

9.2.1 Approximate solution

(see also Kudritzki et al., 1989, A&A 219)

- supersonic → pressure terms vanish
- radially streaming photons → f $(4\pi)^\alpha$ → const

$$v\frac{dv}{dr} = -\frac{GM}{r^2}(1-\Gamma) + \frac{\text{const}\cdot L}{r^2}\dot{M}^{-\alpha}\left(r^2 v\frac{dv}{dr}\right)^\alpha$$

$\Rightarrow\; y + A = \text{const}\cdot L\cdot\dot{M}^{-\alpha}y^\alpha \quad\Rightarrow\quad y$ is constant

with $A = GM(1-\Gamma), \qquad y = r^2 v\dfrac{dv}{dr}$

graphical solution (Cassinelli et al. 1979, ARAA 17, Kudritzki et al. 1989)

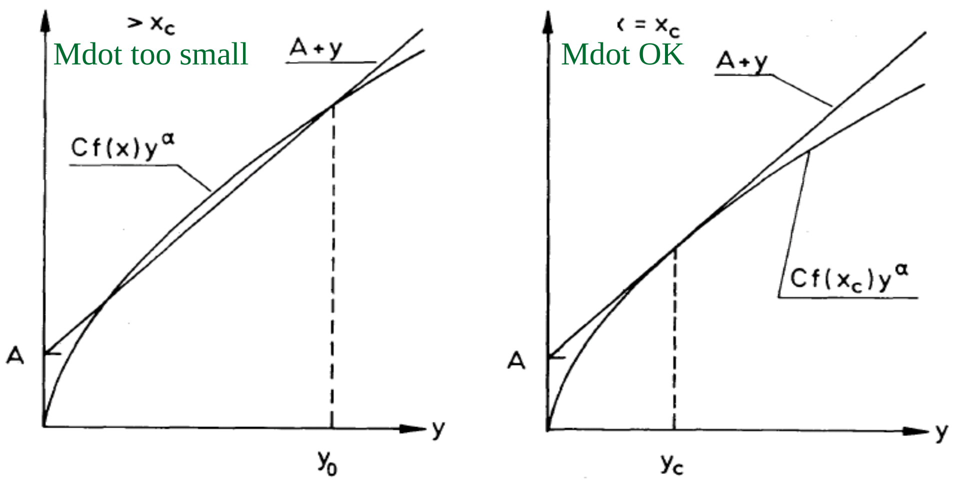

for unique solution, derivatives have to be EQUAL!

$y + A = \text{const}\cdot L\cdot\dot{M}^{-\alpha}y^\alpha$ equation of motion

and equality of derivatives

$1 = \text{const}\cdot L\cdot\dot{M}^{-\alpha}\alpha\, y^{\alpha-1}$ at critical point y_c

$$\dot{M}^{-\alpha} = \frac{1}{\text{const}\cdot L\cdot\alpha}y_c^{1-\alpha}$$

in equation of motion at critical point

$y_c + A = \dfrac{1}{\alpha}y_c, \qquad$ i.e., $y_c\left(1-\dfrac{1}{\alpha}\right) = -GM(1-\Gamma)$

$$y_c = \frac{\alpha}{1-\alpha}GM(1-\Gamma) \overset{!}{=} y$$

finally …

Scaling relations for line-driven winds (without rotation)

- $\dot{M} \propto N_{\text{eff}}^{\frac{1}{\alpha'}} L^{\frac{1}{\alpha'}} \left(M(1-\Gamma)\right)^{1-\frac{1}{\alpha'}}$ scaling law for $\dot{M}$
- $r^2 \mathrm{v} \dfrac{d\mathrm{v}}{dr} = \dfrac{\alpha}{1-\alpha} GM(1-\Gamma)$

  $\rightarrow$ Integration between ∞ and R_*
- $\mathrm{v}(r) = \mathrm{v}_\infty \left(1 - \dfrac{R_*}{r}\right)^\beta, \quad \beta = \begin{cases} 0.5 \text{ for approx. solution, "CAK-velocity law"} \\ 0.8 \text{ (O-stars) ... 2 (BA-SG), see next slide} \end{cases}$
- $\mathrm{v}_\infty = \left(\dfrac{\alpha}{1-\alpha}\right)^{\frac{1}{2}} \left(\dfrac{2GM(1-\Gamma)}{R_*}\right)^{\frac{1}{2}}$ scaling law for v_∞
- $\rightarrow \mathrm{v}_\infty \approx 2.25 \dfrac{\alpha}{1-\alpha} \mathrm{v}_{\text{esc}},$ if all subtleties included

Γ Eddington factor, accounting for acceleration by Thomson-scattering, diminishes effective gravity

N_{eff} number of lines effectively driving the wind ($\propto k_{\text{CAK}}$), dependent on metallicity and spectral type

α exponent of line-strength distribution function, $0 < \alpha < 1$
large value: more optically thick lines

$\alpha' = \alpha - \delta$, with δ ionization parameter, typical value for O-stars: $\alpha' \approx 0.6$

NOTE

From $y_c = y = const$ follows from the

CAK velocity law

$$v(r) = v_\infty \left(1 - \frac{R_*}{r}\right)^{\frac{1}{2}}$$

$$\tau_S \sim \frac{k_L \rho}{dv/dr} \sim \frac{1}{y} = const!!!$$

- this basically explains why resonance lines remain optically thick also in the outer wind part
- generalized velocity law
  - from consistent solution
  - from 'β-velocity law'

$$v(r) = v_\infty \left(1 - \frac{R_*}{r}\right)^{\beta}, \quad \text{in most cases } \beta = 0.8...1.3$$

... consistent solution
of complete equation
–- β=0.8 velocity law
+ photospheric structure
(see Santolaya Rey,
Puls, & Herrero, 1997,
A&A, 488)
with same mass-loss rate
and terminal velocity as
in consistent solution

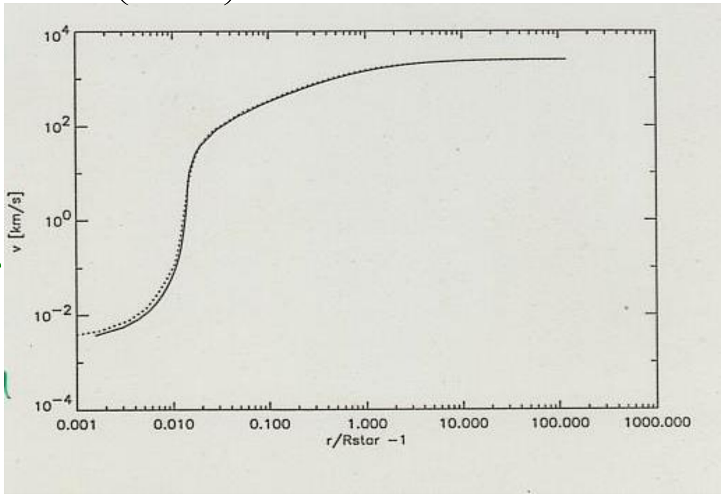

consistent solution

- inclusion of finite cone-angle and $(n_E/W)^\delta$ term:
  Pauldrach, Puls & Kudritzki (1986) and Friend & Abbott (1986)
- major effect
  y no longer constant,
  steeper slope in subcritical,
  flatter slope in supercritical wind
- critical point closer to photosphere
  – lower Mdot, larger vinf

"Cooking recipe" by Kudritzki et al. (1989, A&A 219)

- very fast calculation of Mdot, vinf for given force-multiplier parameters

- use scaling relations for Mdot and v_∞, calculate
  modified wind-momentum rate

$$\dot{M}\, v_\infty \propto N_{\mathrm{eff}}^{1/\alpha'}\, L^{1/\alpha'} \big(M(1-\Gamma)\big)^{1-1/\alpha'} \frac{\big(M(1-\Gamma)\big)^{1/2}}{R_*^{1/2}}$$

$$\dot{M}\, v_\infty\, R_*^{1/2} \propto N_{\mathrm{eff}}^{1/\alpha'}\, L^{1/\alpha'} \cancel{\big(M(1-\Gamma)\big)^{3/2-1/\alpha'}}$$

9.2.2 The wind-momentum luminosity relation (WLR)

- use scaling relations for Mdot and v_∞, calculate

modified wind-momentum rate

$$\dot{M}\, v_\infty R_*^{1/2} \propto N_{\mathrm{eff}}^{1/\alpha'} L^{1/\alpha'} \qquad \text{since } (\alpha' \approx \frac{2}{3})$$

independent of M and Γ!!!!!

$$\boxed{\log(\dot{M}\, v_\infty R_*^{1/2}) \approx \frac{1}{\alpha'} \log L + const(z,\ \text{sp.type})}$$

▸ stellar winds contain info about stellar radius!!!

(Kudritzki, Lennon & Puls 1995)

- (at least) two applications

(1) construct observed WLR, calibrate as a function of spectral type and metallicity (N_{eff} and α' depend on both parameter)

– **independent tool to measure extragalactic distances** from *wind-properties*, *T*eff and metallicity

(2) compare with theoretical WLR to test validity of radiation driven wind theory

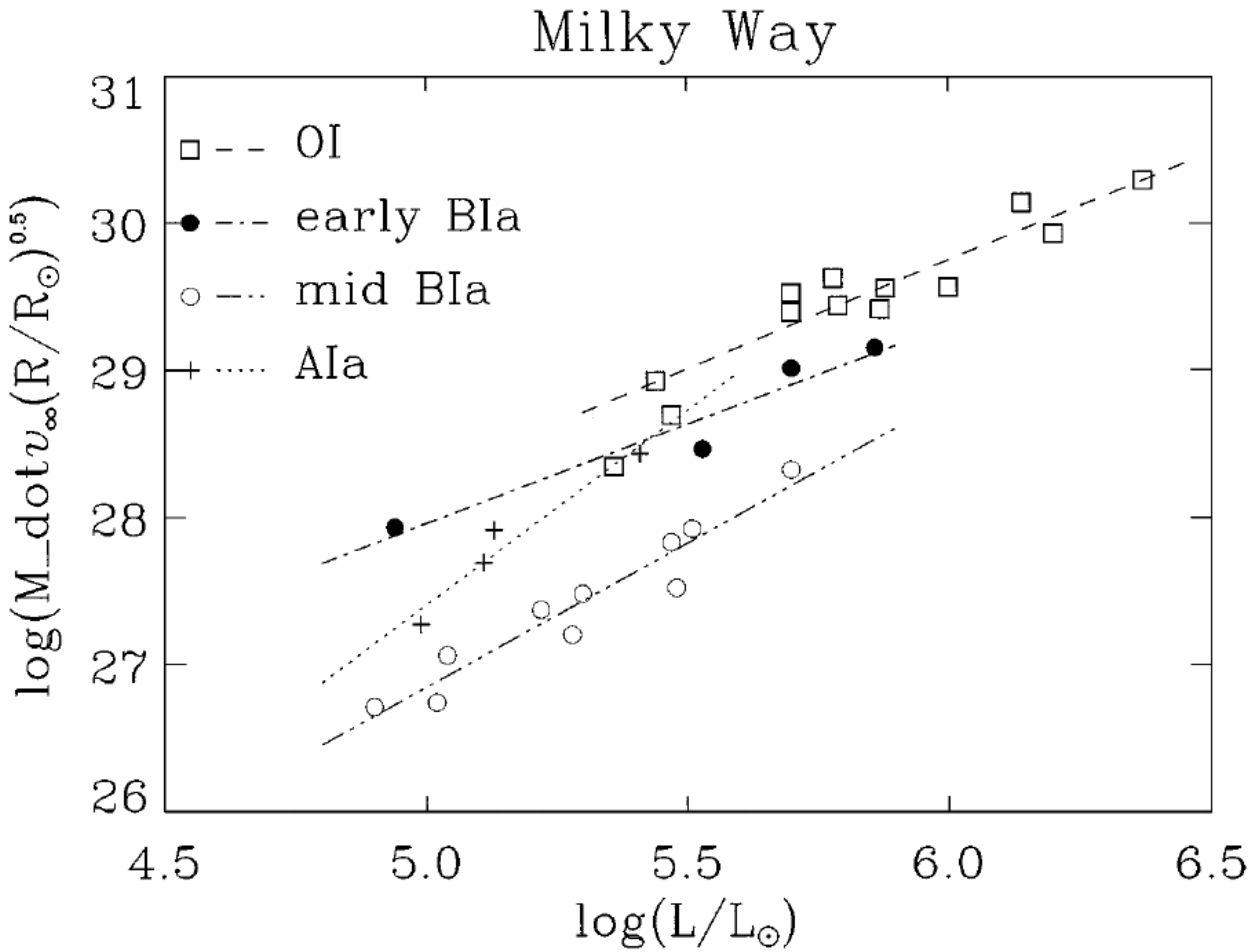

Modified wind momenta of Galactic O-, early B-, mid B- and A-supergiants as a function of luminosity, together with specific WLR obtained from linear regression. (From Kudritzki & Puls, 2000, ARAA 38).

9.2.3 Why α ≈ 2/3?

Simple, however interesting argument
(cf. Puls et al., 2000, A&ASS141)

Remember

$$\frac{dN(k)}{dk} \propto -k^{\alpha-2}, \qquad k \propto \frac{n_{abs}}{\rho} \underbrace{\frac{\pi e^2}{m_e c} f}_{\text{cross section}}$$

for resonance lines *k* ~ *f*
(lower level = ground state of ion)

The most simple case: The hydrogen atom

'Kramersformula' for resonance lines, from Q.M.

$$f(1,n) = \frac{32}{3\sqrt{3}\pi}\left(1-\frac{1}{n^2}\right)^{-3}\frac{1}{n^3} \approx \frac{C}{n^3}$$

(summed over all contributing angular momenta)

Number of lines until principal quantum number $n_{\max}$:

$$N(n_{\max}) = n_{\max} - 1$$

$$f(n_{\max}) = \frac{C}{n_{\max}^3}$$

$$n_{\max} = \left(\frac{C}{f(n_{\max})}\right)^{\frac{1}{3}}$$

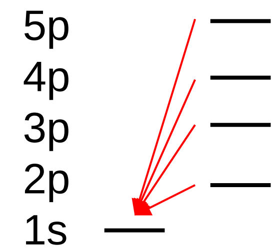

example: 4 resonance lines until n=5

$$N(f > f(n_{\max})) = C^{\frac{1}{3}}\left(f(n_{\max})\right)^{-\frac{1}{3}} - 1$$

= number of lines with f-values larger than a given one

$\Rightarrow$ distribution function

$$\boxed{\frac{dN}{df} \propto -f^{-\frac{4}{3}}}$$

powerlaw, compare with

$$\frac{dN}{dk} \propto -k^{\alpha-2}$$

$$\Rightarrow \alpha = \frac{2}{3} \quad !!!$$

- inclusion of other (non hydrogenic) ions (particularly from iron group elements) complicates situation
- general trend: α decreases !

9.2.4 Predictions from line statistics

Let *Z* be the (global) abundance relative to its solar value, i.e., solar comp. is *Z* =1

- number of effective lines scales (roughly) with $Z^{1-\alpha}$
  - more metallicity => more lines
- **consequence**

  both mass-loss and wind-momentum should scale with

$$Z^{\frac{1-\alpha}{\alpha'}} \approx \sqrt{Z} \quad \text{for } \alpha,\alpha' \approx 2/3 \text{ (O-type winds)}$$

$$\ldots Z^{1.5} \quad \text{for } \alpha,\alpha' \approx 0.4 \text{ (A-type winds)}$$

- example for Z=0.2 (≈ SMC abundance)
  - Mdot (40kK) factor of 0.45 decrease
  - Mdot (10kK) factor of 0.09 decrease

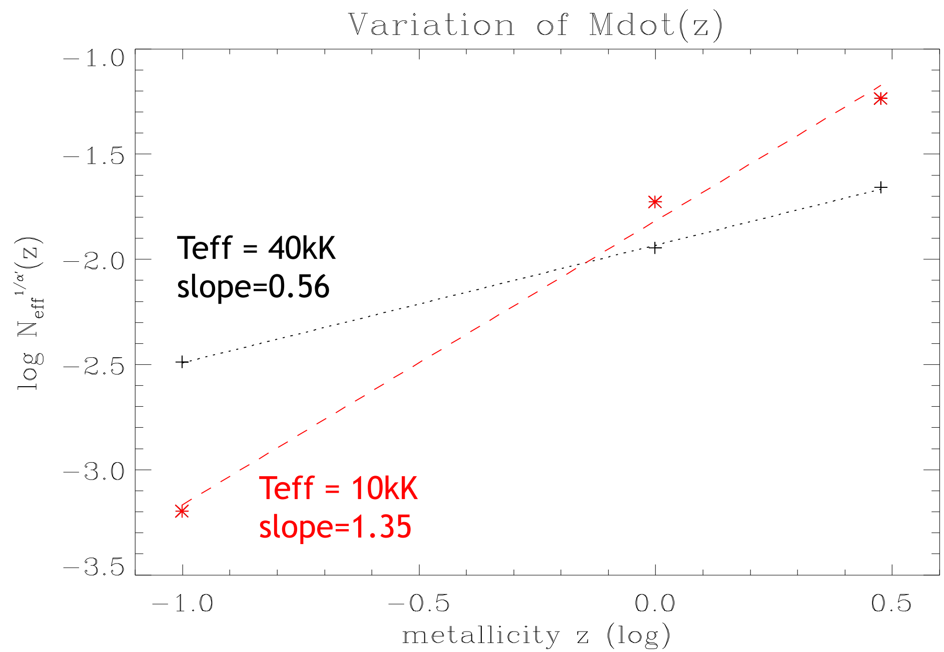

adapted from Puls et al., 2000, A&ASS 141

Predictions from line statistics

- Differential importance of Fe-group and lighter elements (CNO)
  - cf. Pauldrach 1987; Vink et al. 1999, 2001; Puls et al 2000; Kriticka 2005
  - lines from Fe group elements dominate acceleration of lower wind

    $\rightarrow$ determine mass-loss rate Mdot
  - lines from light elements (few dozens!) dominate acceleration of outer wind

    $\rightarrow$ determine terminal velocity v_∞

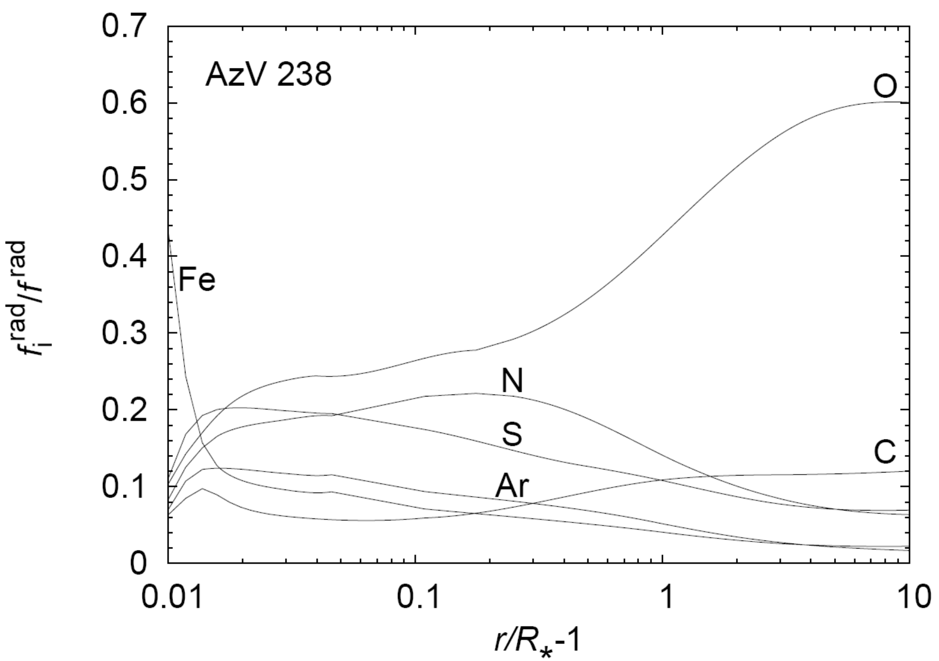

From Kritcka, 2005

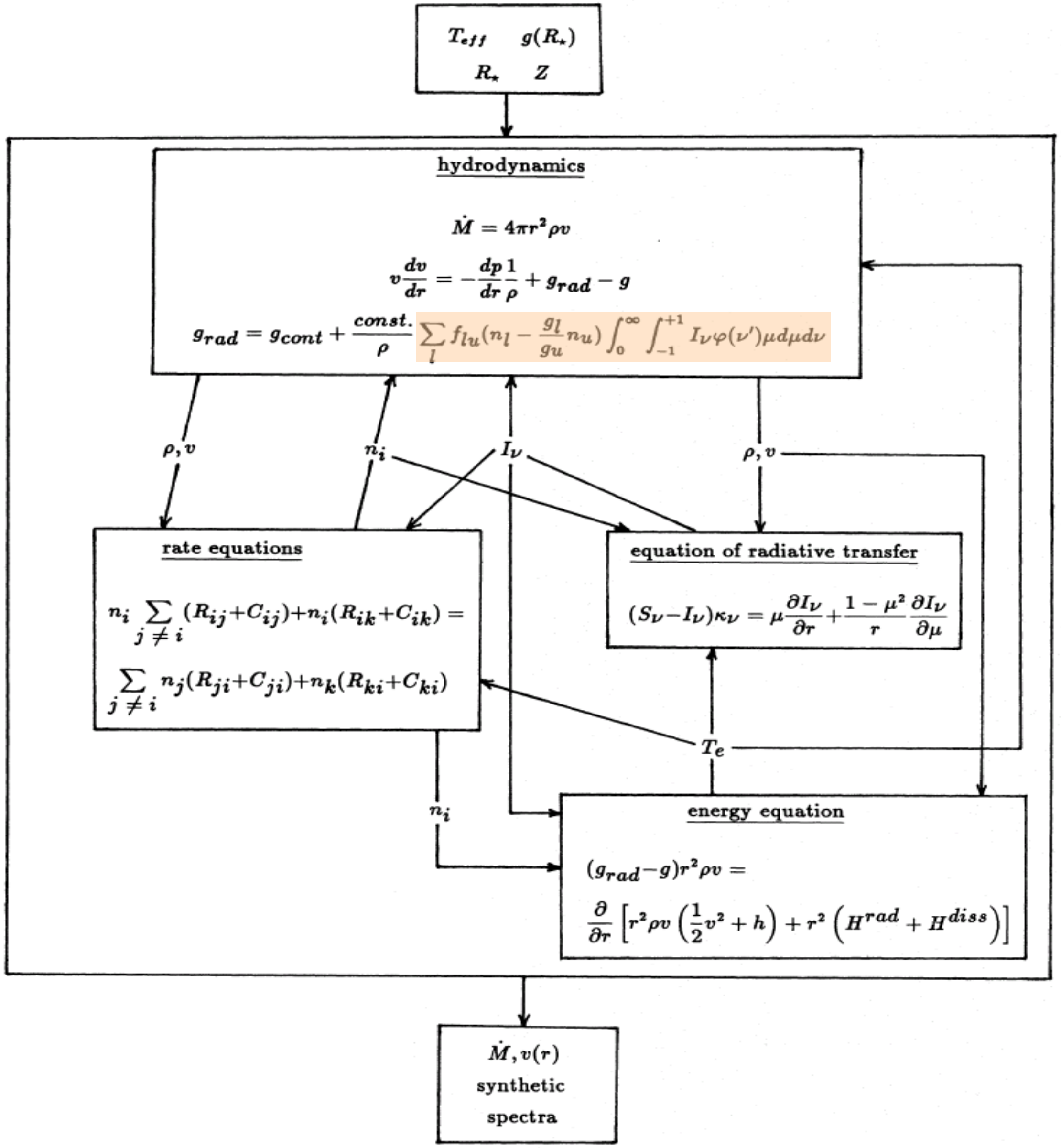

- Pauldrach (1987) and
  Pauldrach et al. (1994/2001): "WM-basic"
  consistent hydrodynamic solution, force-multiplier from regression to NLTE line-force
- NLTE, since strong radiation field and low densities
- 150 ions in total (≈ 2 MegaLines), reduced computational effort due to Sobolev line transfer
- since 2001, line-blocking/blanketing and multi-line effects included

From Pauldrach et al (1994)

(see also Pauldrach et al. 2001 for inclusion of line-blocking/blanketing)

- Vink et al. (2000/2001)
  - Monte-Carlo approach following Abbott & Lucy (1985):
  - derive (iterate) Mdot from **global** energy conservation

$$\frac{1}{2}\dot{M}\,(v_\infty^2 + v_{esc}^2) = L(R_*) - L(\infty)$$

input: $v_\infty, v_{esc}, \beta, L(R_*), \dot{M}_i$

calculate via Monte-Carlo: $L_i(\infty)$

calculate new estimate: $\dot{M}_{i+1}$ from $L_i(\infty)$, update occupation numbers, calculate $L_{i+1}(\infty)$

iterate until $\dot{M}_i$ converges

  - occupation numbers: NLTE, with Sobolev line transfer
  - advantage: precise treatment of multi-line scattering
  - disadvantage: only scattering processes can be considered,
    no line-blocking/blanketing in NLTE
- Krticka & Kubat (2000/2001/2004), Krticka 2006
  - similar approach as Pauldrach et al., but
    - disadvantage: no line-blocking, no multi-line effects
    - advantage: more component description (metal ions + H/He)
    - allows to investigate de-coupling in stationary wind-models
- Kudritzki (2002, based on Kudritzki et al. 1989)
  - “cooking recipe” coupled with approx. NLTE, very fast
    - allows for depth-dependent force-multiplier parameters

Validity of WLR concept

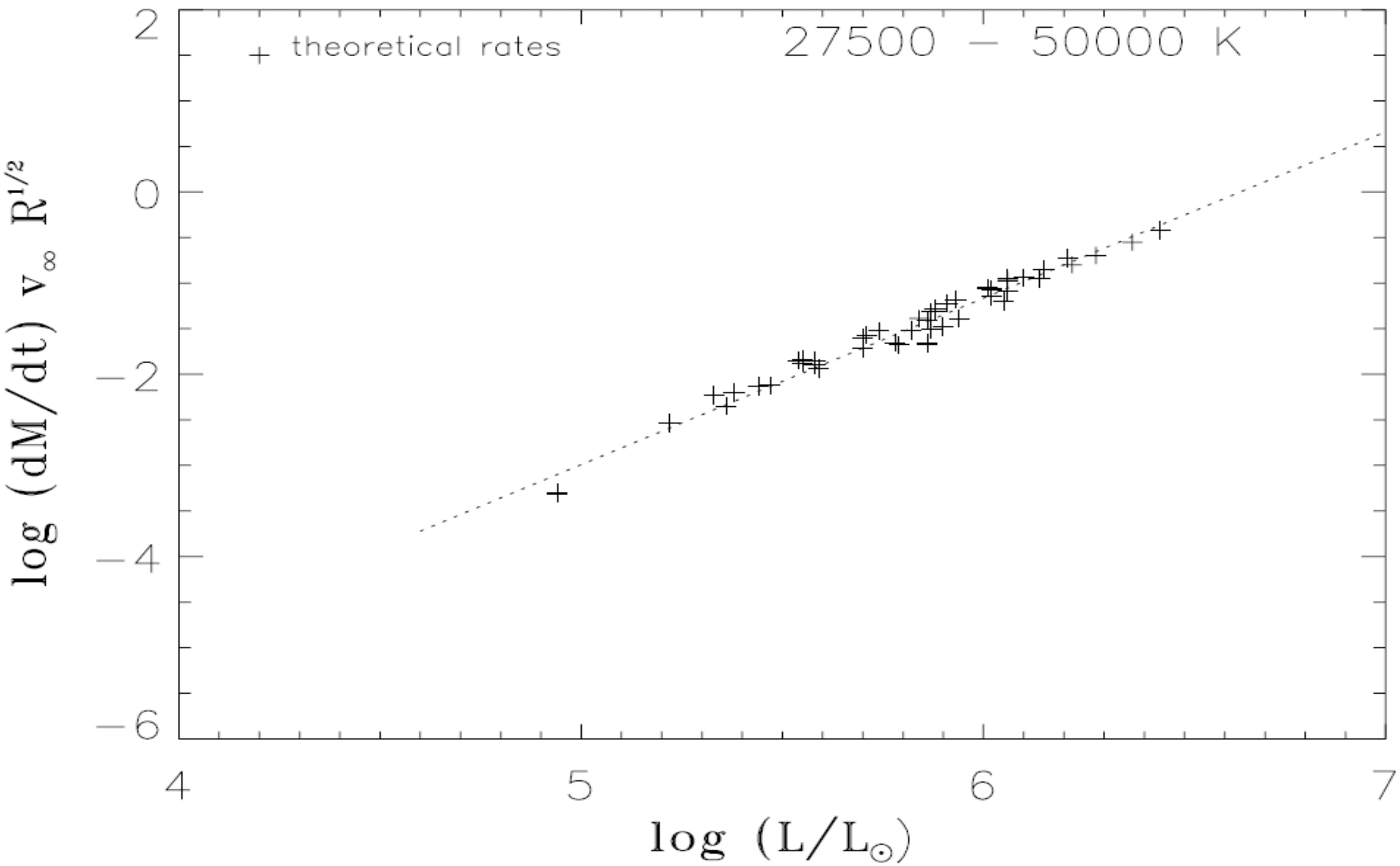

Theoretical wind-momentum rates as a function of luminosity, as calculated by Vink et al. (2000). Though multi-line effects are included, the WLR concept (derived from simplified arguments) holds!

Consistency of different codes

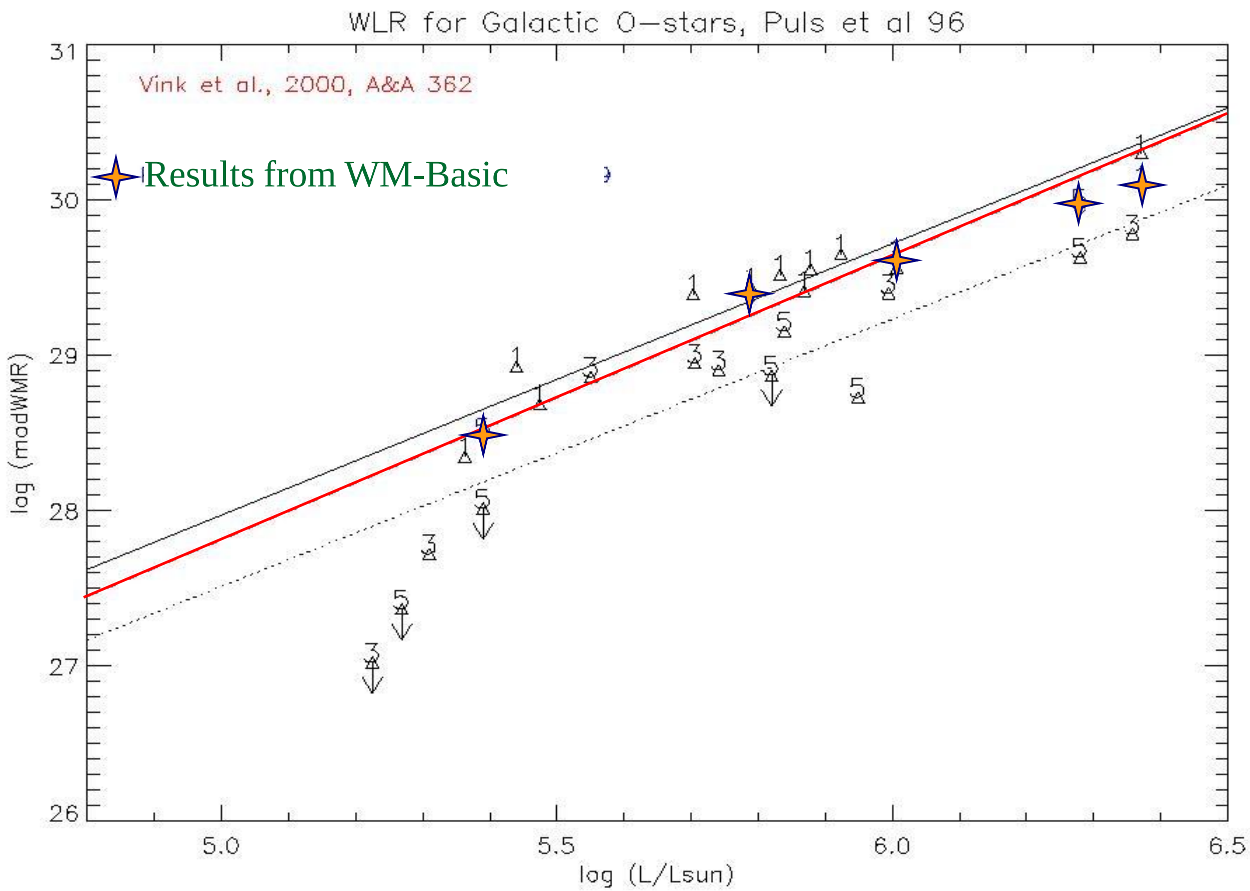

From Puls et al. 2003 (IAU Symp. 212)

9.2.6 Predictions from hydrodynamical models

- OB stars:
  - Vink et al. (2000): “Mass-loss recipe” for solar abundances

    in agreement with independent models $v_\infty \propto z^{0.12}$
    - by Kudritzki (2002), with
    - by Puls et al. (2003), using WM-Basic (A. Pauldrach and co-workers)
    - by Krticka & Kubat (2004)

  - Vink et al. (2001): $\dot{M} \propto z^{0.69}$ for O-stars,

    $\dot{M} \propto z^{0.64}$ for B-supergiants

  - Krticka (2006): $\dot{M} \propto z^{0.67}$ for O-stars

    $v_\infty \propto z^{0.06}$

Summary Chap. 9

- radiative line acceleration:

$$g_{\mathrm{rad}} \propto \frac{\mathrm{dv}}{\mathrm{d}r} \text{ for optically thick lines, } \propto \left(\frac{\mathrm{dv}}{\mathrm{d}r}\right)^{\alpha} \text{ for ensemble of lines}$$

Doppler-effect!

- scaling relations for line-driven winds

$$\mathrm{v}_{\infty} \propto \mathrm{v}_{\mathrm{esc}}$$

$$\dot{M} \propto L^{\frac{1}{\alpha'}} M_{\mathrm{eff}}^{1-\frac{1}{\alpha'}}$$

$$\mathrm{v}(r) = \mathrm{v}_{\infty}(1 - \frac{R_*}{r})^{\beta}$$

- wind-momentum luminosity relation (WLR)

$$\log \dot{M} \mathrm{v}_{\infty} (R / R_{\odot})^{\frac{1}{2}} = x \log L / L_{\odot} + D$$

  - mass-dependency vanishes or weak, since 1/x= α´≈0.6 (for OB-stars)
  - offset D (and, to a lesser extent, slope x) depend on spectral type and metallicity

- predictions from theoretical models
  - metallicity dependence

Determine atmospheric parameters from observed spectrum

Required

T_{eff}, log g, R, Y_{He}, Mdot, v_∞, β (+ metal abundances)
(R stellar radius at $\tau_R = 2/3$)

also necessary

v_{rad} (radial velocity)
v sin i (projected rotational velocity)

Given

- *reduced* optical spectra (eventually +UV, +IR, +X-ray)
- λ/Δλ, resolution of observed spectrum
- Visual brightness V
- distance d (from cluster/association membership), partly rather insecure
- NLTE-code(s), "model grid"

1. Rectify spectrum, i.e. divide by continuum (experience required)

2. Shift observed spectrum to lab wavelengths (use narrow **stellar** lines as reference):

$$\lambda_{\mathrm{lab}} \approx \lambda_{\mathrm{obs}} \left(1 - \frac{v_{\mathrm{rad}}}{c}\right), \quad v_{\mathrm{rad}} \text{ assumed as positive if object moves away from observer}$$

- **Alternative set of parameters**

  L, M, R *or*
  L, M, T_{eff} *or*
  T_{eff}, log g, R …

- **interrelations**

$$L = 4\pi R_*^2 \sigma_B T_{\mathrm{eff}}^4$$

$$g = \frac{GM}{R_*^2}$$

- **Useful scaling relations**

  If L, M, R in *solar units*, then

$$R_* = \frac{L^{0.5}}{T_{\mathrm{eff}}^2} \cdot 3.327 \cdot 10^7$$

$$\log g = \log\left(\frac{M}{R_*^2} \cdot 2.74 \cdot 10^4\right)$$

$$v_{\mathrm{esc}} = \sqrt{R_* g (1-\Gamma) \cdot 1.392 \cdot 10^{11}}$$

$$\Gamma = s_e T_{\mathrm{eff}}^4 / g \cdot 1.8913 \cdot 10^{-15}$$

$$s_e = 0.4 \frac{1 + I_{\mathrm{He}} Y_{\mathrm{He}}}{1 + 4 Y_{\mathrm{He}}}$$

with I_{He} number of free electrons per Helium atom (e.g.,=2, if completely ionized)

rectified
optical spectrum,
("blue" and "red")
corrected for v_{rad},
of the late O-SG
19 Cep

___ Hydrogen
...... Helium I
- - - Helium II

in "red":
"strategic" lines to derive atmospheric parameters in hot stars

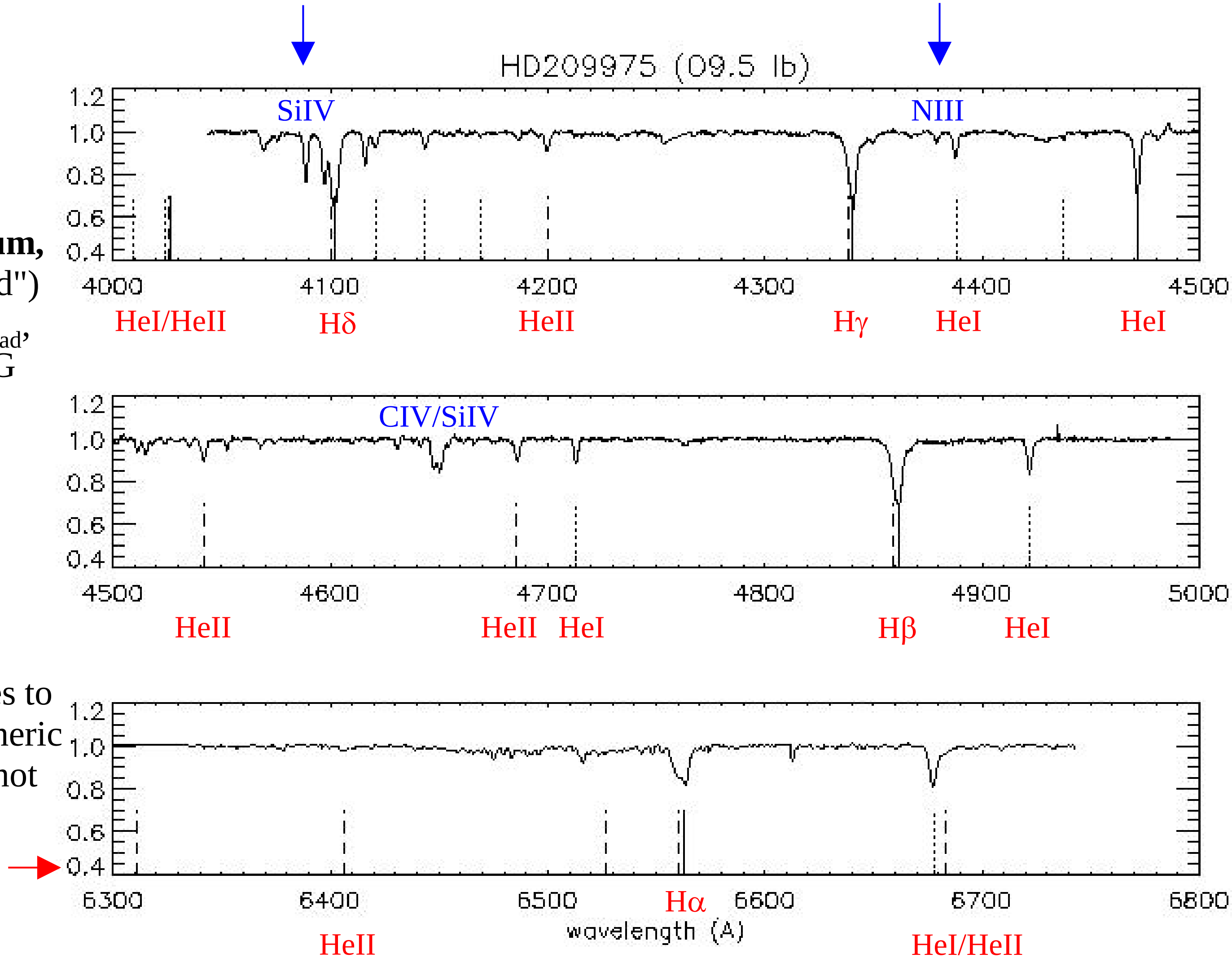

remember equivalent width $W_\lambda = \int\limits_{\text{line}} \frac{H_{\text{cont}} - H_{\text{line}}(\lambda)}{H_{\text{cont}}} d\lambda = \int\limits_{\text{line}} \left(1 - R(\lambda)\right) d\lambda,$

area of profile under continuum, $\dim[W_\lambda]$ = Angstrom or milliAngstrom, mÅ

corresponds to width of saturated profile ($R(\lambda) = 0$) with same area

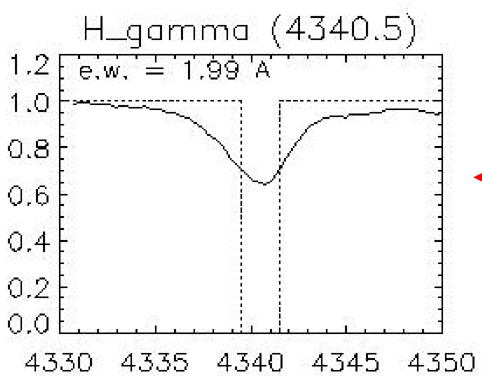

strong line

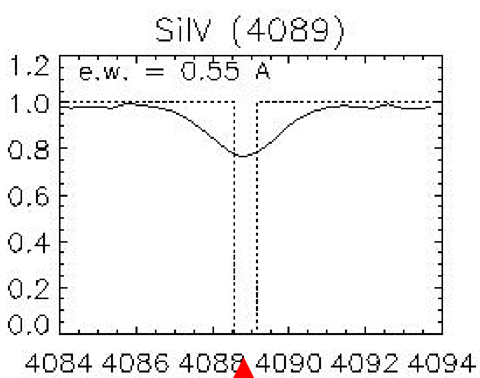

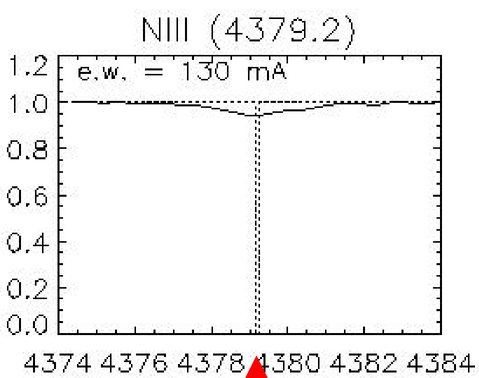

intermediate line

weak line

Determine projected rotational speed v sin i

Use weak metal lines
to derive v sin i:
Convolve theoretical line
with rotational profile.

Convolve finally with
instrumental profile
(~ Gauss) according
to spectral resolution

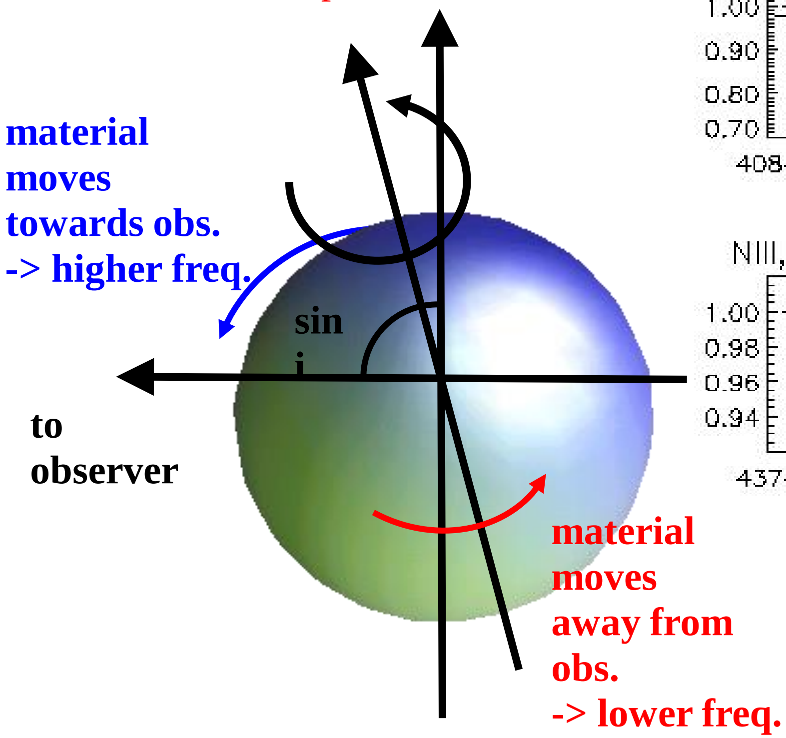

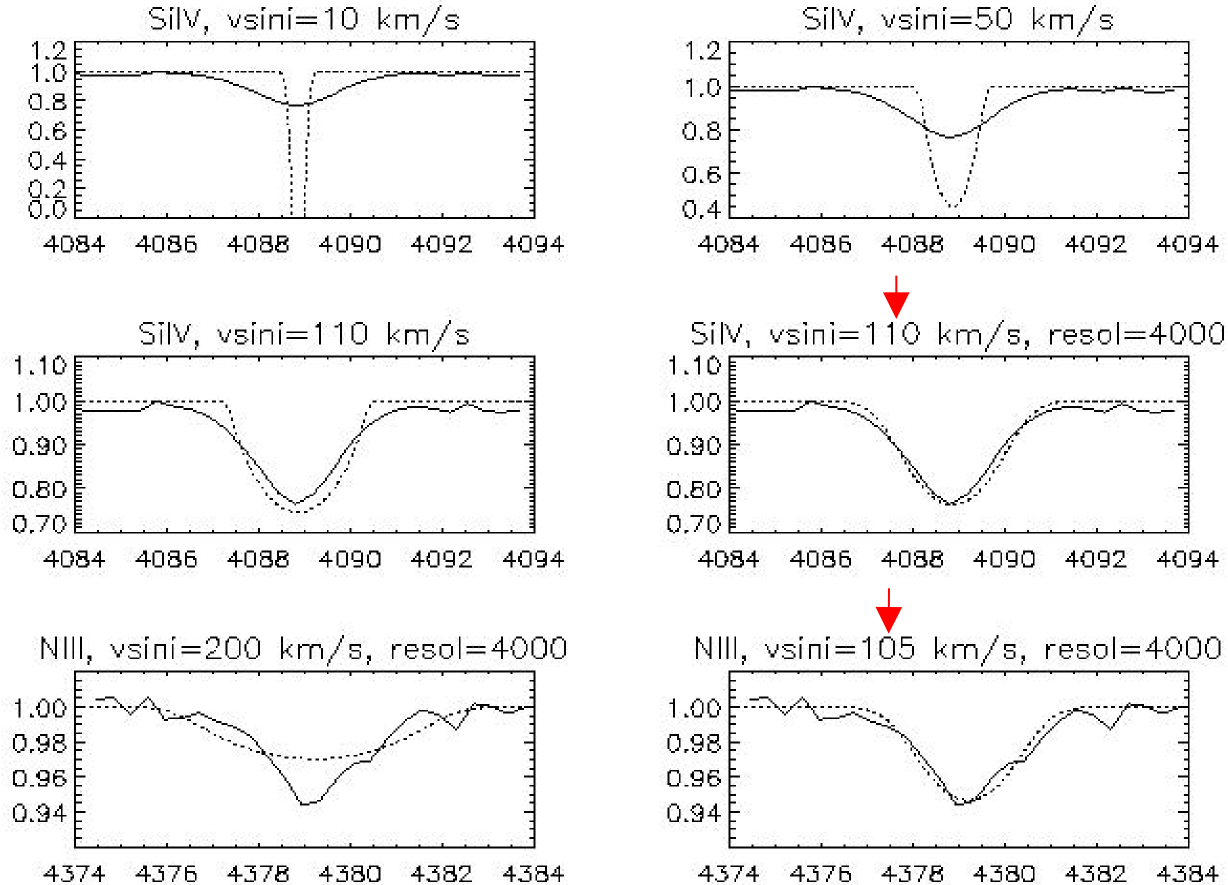

Convolution with rotational and instrumental profile conserves equivalent width!!!

Hγ - log g and T_{eff}

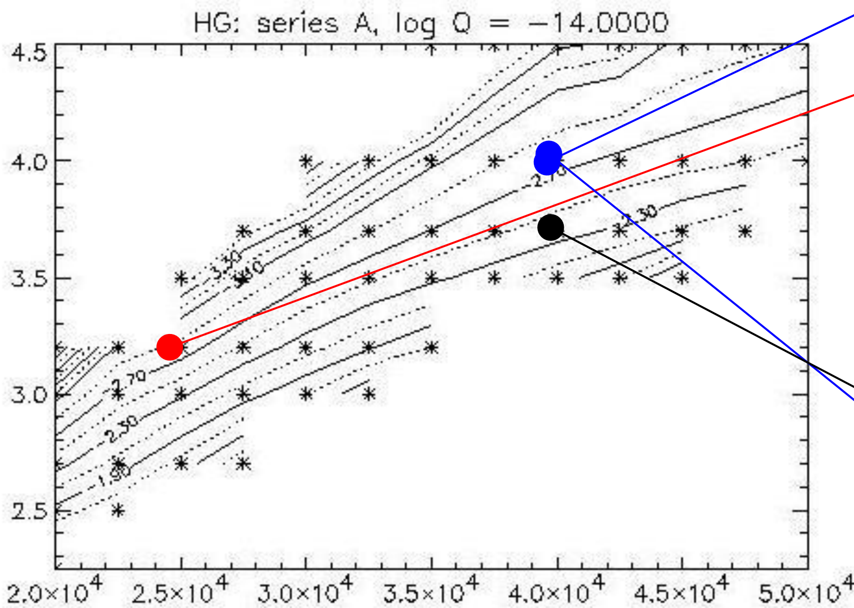

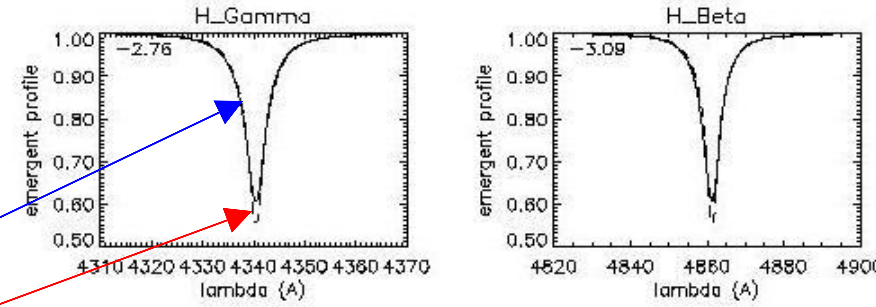

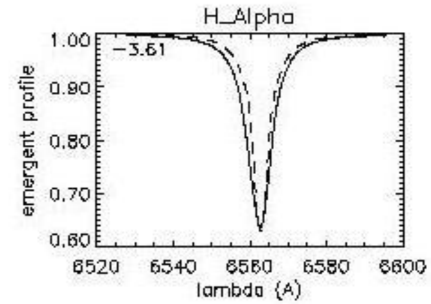

degeneracy of profiles:
(almost) identical lines for
T_{eff} =40,000 and log g=4.0
and
T_{eff} =25,000 and log g=3.2

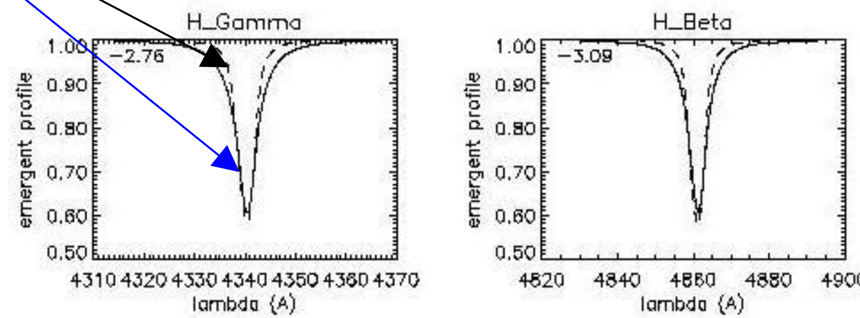

Iso-contours of equiv. widths for Hγ (from model grid),
for solar Helium abundance and (very) thin winds

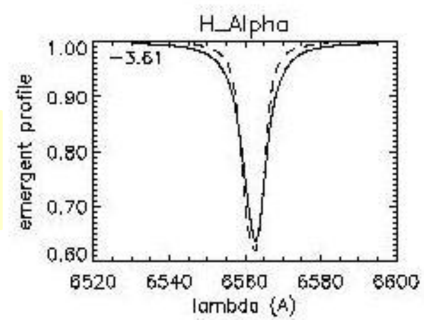

to derive T_{eff}, log g and Y_{He},
at least 3 lines have to be fitted in parallel
(if no wind is present):

Hγ defines **log g** (for given T_{eff})
HeII/HeI define $\mathbf{T_{eff}}$ (for given log g)
absolute **strength of He lines** define $\mathbf{Y_{He}}$

usually, wind emission has to be accounted for (profiles shallower)

wings of Balmer lines
(Stark-broadened)
react strongly on electron-density (as a function of τ)
=> perfect gravity indicator

Coarse fit - analysis of equivalent widths

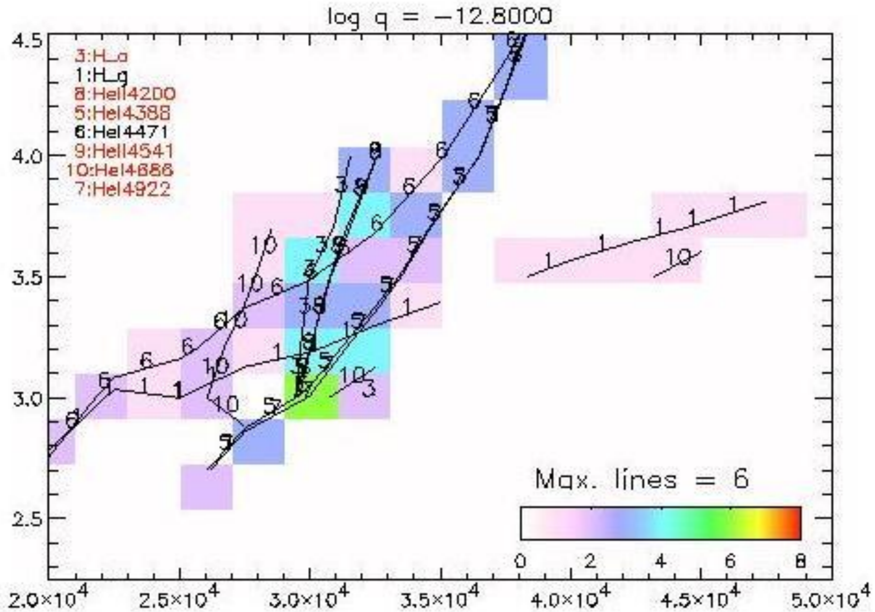

Fit diagram for Y_{He} = 0.1 (best fit at log Q = -12.8)

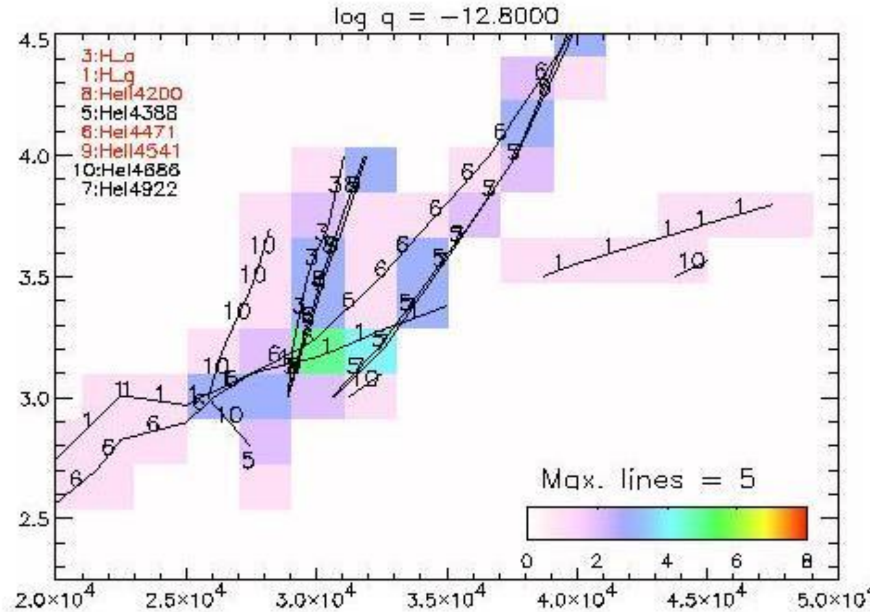

Fit diagram for Y_{He} = 0.15 (best fit at log Q = -12.8)

Measured equivalent widths

Balmer lines	HeI	HeII
Hγ 1.99	4387 0.32	4200 0.25
Hα 1.33	4471 0.86	4541 0.31
	4922 0.46	4686 0.27

Note: Hα and HeII 4686 mass-loss indicators

Result: $T_{eff} \approx$ 30,000 K, log g ≈ 3.0 ...3.2, $Y_{He} \approx$ 0.10 ... 0.15, log Q ≈ -12.8

Fit diagram constructed from model grid with

$$20{,}000\text{ K} < T_{eff} < 50{,}000\text{ K with } \Delta T = 2{,}500\text{ K}$$

$$2.2 < \log g < 4.5 \text{ with } \Delta\log g = 0.25$$

$$-14 < \log Q < -11 \text{ with } \Delta\log Q = 0.3,\ Y_{He} = 0.10, 0.15, 0.20$$

Note: Wind parameters can be cast into one quantity

$$\log Q = \frac{\dot{M}}{(R_* v_\infty)^{1.5}}$$

For same values of Q (albeit different combinations of Mdot, v_∞ and R_*), profiles look almost identical!

P Cygni profile formation and v_∞

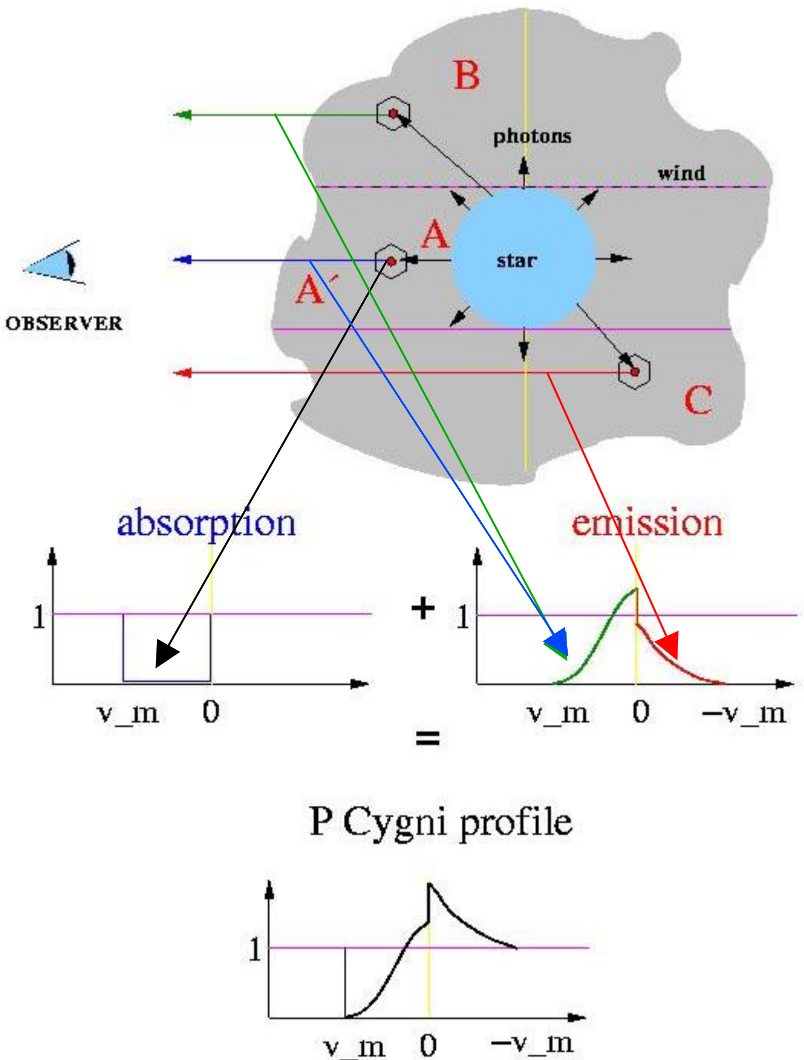

$$\nu_{obs} = \nu_0 \left(1 + \frac{\mu v(r)}{c}\right); \quad \nu_0 \text{ line frequency in CMF}$$

DOPPLER-EFFECT!!!

$\mu v(r) > 0: \quad \nu_{obs} > \nu_0$ blue side

$\mu v(r) < 0: \quad \nu_{obs} < \nu_0$ red side

$$\frac{v_m}{c} = \frac{\nu_{max} - \nu_0}{\nu_0} = 1 - \frac{\lambda_{min}}{\lambda_0}$$

NOTE: Absorption/Reemission in

atomic = fluid frame

at $\nu = \nu_o \pm \Delta\nu, \quad \Delta\nu \ll \nu_{max} - \nu_o$

Note: interpretation of $v_{max} \approx v_\infty$ (wind) requires large interaction probability $\sim 1\text{-}\exp(-\tau)$, i.e., optical depth τ must be large at large radii and low densities ????

P Cygni profile formation and v_∞

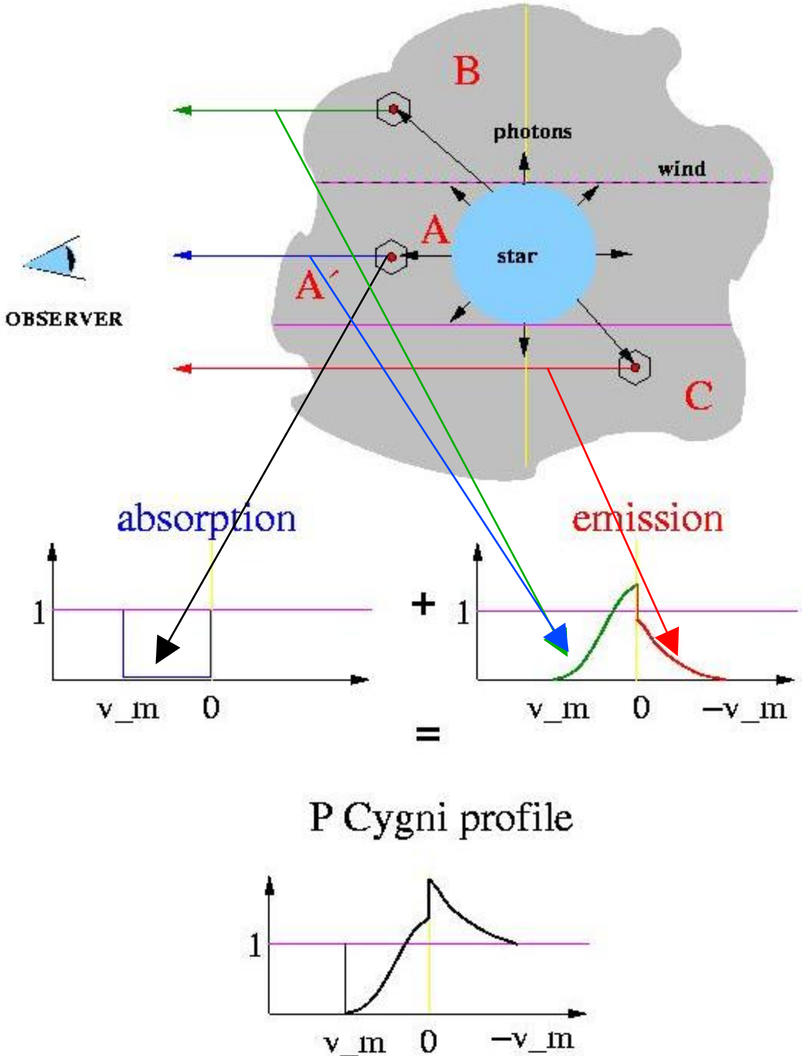

$$\nu_{\rm obs} = \nu_0 \left(1 + \frac{\mu v(r)}{c}\right); \quad \nu_0 \text{ line frequency in CMF}$$

DOPPLER-EFFECT!!!

$\mu v(r) > 0: \quad \nu_{\rm obs} > \nu_0$ blue side

$\mu v(r) < 0: \quad \nu_{\rm obs} < \nu_0$ red side

$$\frac{v_m}{c} = \frac{\nu_{\max} - \nu_0}{\nu_0} = 1 - \frac{\lambda_{\min}}{\lambda_0}$$

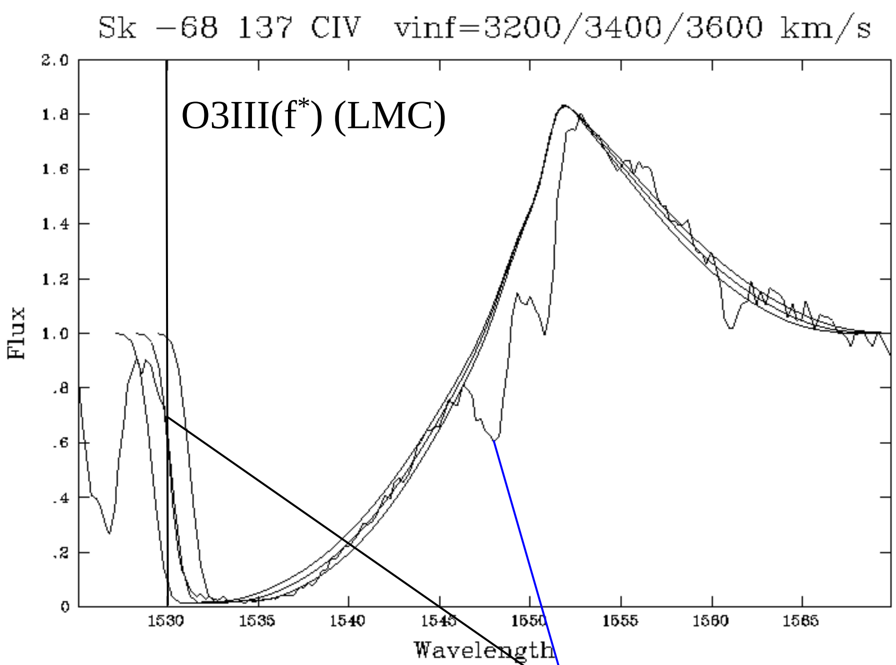

$$v_m \approx 2.998 \cdot 10^5 \left(1 - \frac{1530}{1548}\right) \approx 3{,}480 \text{ km/s}$$

Determination of terminal velocity from UV-P Cygni profiles

observation with IUE (International Ultra- violet Explorer)
no longer active

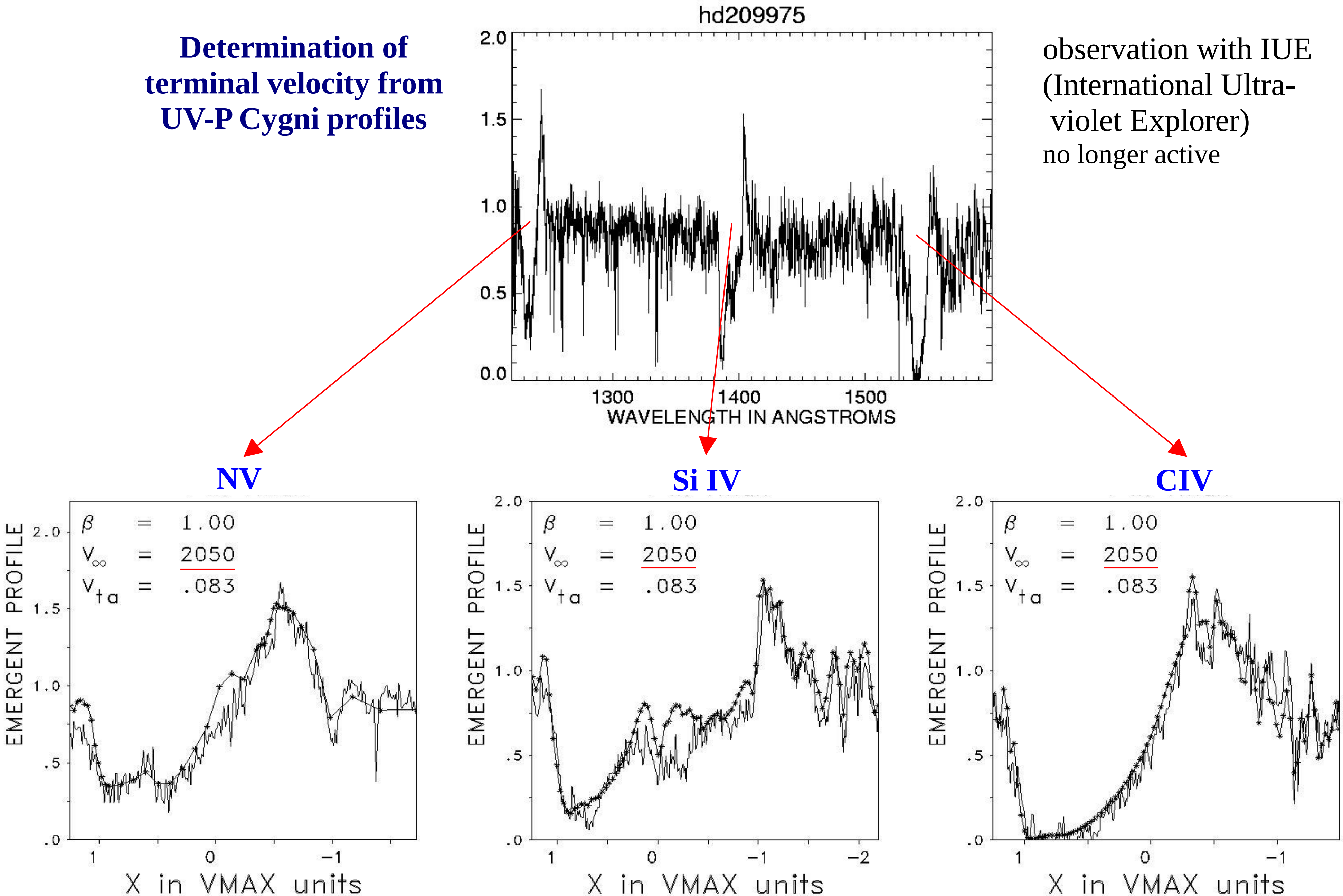

Fine fit - detailed comparison of line profiles

___ Hydrogen
...... Helium I
- - -Helium II

indicated lines used for fits

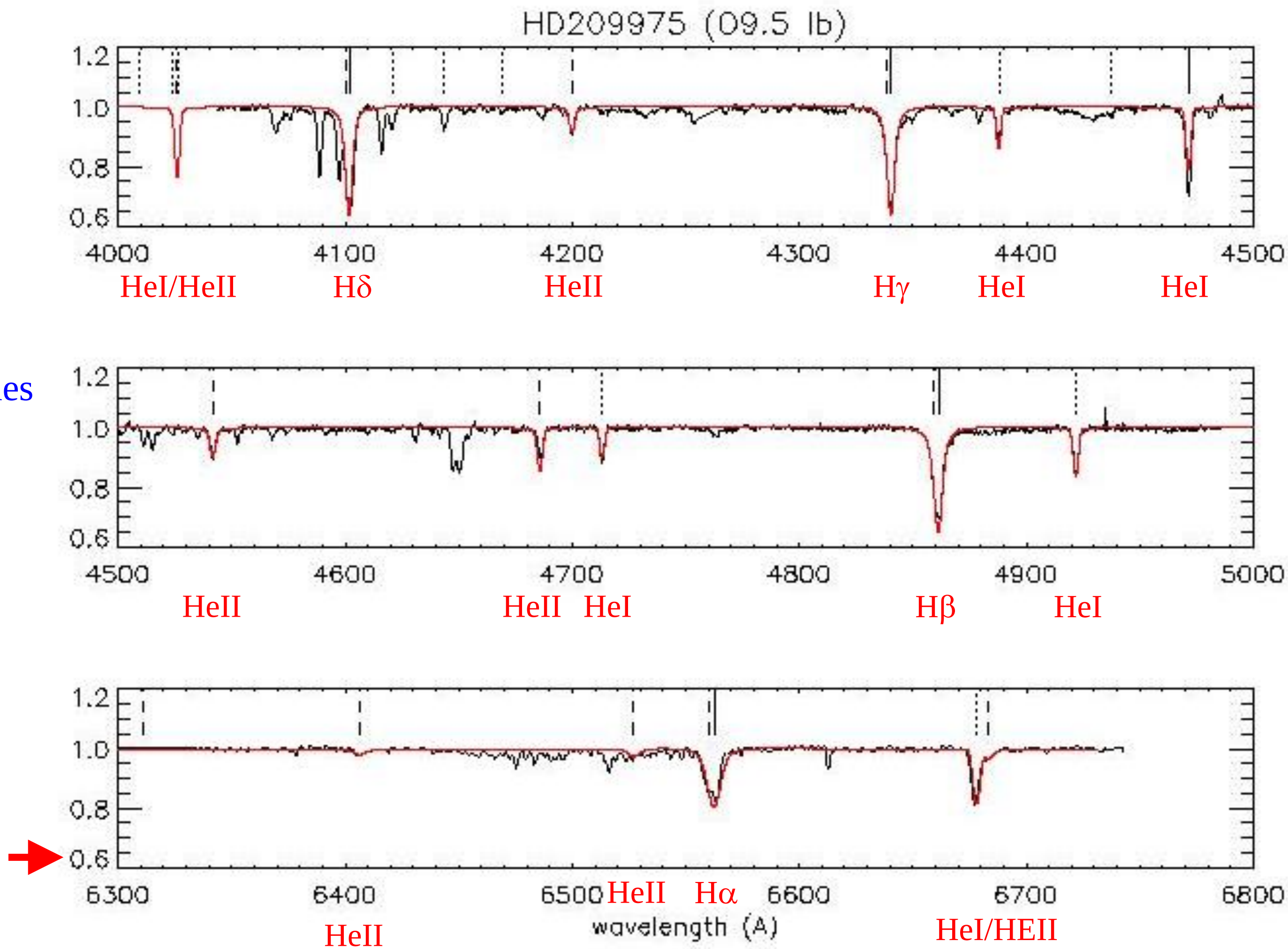

derived parameters

T_{eff} = 31,000 K
log g = 3.17
log Q = -12.87
Y_{He} = 0.10
β = 1.0

with v_∞ = 2050 km/ s we have

$$\log(\dot{M}/R_*^{1.5}) = -7.9$$

Determination of stellar radius – if it cannot be resolved

- **IF** *you believe in stellar evolution*
  - use **evolutionary tracks** to derive M from (measured) T_{eff} and log g **=> R**
  - transformation of conventional HRD into log T_{eff} - log g diagram required
  - problematic for evolved massive objects, "mass discrepancy": spectroscopic masses (see below) and evolutionary masses not consistent, inclusion of rotation into stellar models improves situation

- **IF** *you know the distance* **and** *have theoretical fluxes* (from model atmospheres), proceed as follows

- **IF** *you believe in radiation driven wind theory*
  - use **wind-momentum luminosity relation**

$$V = -2.5\log \int_{\text{filter}} \mathcal{F}_\lambda S_\lambda d\lambda + \text{const}$$

S_λ spectral response of photometric system

absolute flux calibration

$V = 0$ corresponds to $\mathcal{F}_\lambda = 3.66 \cdot 10^{-9}$ erg s^{-1} cm^{-2} Å^{-1} at $\lambda_0 = 5{,}500$ Å outside earth's atmosphere

λ_0 *isophotal* wavelength such that $\int_{\text{filter}} \mathcal{F}_\lambda S_\lambda d\lambda \approx \mathcal{F}(\lambda_0) \int_{\text{filter}} S_\lambda d\lambda$, $\int_{\text{filter}} S_\lambda d\lambda \approx 2895$ for Johnson V-filter

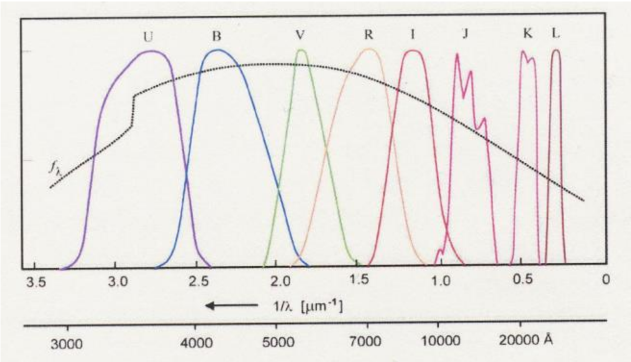

$\Rightarrow$

$$\text{const} = -2.5\log(3.66 \cdot 10^{-9} \cdot 2895) = -12.437$$

$$M_V = -2.5\log\left[\left(\frac{R_* R_{\text{sun}}}{10\text{ pc}}\right)^2 \int_{\text{filter}} \mathcal{F}_\lambda S_\lambda d\lambda\right] + \text{const}$$

$$5\log R_* = 29.553 + (V_{\text{theo}} - M_V)$$

if R_* in solar units, M_V the absolute visual brightness (dereddened!) and

$V_{\text{theo}} - 2.5\log \int_{\text{filter}} 4 H_\lambda S_\lambda d\lambda$ with H_λ the *theoretical* Eddington flux in units of [erg s^{-1} cm^{-2} Å^{-1}]

remember relation between M_V and V (distance modulus)

$M_V = V + 5(1 - \log d) - A_V$, d distance in pc, A_V reddening

d from parallaxes (if close) or cluster/ association/ galaxy membership (hot stars)
(note: clusters/ assoc. radially extended!)

For Galactic objects, use compilation by
Roberta Humphreys, 1978, ApJS 38, 309 *and/or*
Ian Howarth & Raman Prinja, 1989, ApJS 69, 527

Back to our example

HD 209975 (19 Cep): M_v = -5.7
check: belongs to Cep OB2 Assoc., d ≈ 0.83 kpc
V = 5.11, A_V = 1.17 => M_V = -5.65, OK

From our final model, we calculate V_{theo}= -29.08 => $R = 17.4\ R_{sun}$

Finally, from the result of our fine fit, $\log(\dot{M}/R_*^{1.5}) = -7.9$, we find $\dot{M} = 0.91 \cdot 10^{-6}\ M_{sun}/\mathrm{yr}$

Finished, **determine metal abundances if required,**
next star ....
but end of lecture …